JDC GEOBYTES

2022

Department of Geology

Jogamaya Devi College

JDC GeoBytes 2022

Department of Geology
Jogamaya Devi College
Kolkata
2022

Kolkata Jogamaya Devi College
92, Shyama Prasad Mukherjee Road, Kolkata 700026 and
5A, Rajeswar Dasgupta Road, Kolkata 700026

Publication Date: 15th April 2023

Publication Data:
JDC GeoBytes 2022/Department of Geology, Jogamaya Devi College
(Jogamaya Devi College Departmental Magazine, Volume 2)

It is great to see the UG students writing scientific articles for departmental magazines. My heartfelt congratulations to the teachers and students of Geology Department for their effort and I hope annual publication of ***GeoByte*** *would eventually become a tradition of Jogamaya Devi College.*

Best wishes

Dr. Srabani Sarkar

The Principal

Jogamaya Devi College

CONTENT

Ex situ Trace fossils and their Equivalences: An Appraisal

Ishika Chatterjee[1], Sampriti Dey[2] and Kankana Paul[3]
Students of 5th Semester Geology Honours Course
[1]*chatterjeeishika23@gmail.com*, [2]*cutesampriti52@gmail.com*, [3]*kankanap083@gmail.com*

Abstract: Trace fossils are the reliable tools for palaeoecological and palaeoenvironmental reconstructions for their common preservation *in situ*. Despite their rarity, *ex situ* traces (emplaced on movable substrates), nonetheless depict a tale tell story of organism-environment interactions along taphonomic pathways. *Ex situ* traces depicts the work of spatially differentiated genres of trace makers on the same substrate. Compound ichnofabrics, on the other hand depict work of genres of trace makers that are differentiated temporally instead spatially. These varied, yet genetically similar trace fossil types should be brought under a rational scheme of classification since all these traces are the work of genres of different trace suites. Varied *ex situ* traces and compound burrows are cited and described in this work to focus on their comparable genetic aspects.

Key Words: Trace fossils, Taphonomy, Compound burrow, Temporal and Spatial traces, Palaeoecology-Palaeoenvironment.

1. Discussion

Ex situ trace fossils include plant/animal traces that are preserved on movable substrates (shells and bones, plant parts or even artificial objects). Subsequent transport of these movable substrates may preserve *ex situ* traces indented on them at varying phases of transport. These traces basically define trace fossil assemblage(s) involving different genres of trace makers interacting with ambient environment in space and time. The *ex situ* trace fossils may sometimes get exhumed (Figure 1) from their original strata, reworked, and transported to younger stratigraphic horizons (Freitas et al., 2020). Compound burrows, on the other hand, involve modifications of the original ichnofabric over a long interval of time (Bromley, 1996). Long period may also involve reversals in the ecological condition in the ambience, inviting burrow modifiers. These modified ichnofabrics, in effect, represent the ecologically differentiated trace fossil suites. A reappraisal of varied *ex situ* traces and compound traces deem overdue to bring them under a broad frame of classification. *Ex situ* traces and their equivalences have been described here with few examples.

2. *Ex situ* traces

Varied examples include-

- Traces of some gastropod drilling holes on bivalve shell found in deep marine environment created by some boring gastropods (shallow marine organisms) due to post mortem transport (Figure 2). An important component of the Mesozoic and Cenozoic shallow water marine communities are the fossil oysters. Their shells act like a substrate for the encrusters and also for other bioeroding organisms during (and beyond) the Oyster's life. Circular to subcircular boreholes were found on the surfaces of three

different bivalve shells (*Mactra chinensis*, *Felaniella usta*, and *Nuttallia japonica*) are characterized by beveled holes that are parabolic in cross section. The boreholes are classified into the ichnospecies Oichnus paraboloides, probably drilled by a naticid gastropod Glossaulax didyma didyma living in the Baengnyeong tidal flat.

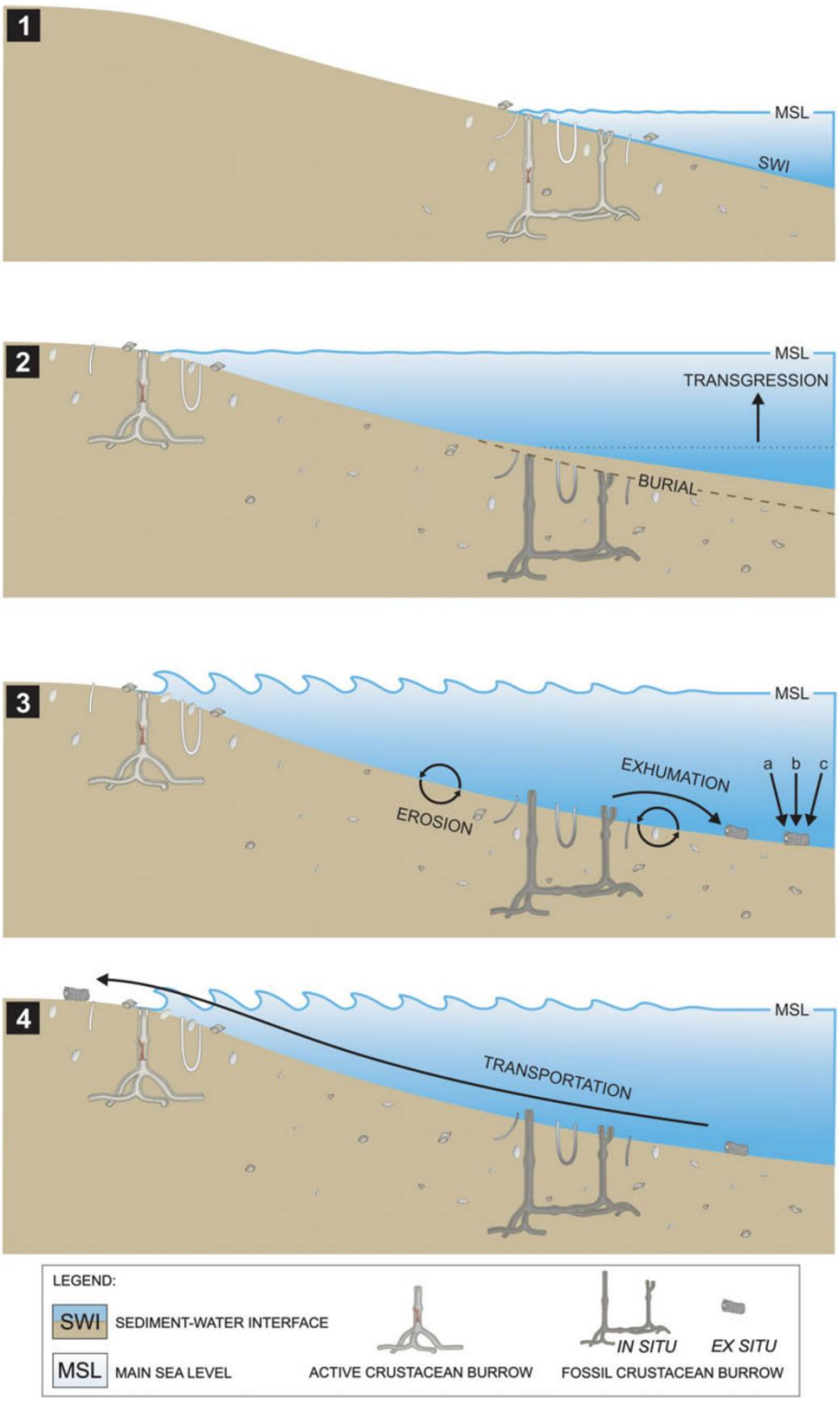

Figure 1: Cartoon showing stages in the formation of ex situ traces in a transgressive milieu (after Freitas et al., 2020).

Figure 2: Gastropod drilling in the umbonal zone of a bivalve shell suggesting it's emplacement during life. This may have a strong potential to be preserved as ex situ trace fossil. The clustered distribution of the boreholes in the umbo area indicates a strong site selectivity for boreholes that is quite a common phenomenon in many Naticid gastropods. (TFF 2021)

Figure 3: Gravity-flow deposition and bioturbation in marine oxygen-deficient environments suggesting a unique situation where ex situ traces may generate (after Föllmi & Grimm, 1990).

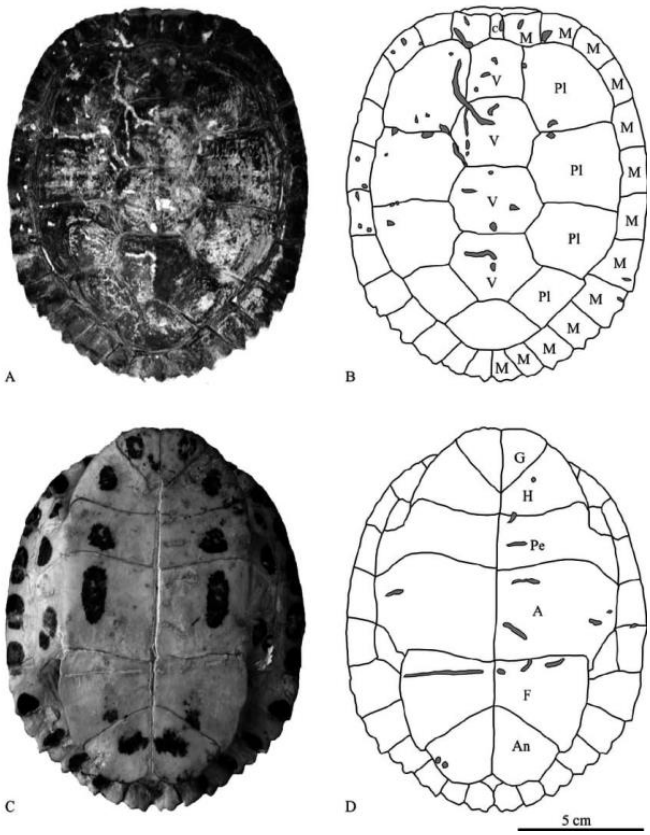

Figure 4: The turtle carapace bears several prominent bite lesions and scrapings (after Milàn et al., 2010).

Doomed pioneers (Figure 3) represented by unusual, mixed shallow and deep-water trace fossil association ((Föllmi and Grimm, 1990; Figure 2c). Here the shallow water substrate moves *en masse* to carry the shallow water ichnocoenoses to deep water realm. In having

the ichnogenera Chondrites, Planolites, and Zoophycos, the "doomed-pioneer" assemblages differ significantly from *in situ* Thalassinoides associations of well-oxygenated environments. The presence of Thalassinoides in association with other ichnogenera (e.g., *Chondrites*, *Planolites*) in otherwise non-bioturbated hemipelagic sediments has been interpreted as an indication of bottom-water ventilation and basin-wide reoxygenation (Savrda et al., 1984). This persistent association within otherwise nonbioturbated sediments, the lack of tiering relations, and the absence of accompanying ichnogenera such as Chondrites, Zoophycos, and Planolites led us to conclude that the organisms which created these prominent burrows were foreign to the oxygen depleted paleoenvironment and were externally derived. It is concluded that deposition from gravity flows in oxygen-depleted environmental settings may be linked with the importation of allochthonous infauna and perhaps oxygenated water, leaving the conspicuous signature of solitary burrowed horizons in laminated host sediments.

- Abundant bite marks on turtle shell are also an example of *ex situ* trace fossil (Figure 4).

- Association of algal boring on deep-water marine shells probably indicate post-mortem transport of the later on which they dwell (Figure 5).

- Plant-animal interactive traces are good examples of *ex situ* preservation of insect-mediated plant damage structures along the taphonomic pathways (Chakraborty, verbal communication). These pre- and post-depositional plant-animal activities (Figure 6) preserve an array of feeding traces of herbivory and detritivory (Labandeira, 2002) including leaf mining (Figure 7A), hole feeding (Figure 7B), lamina eating (Figure 7C), margin feeding (Figure 7D), Frass marks (Figure 7E). Presence of pre- and post-depositional emplacement of insect mediated damage structures on leaf fossil may offer a tale-tell story of taphonomic modification of the trace fossil association (Figure 8).

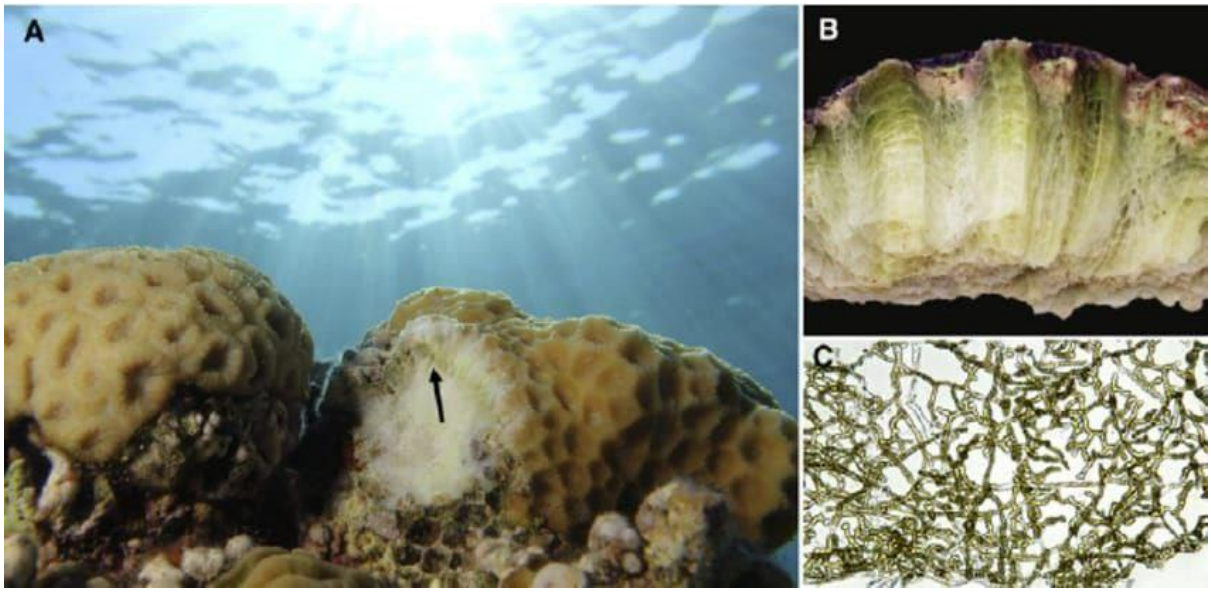

Figure 5. Boring algae. Boring algae of the genus Ostreobium growing in the limestone skeleton of corals. (A) Fractured coral colony with a greenish band of boring algae indicated

by the arrow. (B) Close-up of a coral colony with green boring algae inside the skeleton. (C) Microphotograph of the meshwork of Ostreobium siphons revealed by decalcification of the skeleton (after Verbruggen and Tribollet, 2011).

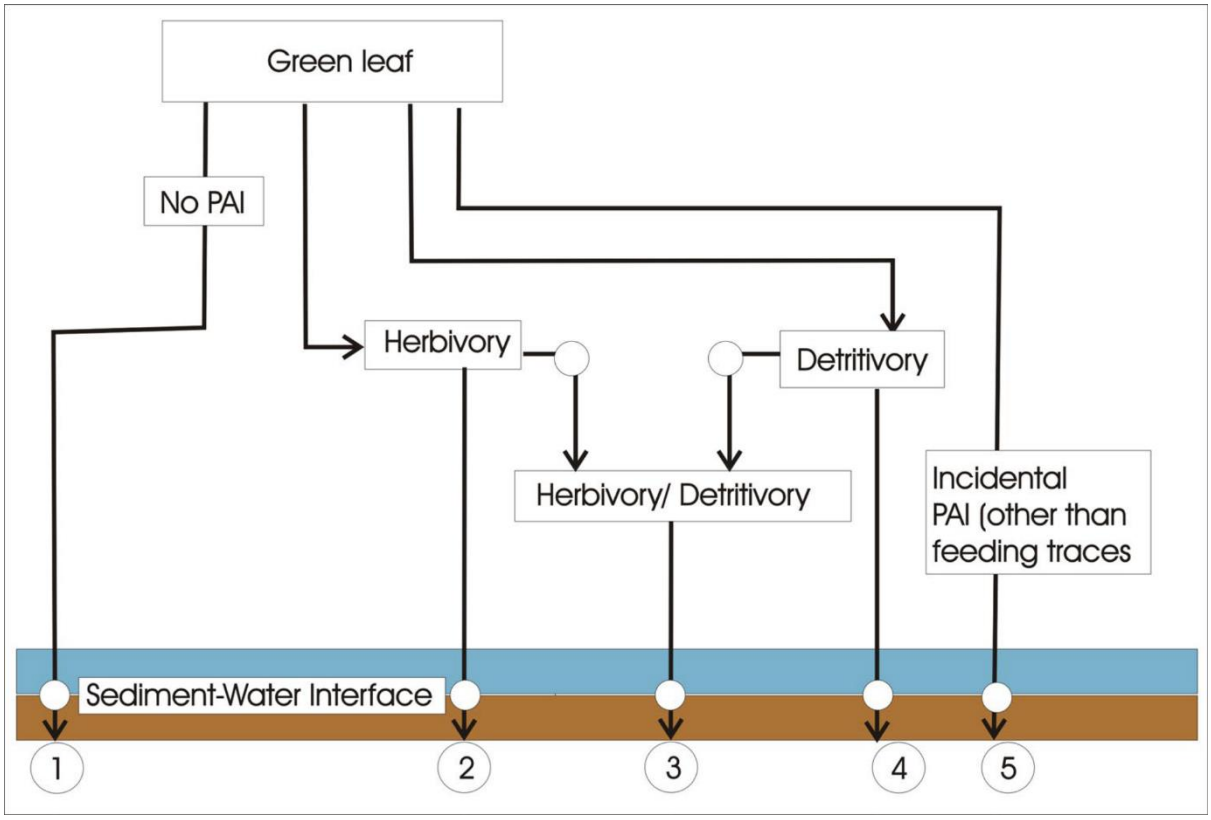

Figure 6: Varied taphonomic pathways showing possibilities of emplacement of pre- and post-event traces, recorded in plant-animal interactive traces (after Chakraborty et al., 2023).

3. Compound traces:

Examples include –

- Modification of rhizohalos by crustaceans (Figure 9) suggesting temporal modification of water table conditions (high/low) (Chakraborty et al., 2013, Figure 2a). These are not *ex situ* traces *sensu stricto* though the substrate hosts varied ichno-taphofacies complying with the essential feature of *ex situ* ichnocoenoses.

- Substrate sharing among the bottom dwellers may have important bearing on the ichnocoenoses. For example, coprophaegus gastropods may retrace and modify the V-shaped profile of bivalve trails with a crescent profile (Figure 10) yielding a compound ichnofabric (conceptual line drawing by A. Chakraborty).

- Burrow modification involving *Phycodes isp*. and *Thalassinoides isp*. (Figure 11) (Chrząstek and Wypych, 2018) indicate *in situ* formation of compound burrows.

Figure 7: Varied traces of insect-mediate damage structures on leaf fossils (after Labandeira et al. 2007).

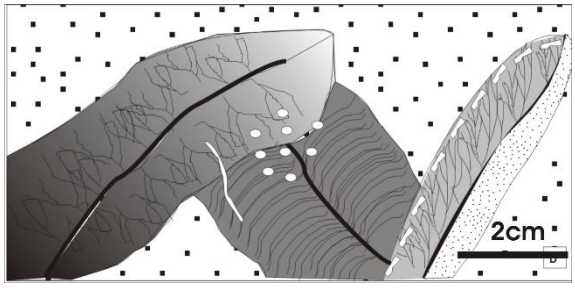

Figure 8: Pre- and post-depositional plat-animal Interactions (conceptual line drawing from A. Chakraborty).

Figure 9: Compound traces showing crustacean trace makers re-burrowing and modifying root traces to keep pace with changing paleo-hydrologic surface (after Chakraborty et al., 2013).

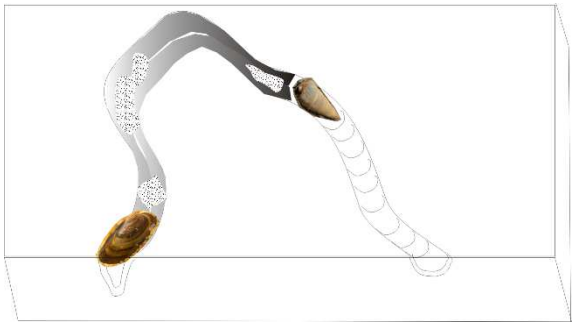

Figure 10: Conceptual line drawing showing compound traces produced by the superposed trails of bivalve and gastropod trace makers.

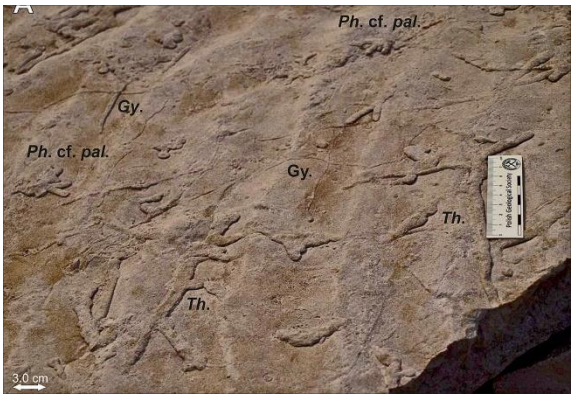

Figure 11:Compound traces showing elements of *Phycodes isp*. And *Thalassinoides isp*. (after Chrząstek and Wypych, 2018).

4. Conclusion

Ex situ trace fossils are rare but significant for their relevance in taphonomic studies. *Ex situ* trace fossils on movable substrates may provide important information on the arrays of spatio-temporal events. Compound trace fossils do also comprise equivalent imprints of temporally differentiated traces made by organisms utilizing the same substrate. However, there is no spatial shift in the substrate, on which a compound trace is grown and modified with time. A broad frame of classification deem necessary to include *ex situ* trace fossils and their equivalences (viz. Compound traces) which might cast light on the spatio-temporal aspect of the trace fossils and improve the fidelity of ichnological data.

ACKNOWLEDGEMENT

We would like to express our sincere gratitude to our mentor Abhijit Chakraborty, Department of Geology, Jogamaya Devi College, for providing guidance and support for writing this article.

REFERENCES

[1] Bromley, R.G., 1996. Trace fossils: Biology Taphonomy and Application, Second Edition, Chapman and Hall, 361p.

[2] Chakraborty, A., Hasiotis, S.T., Ghosh, B and Bhattacharya, H.N. 2013: Fluvial trace fossils in the Middle Siwalik (Sarmatian-Pontian) of Darjeeling Himalayas, *India. J. Earth Syst. Sci*. V.122(4), pp.1023–1033.

[3] Chakraborty A., Mandal S. and Jain, S. 2022. Taphonomic overprinting on the late Palaeozoic terrestrial plant–animal interactions: a noise in the record. *Ichnos*, V.29, pp.166-184, DOI: 10.1080/10420940.2023.2182297.

[4] Föllmi, K. B., & Grimm, K. A. (1990). Doomed pioneers: Gravity-flow deposition and bioturbation in marine oxygen-deficient environments. *Geology*, V.18, pp.1069–1072.

[5] de Freitas G.P., Francischini H., de Souza Tâmega F.T., Spotorno P. and Dentzien-Dias P. 2020. On ex situ *Ophiomorpha* and other burrow fragments from the Rio Grande do Sul Coastal Plain, Brazil: paleobiological and taphonomic remarks. *Journal of Paleontology*, V.94(6) pp.1148 - 1164. DOI: 10.1017/jpa.2020.29.

[6] Labandeira, C.C., Wilf, P., Johnson, K.R., and Marsh, F. 2007. Guide to Insect (and Other) Damage Types on Compressed Plant Fossils. Version 3.0. Smithsonian Institution, Washington, D.C. 25 p.

[7] Milàn J., Kofoed J. and Bromley R.G. 2010 Crocodylian-chelonian carnivory: bite traces of Dwarf Caiman, Paleosuchus palpebrosus, in Red-eared slider, Trachemys scripta, carapaces, pp.195–200; *In* Milàn, J., Lucas, S.G., Lockley, M.G. and Spielmann, J.A., eds., 2010, Crocodyle tracks and traces. New Mexico Museum of Natura l History and Science, Bulletin 51.

[8] ScienceDirect 2021. Burrowing, *From: Encyclopedia of Geology, 2005*. Available at: https://www.sciencedirect.com/topics/earth-and-planetary-sciences/burrowing. Accessed on: 01-12-2021

[9] TFF 2011. What's The Predator That Drills Holes On Bivalves? [*The Fossil Forum: By Steve P., August 9, 2011 in General Fossil Discussion*] Available at: http://www.thefossilforum.com/index.php?/topic/22954-whats-the-predator-that-drills-holes-on-bivalves/. Accessed on: 01-12-2021

[10] UC 2021. Burrow Modification: Belding's ground squirrel. Division of Agriculture and Natural Resources, the University of California, Available at: http://www.groundsquirrelbmp.com/burrowmod-beldings.html. Accessed on: 01-12-2021

[11] Vallon, L. H., Rindsberg, A. K., Röper, M., Rothgaenger, M. and Rothgaenger, K. 2020. Move, burrow, feed – repeat! A compound trace fossil from the Solnhofen Plattenkalke possibly made by holothurians. *Ichnos*, pp.1–10. DOI:10.1080/10420940.2020.1784159

[12] Verbruggen, H., Tribollet, A., 2011. Boring algae. Current Biology, V.21(21), pp.876-877.

[13] Wikipedia-1 2021. Taphonomy. Available at: https://en.m.wikipedia.org/wiki/Taphonomy#. Accessed on: 01-12-2021

[14] Wikipedia-2 2021. Fossorial. Available at: https://en.wikipedia.org/wiki/Fossorial. Accessed on: 01-12-2021

[15] William Miller III (ed) 2007. Trace Fossils- Concepts, Problems, Prospects. Elsevier, 611p.

An Overview of Geobaric and Geothermal Gradients and Terrestrial Heat Flow Pattern

Ankita Chatterjee[1], Purbita Sarkar[2] and Sudarsana Halder[3]
Students of 3rd Semester Geology Honours Course
[1]*ankitachatterjee998@gmail.com*, [2]*purbitasarkar1510@gmail.com*, [3]*moutushihalder25@gmail.com*

Abstract: Temperature and pressure increases from the surface of the earth with increase in depth. But the increase is not uniform and shows significant variation. The formation of different types of rocks at different depths within the interior of the Earth, and the mineralogical, textural and rheological attributes of those rocks are largely controlled by the ranges of pressure and temperature in those depths. The flow of heat from the hot interior of Earth to its relatively cold exterior is the primary source of energy that drives the lithospheric processes. The flow of thermal energy is also involved in magmatic rock-forming processes. This article presents an overview of the pressure and temperature gradients of the Earth, and the heat flows in different tectonic settings.

1. Introduction

In physics, **gradient** refers to the rate of change of a variable physical quantity with respect to distance, in the direction of the maximum change. When depicted graphically with the variable quantities plotted in an appropriate coordinate system, this rate of change can be represented by a curve (Figures 1 & 2).

The magnitudes of two physical quantities, pressure and temperature, vary considerably from the surface of the Earth to its centre; and their rates of variation with depth are termed as the pressure (or geobaric) gradient and the temperature (or geothermal) gradients respectively.

The force of gravity acts on mass to produce pressure, P, in the interior of the Earth, and the rate at which P increases into the interior of the Earth is the **pressure gradient** or **Geobaric gradient**. (Best 2003).

Geobaric gradient in the interior of the Earth is expressed as $\Delta P/z$, where z is the depth. It is related to the overburden of the overlying rocks and is referred to as lithostatic pressure gradient. It is about 3 kilobar/km. This is equal to an increase of 4,410 lbs/in^2 or 3.1×10^6 Kg/m^2 per kilometre increase in depth.

Geothermal gradient is the rate at which temperature (T) increases into the interior of the Earth, or $\Delta T/z$. (Best 2003).

Thermal energy always tends to be conducted through a solid medium from the high temperature zone to the low temperature zone. That is why there is an intermittent dissipation of heat from within the Earth to the surface in response to temperature gradients, which is

termed as the '**Geothermal Heat Flow'**. This continuous heat flow, into the base of the crust from the mantle below, started early in the Earth's history.

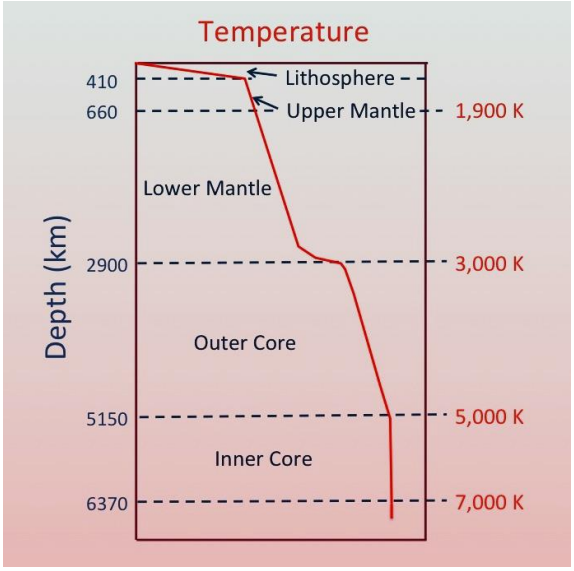

Figure 1: Temperature profile of inner Earth, schematic view (Wikipedia 2022).

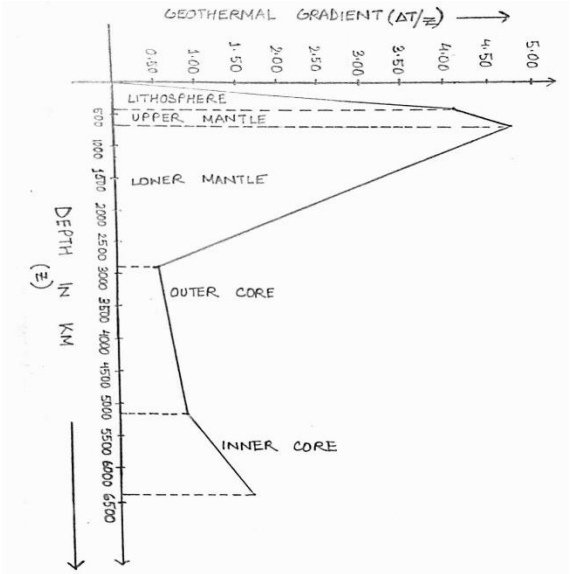

Figure 2: Variation in the geothermal gradient with depth Constructed by the authors, using the data given in Fig. 1

This geothermal heat is the driving force for a variety of multi-scale geologic processes taking place in the Earth's lithosphere, among which the movement of the lithospheric plates is one of the most important phenomena.

Human beings are have already started utilizing the geothermal energy that finds its way to the Earth's surface in the form of geothermal reservoir. These are naturally occurring areas of hydrothermal resources. They are located deep underground and are difficult to detect from above the ground. Geothermal energy moves up to the surface through volcanoes, fumaroles, hot springs and geysers. Most of the active geothermal resources are discovered along the major tectonic plate boundaries where most volcanoes are located, like the Pacific Ring of Fire encircling the Pacific Ocean. This energy can be harnessed for heating and cooling structures through geothermal heat pumps, generating electricity through power plants, also heating through direct application. Among all the countries, California generates the most electricity from geothermal energy. The Geysers dry steam reservoir in Northern California is the largest dry steam field in the world, from which electricity is being generated since 1960. Although geothermal power generation is mainly concentrated in the Western U.S.A., it is expected that these applications would expand geographically with time.

2. Geobaric Gradient

The pressure gradient vividly narrates a differential form of the Pressure-Depth relationship inside the Earth with the variation of density 'ρ' and gravitational acceleration (g) and then integrated over the depth range, to obtain the gradient. Density increases with depth as the rock gets compressed due to the increasing overlying materials and 'g' decreases as depth

increases. However, the changes in 'g' and density of a given rock type are relatively minor in the lithosphere and they tend to offset each other.

2.1 Variation of geobaric gradients from the surface to the centre of the earth

2.1.1 Geobaric gradients in different parts of the crust

In the continental crust, where the mean density is 2.7 g/cm^3, and the average geobaric gradient, $\Delta P/z$= 270 bar/km (~27 MPa/km). In the basaltic oceanic crust, on the other hand, the mean density is ~3.0 g/cm^3, $\Delta P/z$ = 300g/cc. Since the thickness of the crust and the density of its constituents vary significantly in different tectonic settings, the geobaric gradient is not uniform in the crust. In the oceanic crust, having thickness 6 – 10 km, the pressure at the base can be in between 2 – 3 kb.

The continental crust is much thicker, and its thickness varies significantly in the different tectonic settings. In normal continental crust setup with thickness in between 35 – 40 km, the pressure experienced by the base is in between 10 – 12 kb.

In the active plate margins, with a crustal thickness of 60 – 80 km, the pressure can be in between 18 kb to 25 kb.
In the areas of collisional orogeny where crustal thickness can reach up to 80 – 100 km, the basal pressure is 24 – 30 kb.

Table 1: Thickness and Pressure at the bases of different crusts

Type of crust	Thickness of the crust	Pressure at base	Example
Normal continental crust	35 – 40 km	10 – 12Kb	Canadian shield
Active margin	60 – 80 km	18 – 25 Kb	Sierra Nevada, Andes
Collisional Orogen	80 – 100 km	24 – 30 Kb	Himalayan orogenic belt
Oceanic crust	6 – 10 km	2 – 3 Kb	Atlantic Ocean

2.1.2 Geobaric gradient in mantle and core

The upper mantle extends from the crust to a depth of about 410 kilometres (255 miles). It is mostly solid, but its more malleable regions are associated to tectonic activities. The upper mantle is rheologically divided into the **lithospheric mantle**, which extends up to 100 km (62 miles) beneath the earth's crust; and the **asthenosphere**, which lies between 100 kilometres (62 miles) and 410 kilometres (255 miles) beneath Earth's surface. The mean density of the upper mantle is ~3.3 g/cm^3 and the geobaric gradient ($\Delta P/z$) is 330 bar/km. The Pressure at Lithosphere-Asthenosphere boundary is 140 kb.

The asthenosphere is the denser, weaker layer beneath the lithospheric mantle. The pressure along with the temperature of the asthenosphere is so high that rocks soften and partly melt, becoming semi-molten. Here the mantle deforms by plastic flow in response to applied pressures that ranges from about 140 kb to 240 kb, increasing with depth. The maximum

pressure experienced by the upper mantle is at the lower boundary of Asthenosphere and the value is 240 kb.

Pressures in the lower mantle start at 237,000 times atmospheric pressure (240 kb) and reach 1.3 million times atmospheric pressure (1360 kb) at the core-mantle boundary.

As we move towards the centre of the Earth, the pressure gradient also increases since the mass of the overlying rocks increases so as the confining pressure. The pressure in the Earth's inner core is slightly higher than it is at the boundary between the outer and inner cores: It ranges from about 330 to 360 gigapascals (3,300,000 to 3,600,000 atmosphere).

3. Geothermal / Temperature Gradient: Its sources and variations with depth

The Earth's internal heat comes from a combination of residual heat from planetary accretion, heat produced through radioactive decay, and possibly heat from other sources. The major heat-producing isotopes in the Earth areK^{40}, U^{238}, U^{235}, and Th^{232}.

3.1 Major heat sources of earth:

3.1.1. Heat originating from planetary accretion

One of the major sources of heat is the original heat from the formation and gravitational compression of the earth from the solar nebula.

3.1.2. Heat produced by radioactive decay

The decay of radioactive elements, like Al^{26}, generated heat energy in the early stages of the earth formation. The ongoing decay of the long-lived radioactive elements like Uranium has been generating heat for a long time.

3.1.3. Heat from other sources

Geothermal Heat is contributed by radiogenic heat (at shallower crustal levels) and residual heat generated by cooling core. Besides, shear heating generated by plate movements is also considered as a contributing factor. It decreases with depth as the concentration of the heat producing radioactive elements in the near surface rocks produces a heat that decreases with depth.

3.2. The variation of geothermal gradient with depth

The geothermal gradient is not constant with respect to depth as we can see in Figure 2. There are at least two possible reasons for a substantially reduced geotherm at depth in the Earth.

One is that, mechanism of more efficient heat transfer prevails in the deep mantle, and the other is the presence of a concentration of heat producing minerals nearer the surface.

Most of the heat within the Earth is generated by radioactive decay. For this reason, temperature generally increases with depth in the Earth. But most the radioactive isotopes, in spite of their high densities, are concentrated in the crust and the asthenosphere. There are areas in the continental crust with high concentrations of radioactive elements. The continuous radioactive disintegration in those areas have locally raised the temperature, which is high enough to cause metamorphism. But such areas are not common in the continental crust.

Heat conductivity inside the earth is not same everywhere. The geothermal gradient must decrease sharply a short distance into the earth, otherwise the mantle would be at temperatures above the melting point. Seismic evidence seems to indicate a solid, not molten, mantle, so the geothermal gradient must drop to 1°C/km within the mantle. The rate of change in temperature is much higher in the lithosphere than in the mantle because the mantle transports heat primarily by convection. This makes the geothermal gradient much steeper in the lithosphere than the mantle. This leads to the geothermal gradient to be determined by the convection cells, though conductive heat transfer processes occur in the lithosphere.

On an average, the temperature increases by about 25°C for every kilometre of depth inside the Earth. Data show the geothermal gradient, on the average, to be about 3°C for each 100 meters (30°C/km) of depth in the upper part of the crust, and decreasing in the mantle. The average change in geothermal gradient with depth is represented graphically in Figure 2.

Away from tectonic plate boundaries, the gradient is about 25°C per km of depth (1°F per 70 feet of depth) in most parts of the plate interiors.

In areas where the continental lithosphere has been stretched and thinned, such as Nevada's Great Basin, the heat transfer is higher, so the geothermal gradientis steeper (for example, 50°C per kilometre of depth). In areas where the continental lithosphere is old and thick, such as central North America, the heat transfer is slower and lesser, so the geothermal gradient is gentler (for example, 20°C per kilometre of depth).

The Geotherm has been found to vary from hundreds of degrees centigrade per kilometre beneath oceanic spreading ridges to about 20–30°C/km in active orogenic belts alongside convergent plate junctures to as low as 7°C/km in the nearby deep-sea trench.

At the centre of the Earth, the temperature may be up to 7,000 K. The interior of the Earth is extremely hot, and reaches temperatures over 5000°C near the core, which is not much colder than the surface of the Sun (the interior of the sun however is much hotter).

Estimates of Earth's internal temperatures are 3,700 °C at the core–mantle boundary, 6,300°C ± 800°C at the inner-core/outer-core boundary, and 6,400°C ± 600 °C at Earth's centre (hotter than the surface of the sun). All these changes in temperature with depth, inside the Earth, is represented graphically in Figure 1. Figure 2 represents the changes in geothermal

gradient with depth. The depth is measured in kilometres whereas the temperature is measured in Kelvin.

4. The terrestrial heat flow

Heat flow is measured as the amount of heat (energy) transferred across an isothermal surface in a unit time. It is the transfer of thermal energy, commonly when there is a temperature difference. Thermodynamically, energy can be produced or transferred as heat by thermal conduction, by thermal radiation, by friction and viscosity, and by chemical dissipation.

Heat flow has the same dimensions as power and is measured in watts (W) or kilo-calories per hour (kcal/hr); 1 W = 0.86 kcal/hr.

Heat flow pattern on earth surface is deciphered based on present data strength which is subjected to continuous evaluation. A thin plate of thickness z with temperature difference ΔT experiences heat flow $(Q)= -k(\Delta T/z)$ where k is the thermal conductivity and $\Delta T/z$ is the thermal gradient.

4.1 Unit of heat flow

Basic heat flow unit for terrestrial heat flow measurement is not done in SI system. So smaller unit (Milli Watts per square meter: mWm^{-2}) is derived for all practical purposes. Similarly, some derived CGS unit (HFU) has been used for heat flow measurement. I HFU= I micro calorie per square cm per second ($10^{-6}cal/cm^2$ /sec) = 41.8 mWm^{-2} (SI Unit) = 0.013228 $BTU/ft^2/hr$.1 HFU can be defined as the amount of heat required to raise the temperature of 1 pound (lb) of water in 1 degree Fahrenheit. (Winter 2014, Philpotts & Ague 2009)

4.2 Heat flow processes: Processes that conduct the vertical movement of heat flow

(a) Conduction

The conduction of heat occurs when thermally agitated atoms and molecules collide one another, mechanically transferring kinetic energy from a hotter region to a cooler one. The conduction of heat through the outer surface of the lithosphere causes the lithosphere to cool slowly. As it cools, it thickens, contracts and becomes denser with decreasing temperature. Conduction in lithosphere describes a wide variety of geologic phenomenon like, the subsidence of passive continental margins and thermal subsidence basins. It explains why the amount of heat flowing out of oceanic lithosphere is high near spreading centres and decreases as the oceanic lithosphere gets older, and it describes why the average thickness of the oceanic lithosphere is about 100 km which is one of the major contributions in plate tectonics.

(b) Convection

Movement of material having temperature difference from one place to another is convection. Unlike heat transfer by conduction, convection depends upon gravity. The solid mantle transmits seismic shear waves and the fluid mantle capable of convection by presence of viscous bodies. Seafloor spreading and plate movements are direct evidence of this solid-state convection at work. The hot mantle material that rises under mid-ocean ridges builds new lithosphere, which cools as it spreads away. In time, it sinks back into the mantle at subduction zones, where it is eventually reheated. Through this process, heat is carried from Earth's interior to its surface.

(c) Advection

Advective transfer of heat associated with magmas ascending from the mantle elevates geothermal gradients in the crust above subduction zones and in rifts. As a result, deeper crustal temperatures locally reach the solidus and cause magma generation. The geothermal gradient does not intersect the zone of partial melting. At all depths, the temperature is not high enough to allow the rock to melt, and no magma is forming. In order for magma to form, conditions must change so that the geothermal gradient can intersect the zone of partial melting.

(d) Radiation

R**adiation occurs** from one surface to another without medium. **Radiation heat transfer** is mediated by **electromagnetic radiation**, **thermal radiation** that arises due to the temperature of a body. Thermal radiation heat transfer can occur between two bodies separated by a medium colder than both bodies. For example, solar radiation reaches the surface of the earth after passing through cold layers of atmosphere at high altitudes.

4.3 Average heat flow in different parts of Earth Crust

Here, Figure 3 describes the heat flow pattern across the earth. The darker region represents higher heat flow and lighter region depicts lower heat flow. Dark red sections signify the areas of highest heat flow while blue coloured sections signify area of lowest heat flow, and the intermediate colours represent the intermediate amounts of heat flow as mentioned in the figure accordingly.

The average heat flow from the continents is the same as the average heat flow from the sea floor. The greater concentration of radioactive material in continental rock would suggest that the continental rocks should have a higher heat flow. The unexpectedly high average heat flow under the ocean crust may be due to hot mantle rock rising slowly by convection under parts of the ocean crust. Heat flow is higher in areas with either high radioactivity or where the Earth's crust is thinner, such as the mid-oceanic ridges or the Basin and Range Province of the Western United States. Additionally, there are areas with heat flow 'anomalies' that have higher than average crustal heat flow without a clearly identified tectonic or radioactive explanation, usually related to fluid flow such as in South Dakota.

The averages of oceanic and continental heat flux data are 70 and 80mW/m^2, respectively. For example, high heat flow has been observed in the Atlantic ridges. Moderate heat flow of 40-60 mW/m^2 has been observed in the Himalayan Mountain regions and low heat flow of about 0-40 mW/m^2 is observed in deep sea trenches and subduction zones. The average oceanic heat flux is found to be 101mW/m^2. The mid oceanic ridge shows higher heat flow. Here the heat-flow is greater than that from normal ocean floor or from the continent. The highest heat flow values are observed along ridge crest, though considerable variations are formed along the crust. In orogenic belts, crustal flow may be greatly facilitated by heating due to crustal thickening, magmatic advection of mantle heat into the crust, or heat conduction through a thinned lithospheric mantle, resulting in partial melting and mechanical weakening of the orogens.

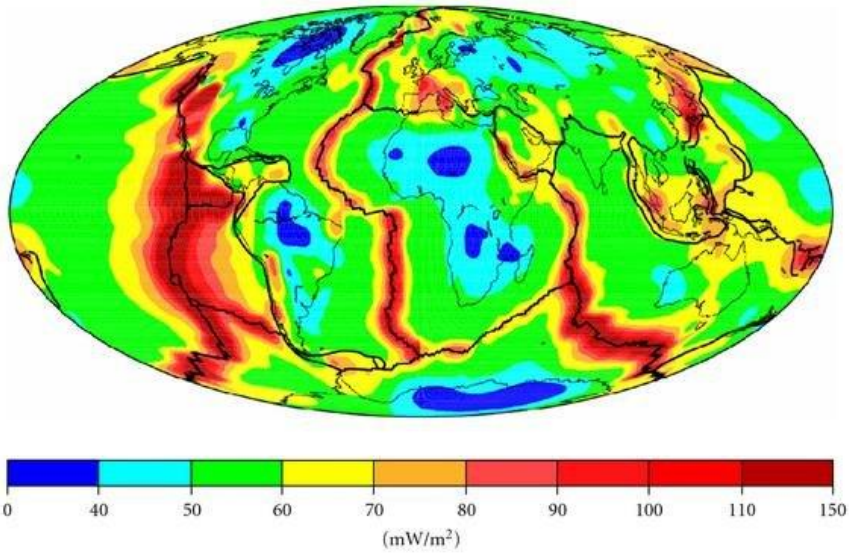

Figure 3: Heat flow pattern across the earth (Hamza et al. 2010)

So, we understand that, heat flow in the ocean basins is also highly variable. The highest values correspond to the mid-ocean ridges. Heat flow decreases away from the mid-ocean ridges and is at a minimum over the convergent plate boundaries, deep ocean trenches or subduction zones. In general lithosphere is hot where the underlying asthenosphere is hot, and cold here it is cold. This observation strongly supports the concept that plate tectonics is largely driven by convection within the asthenosphere. Sites characterized by upwelling of hot asthenosphere (the rising limbs of convection cells) have high heat flow (e.g., mid-ocean ridges). In contrast areas where the convection cells turn and sink back into the deep interior are cold (e.g., subduction zones).

4.4 Heat flow at different tectonic settings

A. Normal situation: In most of the plate's interior or stable cratonic parts, the average heat flow is minimum. If we represent this situation graphically (Figure 4A), with geotherm line and solidus line, here both the lines move without intersecting anywhere, which signifies the absence of molten material in that area.

B. Mid-oceanic ridge: Mid-oceanic ridge is a Divergent plate boundary where two plates move away from each other. Along the ridge axis, the molten basaltic magma upwells, cools down slowly and forms the oceanic crust. Representing the heat flow of this area graphically (Figure 4B), would lead to an extremely steep geotherm at the crustal level. The temperature is so high that it exceeds the solidus curve, indicating the presence of hot, molten magma that reaches the surface. The geotherm curve is steepest across the ridge axis, where the magma upwelling primarily occurs and the oceanic crust is thinner and youngest. As we move away from the axis, the gradient would very slowly become gentler, as we encounter older, thicker and cooler rocks.

C. Hotspot: In the Hotspot situation, high heat flow is observed at the asthenospheric depths. This is due to the presence of mantle plume. Here the magma is hotter than the surrounding magma. This acts as the magma chamber and the heat from the magma plume causes melting and thinning of the rocky crust and widespread volcanic activity. If we represent the heat flow of this area graphically (Figure 4C), we'll notice that the geotherm intersects with the solidus line and even exceeds it at the depths of deep mantle, signifying the presence of molten magma material. Plumes probably originate from the depth of nearby 700km. This phenomenon occurs far away from the plate boundaries. The magma upwells from the chamber and creates Volcanism on the Earth's surface, right above the mantle plume. These are called Hotspots. As the hotspots are formed by mantle plumes, and the lithospheric plates tend to move with time, it may show a chain of volcanoes on the Earth's surface. Hotspots are widely observed at Hawaiian Islands and Yellowstone National Park.

D. Subduction zone: Subduction zone is a tectonic plate boundary where both the plates move towards each other and the denser oceanic plate gets subducted under the lighter continental one. The crustal portion of the subducting oceanic slab contains a significant amount of water molecules. As the subducting slab moves to deeper depths, it progressively encounters greater temperatures and pressures which cause the slab to release water into the mantle wedge overlying the descending plate. Water lowers the melting temperature of the mantle, thus causing fractional melting of the mantle material. The magma produced by this mechanism ranges from basalt to andesite in composition. It rises upward to Earth's surface and produce a linear belt of volcanoes parallel to the oceanic trench, and this chain is known as island arc volcanoes. This phenomenon is seen in the Pacific Ring of Fire, a region of subduction zone volcanism surrounding the Pacific Ocean. If we represent the geothermal gradient of this area graphically (Figure 4D), we'll observe that the geotherm line intersects the solidus line and exceeds it at the asthenospheric depths, representing the partial melting of the mantle wedge.

If we see the heat flow variation of this area, highest heat flow values are observed over the volcanic arc, that are supposedly associated with the partial melting processes. The lowest heat flow is observed over the subduction complex and forearc basin is assumed to result from thermal blanketing effect by the overlying plate and accreted sediments above the subducting oceanic plate.

5. Effects of pressure and temperature on different geological phenomenon

Lithostatic pressure and temperature governs volcanic activities like metamorphism, rock deformation which in turns controls all about the geologic processes in the earth.

If we delve into the situation of Mid-oceanic ridge, we'll notice that the magma is generated in the mid-ocean ridge by decompression melting. The mantle is solid but is slowly flowing under enormous pressure and temperatures due to convection. As mantle rock rises, the pressure is reduced along with the melting point, but the rock temperature remains about the same, and the rising rock begins to melt. Pressure changes instantaneously as the rock rises, but temperature changes slowly because of the low heat conductivity of rock. Thus, hotter rock is now at shallower depth, at a lower pressure, and the new geothermal gradient exceeds the solidus and melting starts. As this magma continues to rise at divergent boundaries and encounters seawater, it cools and crystallizes to form new lithospheric crust. The rate of convection depends on both on the temperature gradient and the viscosity of the material. In the Earth, temperature gradients appear to be high enough and viscosity low enough for convection to occur. Plate tectonics appears to be driven by convection in some form. Anywhere there is a rising convection current, hotter material at depth will rise carrying its heat with it. As it rises to lower pressure (decompression) it will cool somewhat, but will still have a temperature higher than its surroundings. Thus, decompression will result in raising the local geothermal gradient. If this new geothermal gradient reaches temperatures greater than the peridotite solidus, partial melting and the generation of magma can occur.

Volcanoes are the main source of geothermal energy. Compared to the normal geothermal gradient of about 25°C per km of depth in most of the world, when magma (i.e., molten rock generated at the Earth's interior) enters the crust, for example, as a shallow intrusion beneath a volcano, this normal gradient changes locally as temperature rises around the intrusion. The extent and duration of such a thermal anomaly depend mostly on the temperature and volume of the intruded melt. The presence of hot magmas below the surface of active volcanic regions offers the prospect of harnessing a huge amount of geothermal energy.

Contact metamorphism occurs due to heating, with or without burial, of rocks that lie close to a magma intrusion. It is characterized by low P/T gradients, as strong thermal gradients between an intruding magma and adjacent country rock are best established at shallow crustal levels. If rocks lie structurally above or to the side of an intrusion, no change in pressure is expected during metamorphism, though temperature simply increases with proximity. However, if magma spreads laterally, for example forming a thick sill or laccolith, the added load on top of pre-existing crust will cause an increase in pressure *and* temperature.

The Earth's outer core is a fluid layer of about 2,400 km thickness and composed of mostly iron and nickel. The transition between the inner core and outer core is located approximately 5,150 km beneath the Earth's surface. Unlike the inner core, the outer core is liquid in nature. This is due to the pressure-temperature condition that prevails in the deeper parts. We know that as temperature increases, solid materials tend to become fluid, while with increasing

pressure materials become more consolidated. In the outer core, the temperature balances the pressure in such a way that results in the liquid nature of the layer.

Therefore, we can definitely say that we need a precise idea on the geobaric and geothermal gradient along with heat flow pattern of the earth for a better understanding of the different types of geologic phenomena, especially the endogenic processes occurring in the lithosphere. (Best 2003, Grotzinger et al., 2007, Philpotts & Ague 2009).

6. Conclusion

We can conclude here that a proper knowledge regarding the pressure-temperature conditions at different depths of the Earth would help us gather a better understanding of the earth's internal composition and processes. Also, it may help to throw light to several tectonic processes which are not yet properly understood. Apart from the research sectors, a better overview of the terrestrial heat flow and geothermal gradient would also help us discover the geothermal reservoirs from where we can harness the geothermal or hydrothermal (hot springs and geysers) energy for different purposes, mainly electricity. The power output of geothermal power plants is predictable and stable, that can generate electricity 24x7 without any lag. So, with a well insight and better infrastructures, this energy would act as a miracle in this overpopulated world where almost all the fuel resources are nearly exhausted.

Therefore, we can definitely say that it is extremely important for us to delve into these arenas of study, at this point of time.

ACKNOWLEDGEMENT

We would like to express our special thanks of gratitude to respected Professor Bhaskar Ghosh and other respected professors of our department who bestowed us with the golden opportunity to do this wonderful project on the topic **An Overview of Geobaric and Geothermal Gradients and Terrestrial Heat Flow Pattern** which also helped us in doing a lot of research. We got a vivid knowledge about the topic we dealt with.

REFERENCES

[1] Best, M.G., 2003. Igneous and Metamorphic Petrology. 2nd Edition, Blackwell Publishing

[2] Grotzinger, J., Jordan, T.H., Press, F and Siever, R. (2007) Understanding Earth, 5th Edition, W. H. Freeman and company, New York.

[3] Hamza, V.M., Cardoso, R.R., Alexandrino, C.H., 2010, A Magma Accretion Model for the Formation of Oceanic Lithosphere: Implications for Global Heat Loss, https://www.researchgate.net/figure/Global-heat-flow-map-derived-from-mixed-data-sets-For-oceanic-regions-with-ages-less_fig1_44849425. Last visited on: 20th December 2021

[4] Philpotts, A.R., Ague. J.J, 2009. Principles of Igneous and Metamorphic. 2nd Edition, Cambridge University Press
[5] Winter, J.D., 2014. Principles of Igneous and Metamorphic Petrology. 2nd Edition, Pearson Education Limited
[6] Wikipedia, 2022. Geothermal Gradient, https://en.wikipedia.org/wiki/Geothermal_gradient. Last visited on: 20th December 2021

Origin of Dolomite

Aditi Das[1], Sarmistha Das[2], Anwesha Ghosh[3]
Students of 5th semester Geology Honours
[1]aditidas7679@gmail.com, [2]sarmipritiyanka@gmail.com and [3]anwesha2001@gmail.com

Abstract: One of the oldest problems in sedimentology is the origin of dolomite. Dolomite is one of the most common sedimentary carbonate minerals that have high porosities and are important reservoir rocks for oil. Dolomite is not a simple mineral. It can have a variety of origin. For both scientific and economic reasons, many attempts were made to explain the origin of dolomite. It can form as a primary precipitate, a diagenetic replacement, or as a hydrothermal/metamorphic phase, all that it requires is permeability, a mechanism that facilitates fluid flow, and a sufficient supply of magnesium. Dolomite can also form in lakes, on or beneath the shallow seafloor, in zones of brine reflux, and in early to late burial settings. In this article we discuss about the all possibilities of dolomite formation processes or dolomitization processes and gives a brief idea about the hypothetical models of dolomitization.

Key words: Dolomite, Dolomitization

1. Introduction

Dolomite is a very common and familiar translucent anhydrous carbonate mineral composed of calcium magnesium carbonate $CaMg(Co_3)_2$. In late 18th century, French geologist Dolomieu (1750 -1801) discovered it. Based on the chemical analysis and description by Dolomieu and De Saussure, Irish chemist Richard Kirwan named the mineral "Dolomite" (Figure 1) in honour of Dolomieu.

The term "Dolomite" is used for both the mineral and rock, to differentiate the rock from the mineral, dolomitic rocks are sometimes referred to as dolostones, which contain more than 50% of dolomite minerals (Boggs, 2010).

Figure 1: Dolomite

Figure 2: Dolostone

Dolomite makes up approximately 2% of the earth's crust in combination with calcite and aragonite. They occur so frequently in close association with limestones as interbeds in many stratigraphic units throughout the world from Precambrian to Holocene. The limestone to dolomite ratio is 10:1 in Mesozoic, 3:1 in Palaeozoic and 1:3 in Precambrian (Tucker, 1988). Workers reported modern dolomite sediment from Russia, South Australia, the Persian Gulf, the Bahamas, Bonaire Island of the Venezuela mainland, the Florida-keys, the canary island. The most notable mines of dolomite are located in the midwestern United States; Ontario, Canada; Switzerland; Pamplona, Spain and Mexico. In India, major 88% resources are distributed in Madhya Pradesh, Andhra Pradesh, Chhattishgarh, Odisha, Karnataka, Rajasthan (Figure 3), Gujrat and Maharashtra. The remaining 12% resources are distributed in Arunachal Pradesh, Jharkhand, Haryana, Sikkim, Tamil Nadu, Telangana, Uttarakhand, Uttar Pradesh and West Bengal.

Figure 3: Dolomite mine at Udaipur, Rajasthan.

Figure 4: Dolomite ore

Figure 5: Dimension stone

2. Use of Dolomite

Dolomite is used as a source of Magnesium metal (Figure 4) and of Magnesia (MgO), a sintering agent and flux in metal processing and also used in the production of glass, bricks and ceramics. Dolomite serves as the host rock for many Lead, Zinc, and Copper deposits and also serves as reservoir rock for oil and natural gas. It is used for acid neutralization in the chemical industry, in stream restoration projects and as a soil conditioner. Dolostone is crushed and sized for use a road base material, an aggregate in concrete and asphalt, railroad ballast. It is also calcined and cut into the blocks of specific size known as "Dimension stone" (Figure 5).

3. Identification of dolomite

Dolomite crystals are colourless, white, buff-coloured, pinkish (Figure 6) or bluish (Figure 7) and in the field, dolomite can be recognized by its sugar-like shine and weathered surfaces that resemble like elephant skin (Figure 8). It may have a golden-brown and tan colour in contrast to limestone, which are typically grey. In field, a bit of powdered sample of dolomite will cause a weak effervescence while treated with dilute acid. In the laboratory, chemical Alizarin Red S stains calcite and aragonite deep red but does not affect dolomite.

Figure 6: Pinkish dolomite

Figure 7: Bluish dolomite

Figure 8: Elephant skin weathering of dolomite

4. Origin of dolomite

Dolomite has attracted greater attention to geologists. Because origin or formation of dolomite is still puzzling the scientists. Dolomite is formed by the replacement of the calcite ions by magnesium ions in crystal lattice, although large deposits of directly formed (primary) dolomite reported from the past 600 million years.

In the Precambrian, the preferential occurrence of dolomite suggest that sea water had a different composition at that time; so that dolomite could be precipitated directly. Alternative views are that dolomite forming environments were more prevalent through paleogeographic and paleoclimatic consideration (Tucker, M.E. 1988), or older limestones have had more time to come into contact with solutions for dolomitization.

Dolomite originates in warm shallow marine environments where calcium carbonate mud accumulates in the form of shell debris, fecal material, coral fragment. It can also form in lakes, in zones of brine reflux, and in early to late burial settings. It may form from sea waters, continental waters, from the mixing of basinal brines, the mixing of hypersaline brine with sea water, or the mixing of seawater with meteoric water or via the cooling process of basinal brines.

4.1. Dolomitization

Dolomite is thought to form when the calcite in carbonate mud or limestone is modified by magnesium rich groundwater. The available magnesium facilitates the conversion of calcite into dolomite. This chemical change is known as “Dolomitization”. This process can completely alter a limestone into a dolostone or it can partially alter the rock to form a ‘dolomitic limestone’. This process obscures the original texture of rocks.

The term ‘primary’ has been applied when the carbonate material directly precipitated from the seawater and the conversion of $CaCO_3$ minerals into dolomite [$CaMg(CO_3)_2$] may take place soon after the sediment have been deposited that is penecontemporaneously and during early diagenesis. This process is known as “syngenetic dolomitization”. Bacterial metabolism may aid the process of precipitation in settings where sulfate-reducing species flourish and microbial action may control primary precipitation in some hypersaline anoxic lake settings.
In the syngenetic diagenesis, the rocks have a loose structure with large quantity pore water and weak compaction. The primary pore evolution includes intraparticle pores, interparticle pores, and skeleton pores. The syngenetic dolomite evolved into small amount of intracrystal pores. In the early diagenetic stage, the compaction was strengthened so the porous water was quickly expelled and the primary pores reduced clearly. When the burial depth increased, the compaction became even stronger and the early cementation took place, so the primary pore was dramatically reduced or even disappeared. The interparticle fluid dissolved along the contact surface of grains formed afterwards and compaction dissolution fissures. Some intracrystallization pores were formed as a result of mineral transformation and recrystallization. In the middle diagenetic stage, dolomite was developed and dissolution was

strengthened so large amounts of intracrystal pores and various secondary pores appeared, including interparticle pores, intraparticle pores, and intercrystal pores, which made up good reservoir space. At the latest diagenetic stage, the base of secondary pore development in early and middle diagenetic stages, the dissolution was further enlarged to form some moldic pores and superlarge pores. At the same time, the tectonic fractures developed in many stages, spread in the shape of reticula, and finally formed dolomite of high porosity.
The process of recent primary dolomite formation is restricted to extreme eco systems such as bacterial mats in highly saline lakes and lagoons.

4.2. Dolomitization reactions

$$1.\ Ca^{2+} + Mg^{2+} + 2(CO_3)^{2-} \rightarrow Ca\ Mg\ (CO_3)_2$$

This reaction indicates precipitation of dolomite crystals directly from seawater.

$$2.\ Mg^{2+} + 2(CaCO_3) \rightarrow Ca\ Mg\ (CO_3)_2 + Ca^{2+}$$

This reaction involves replacement of individual calcium cation by magnesium cation. It requires the addition of magnesium to the system and the removal of calcium from the system. So, the system must be an open one.

$$3.\ CaCO_3 + Mg^{2+} + (CO_3)^{2-} \rightarrow Ca\ Mg\ (CO_3)_2$$

Dolomitizing fluids provide magnesium cations and carbonate anions. This reaction eliminates the requirement of reaction 2 that calcium ions be removed from original calcite or aragonite.

The majority of dolomites have formed by replacement of pre-existing carbonate minerals. The term ‘secondary’ has been applied when the conversion of $CaCO_3$ minerals may took place in a long time after deposition, usually after the cementation, during later stages of diagenesis. This process is known as “Epigenetic Dolomitization”. Workers found relict limestone textures and structures in coarsely crystalline secondary dolomite rocks. Many fine crystalline dolomites lack textural evidence is of replacement and cannot be proven to have originated by diagenetic alteration of limestones. These fine-grained dolomites created so called ‘**Dolomite problem’** (Boggs, 2010).

5. Models for early formed Dolomite

Various models have been created to explain the formation of early dolomites. some of them are –

- The Hypersaline (Sabkha, Evaporation, Reflux) model
- The Mixing zone (Mixed water) model
- The Seawater (shallow subtidal) model
- The Subsurface (Burial) model

5.1. The Hypersaline Model

Modern or Holocene dolomites are found in hypersaline environments like the Coorong coastal plain on the south eastern coast of Australia, the sabkhas (coastal plains characterized by the presence of evaporites) of the Persian Gulf and the supratidal zones of arid climates.

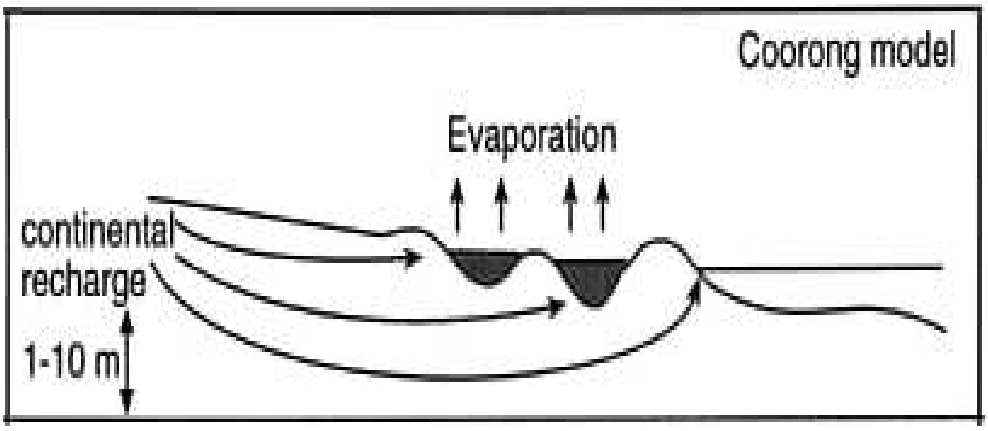

Figure 9: Coorong Model of Dolomitization

5.1.1. Dolomitization process on Coorong coastal plain

During summer season in arid region, the pH in the lakes ranges from 8 to 10 and Mg-Ca ratio in the lake water varies from 1 to 20. Under strongly evaporative conditions, where rates of evaporation exceed rates of precipitation, seawater beneath the sediment surface becomes concentrated by evaporation. This concentration process leads to precipitation of aragonite and gypsum, which preferentially removes Ca^{2+} from the water and increases the Mg^{2+}/Ca^{2+} ratio. The Mg^{2+}/Ca^{2+} ratio in normal seawater is about 5:1. When this ratio rises to sufficiently high levels, possibly in excess of 10:1, then remaining fluids act as the dolomitizing agent and dolomite is believed to form. These dolomites are formed by primary precipitation, so the actual mineral is proto-dolomite that has the appropriate chemical composition of dolomite but lacks the distinctive ordered crystal structure. That's why we can't apply this model widely (Prothero &Schwab, 2004) (Figure 9).

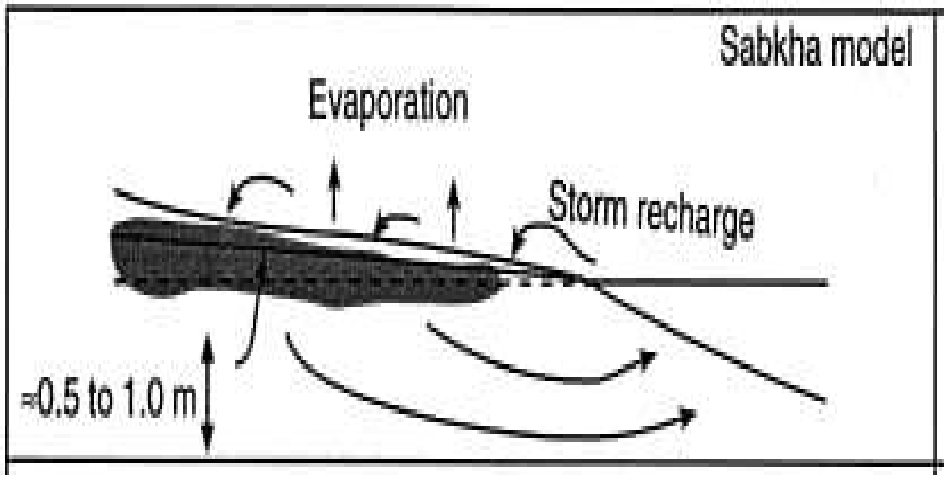

Figure 10: Sabkha Model of Dolomitization

5.1.2. Dolomitization process on Sabkhas

During the long, hot, arid summer season, net evaporation leads to the crystallization of Ca rich evaporite minerals. Brines are concentrated involves evaporation of capillary water in the sediments of Sabkhas. From the saturated groundwater zone, upward flow of water replaces

the water lost by capillary evaporation. This process is called "evaporating pumping". Upward evaporating pumping causes these dolomitizing fluids to react with aragonite mud. The overall volume of dolomite that forms in sabkha environments is believed to be relatively small, and there is still considerable controversy with regard to the exact mechanism by which the dolomite forms. It is not definitely known if it forms by replacement of aragonite or high-magnesian calcite (dolomitization) or if it forms as a primary precipitate of disordered Proto-dolomite, which presumably later develops better ordering to become true dolomite (Prothero &Schwab, 2004) (Figure 10)

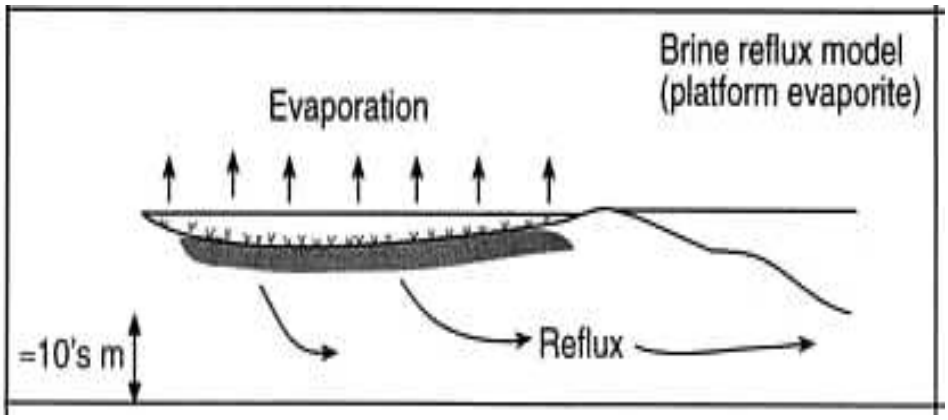

Figure 11: Brine or Seapage reflux Model of Dolomitization

5.1.3. Seapage refluxion

Brines may also be concentrated in surface ponds or bays by surface evaporation of water. These concentrated brines have higher density than normal seawater, causing them to sink downward. Large volumes of Mg-rich brine moving downward through calcium carbonate sediment can favour the dolomitization process that referred to as seapage refluxion. This process requires more time or gradual lateral migration of the evaporite recharge area. The texture and extent of secondary dolomitization are controlled by the porosity and permeability of the carbonate sediment (Sam Boggs, Jr.; fourth edition) (Figure 11).

5.2. The Mixing zone Model

Several studies published since the early 1970s (e.g., Hanshaw, Back, and Deike, 1971; Badiozamani, 1973; Folk and Land, 1975) have suggested that brackish ground waters produced by mixing of seawater with meteoric water could be saturated with respect to dolomite at Mg^{2+} /Ca^{2+} ratios much lower than those required under hypersaline conditions. Mixing of fresh water and saline water in environments such as the subsurface zones of coastal areas where meteoric waters come in contact with seawater is suggested to lower salinities sufficiently so that dolomites can form at Mg^{2+}/Ca^{2+} ratios ranging from normal seawater values of about 5:1 to as low as 1:1. Presumably, dolomite can form at lower Mg^{2+} /Ca^{2+} ratios in these mixed waters compared to seawater because of less competition by other ions in the less saline water (Sam Boggs, Jr.; fourth edition).

The mixing-zone model, or variations thereof, has been referred to also as the Dorag model (Badiozamani, 1973) and the Schizohaline model (Folk and Land, 1975) (Figure 12).

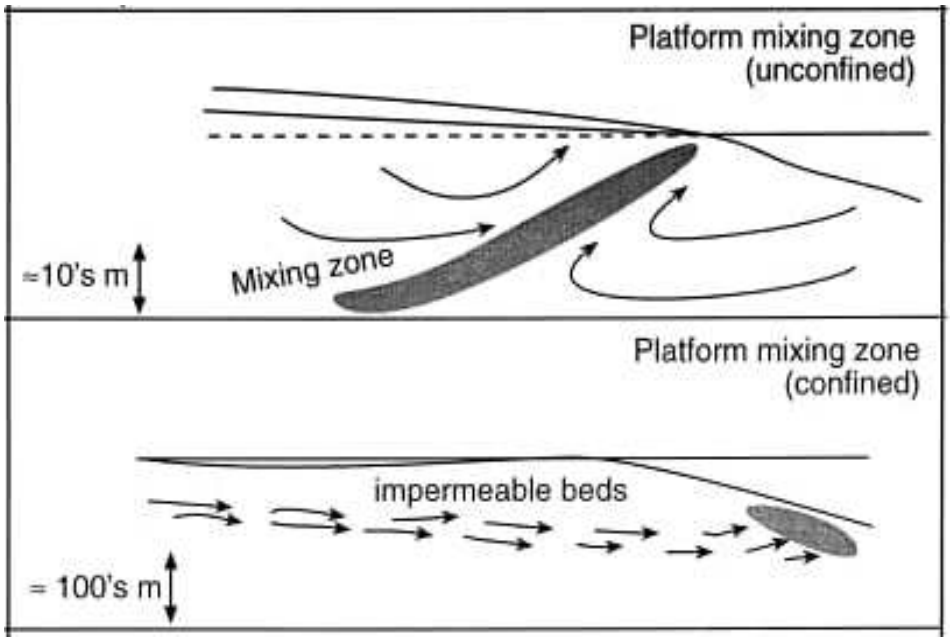

Figure 12: Mixing zone Models of Dolomitization

5.3. The Seawater (Shallow Subtidal) Model

Land (1985) suggested that, if there is an efficient Tidal pump mechanism to move large volumes of seawater through carbonate mud sediments, then dolomite may precipitate as a marine cement directly from pores filled with completely unmodified seawater. Sediments with suitable permeabilities to allow the focused flushing of large volumes of seawater. Thus, each pore volume of water in sediment is constantly being renewed with new seawater. By this mechanism, large quantities of new Mg^{2+} ions are imported into the marine sediment with replaced Ca^{2+} ions. Under these conditions, dolomite is forming (Figure 13).

Mazzullo et al. (1995) referred to dolomite precipitated from seawater as "Subtidal dolomite". Holocene subtidal dolomite forming from unmodified seawater, where dolomite precipitates in modern shallow water deposits and in underlying Pliocene-Pleistocene rocks bathed in normal seawater. Sub tidal dolomite may also have precipitated in cool-water shelf deposits (John Warren, Earth Science Reviews 52, 2000).

According to Lumsden (1988), small volumes of micritic dolomite also takes place in cool marine pore waters within recent deep-water sediments. Such dolomite is interpreted as a direct precipitate from normal seawater and makes up 1% of deep-water marine carbonate worldwide. Mullins et al. (1988) reported the formation of early authigenic dolomite in the Neogene Florida Bahamas platform from marine pore waters where temperature are as low as 1.8°c – 9.8°c. However, in present seawater such above mentioned systems appeared to be precipitating no more than small volumes of dolomite.

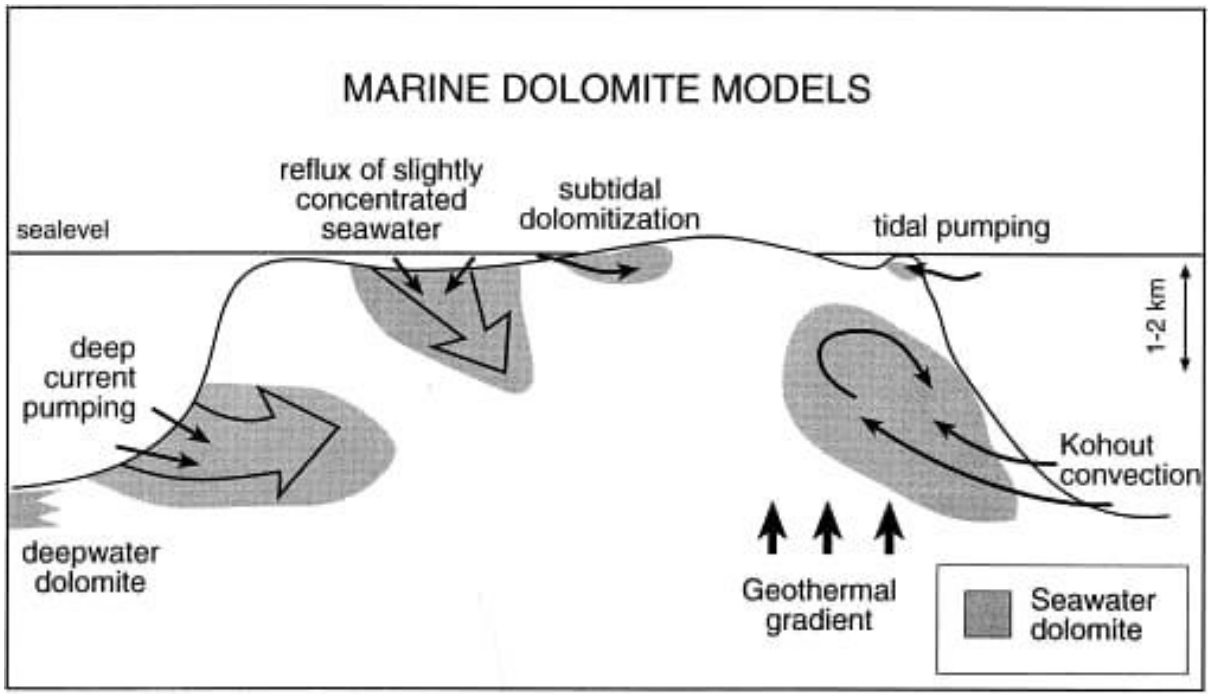

Figure 13: Various models of marine dolomite formation in which Dolomitizing fluid is unmodified seawater that is pumped through porous limestone.

5.4. The Subsurface (Burial) Model

Burial dolomites are subsurface cements and replacements that form below the active phreatic zone (reflux and mixing zones) in permeable intervals flushed by warm to hot Mg-rich basinal and hydrothermal waters. Burial dolomitization occurs readily in buried limestone that has sufficient porosity and permeability to allow circulation of large volumes of Mg-bearing fluids. When buried Mg-rich mudrock is compacted and dewatered at high temperature (above 60°c to 70°c) in the subsurface, then Mg-rich fluids invade and dolomitized the adjacent limestone (Sam Boggs, Jr.; fourth edition).

Burial dolomitization have been divided by Heydari(1997) into three hydrologic realms:

- Passive margin burial diagenesis
- Collision margin burial diagenesis
- Post orogenic burial diagenesis

5.4.1. Passive margin burial diagenesis is characterised by extensional tectonics, growth faulting, relatively slow and steady subsidence. The Gulf of Mexico and Atlantic margin basin during Mesozoic are examples of this realm (Figure 14).

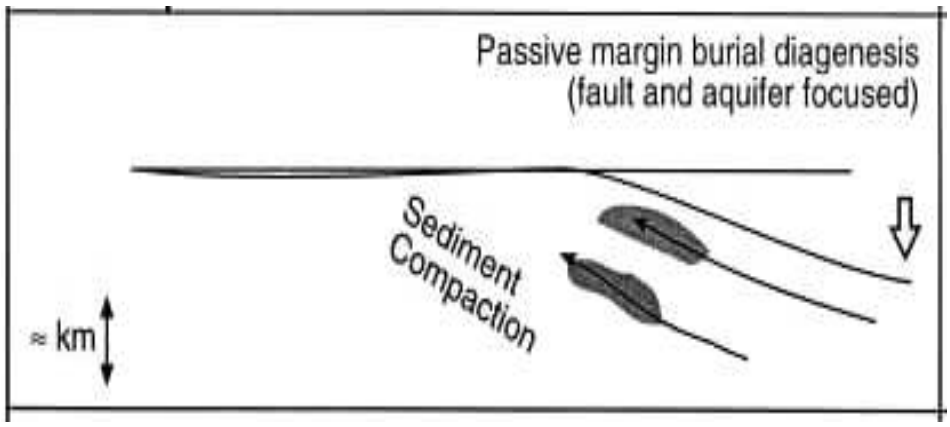

Figure 14: Passive margin burial diagenesis

5.4.2. Collisional margin burial diagenesis is characterised by compressional tectonics, thrust faulting, extensive fracturing of carbonate strata and episodic fluid flow in response to tectonic loading. The Appalachian-Ouachita collision belt is typical example of this realm (Figure 15).

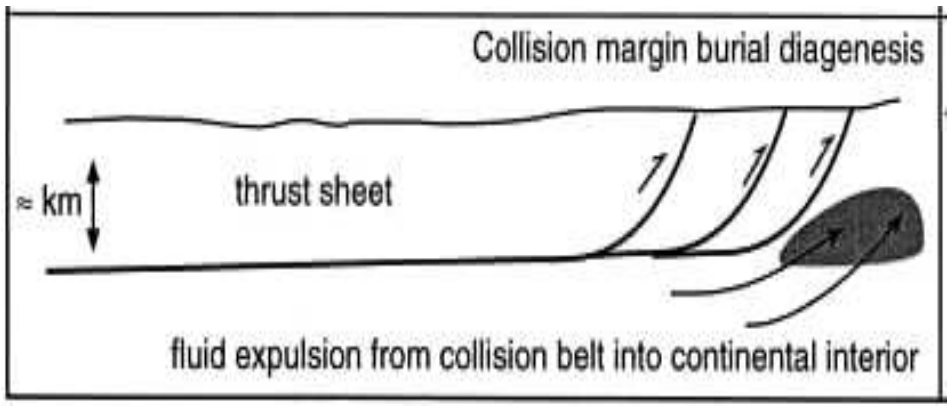

Figure 15: Collision margin burial diagenesis

5.4.3. Post orogenic burial diagenesis is characterised by a lack of tectonic activity, dominance of topographically driven flow and high fluid flow rates ranging from 100-3000 cm/yr. this hydrologic style is thought to exemplify the late-stage dolomites of the US mid-continent (John Warren, Earth Science Reviews 52, 2000) (Figure 16).

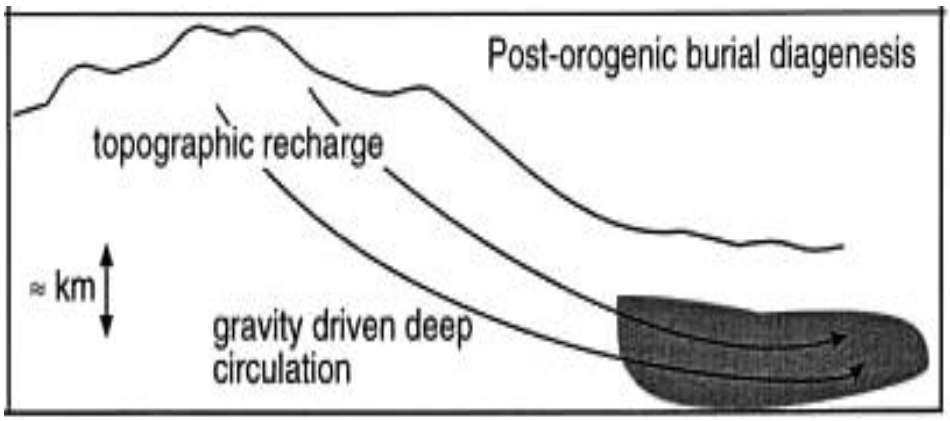

Figure 16: Post-orogenic burial diagenesis

6. Conclusion

Considering all the evidence, there seems to be no escape from the conclusion that the great majority of the stratified dolomites have had their inception on the alteration of limestones. It will not be denied that some dolomitic formations of minor importance have had a different origin. The possibility of direct chemical precipitation of dolomite from the sea by the simple addition of Mg, has not been wholly disproven. Dolomite also forms as a result of evaporation and burial of magnesium containing water upon reaction with limestone. Some impure dolomitic limestones of minor importance may represent original clastic deposits.
So, origin of dolomite is a very complex process. A considerable measure of work and research is anticipating to determine the origin of dolomite.

ACKNOWLEDGMENT

We would like to express special thanks and gratitude to our mentor Asima Kar, Department of Geology, Jogamaya Devi College, who guided and encouraged us throughout this article.

REFERENCES

[1] Boggs, S. Jr., 2005, Principles of Sedimentology and Stratigraphy, 4th Ed., Prentice Hall, New Jersey.
[2] Tucker, M. E., 2001, Sedimentary Petrology – An introduction to the origin of sedimentary rocks, Blackwell, Oxford.
[3] Prothero & Schwab, 2004, Sedimentary Geology — an introduction to sedimentary rocks and stratigraphy, 3rd Edn., W. H. Freeman and Company, New York.

Weblinks (Accessed on 14.02.2022)

[1] https://www.hindawi.com/journals/jchem/2016/7328326/
[2] https://geology.com/minerals/dolomite.shtml
[3] https://www.sciencedaily.com/releases/2012/06/120607105815.htm
[4] https://medcraveonline.com/IJH/dolomite-and-dolomitization-model--a-short-review.html
[5] http://northerndolomite.com/site/index.php?cat=6
[6] https://india.tradeford.com/in761371/dolomite-ore_p1023194.html
[7] https://en.m.wikipedia.org/wiki/Dolomite_(rock)
[8] https://www.online-edelstein.de/en/Minerals/dolomite-specimen-52-mm-sky-blue-moshi-kilimandjaro-tanzania.html
[9] https://elements.envato.com/unpolished-pink-dolomite-rock-isolated-on-white-EMTM23B
[10] http://krishnaminers.com/.
[11] https://www.saltworkconsultants.com/downloads/Dolomite_Warren_2000.

Acid Mine Drainage

Dipannita Das[1], Sreya Sahoo[2], Suravi Mondal[3]
Student of 4th Semester Geology Honours Course
[1]dasdipannita0028@gmail.com, [2]gr8sreyasahoo@gmail.com, [3]mail2suravimondal@gmail.com

Abstract: Acid Mine Drainage deals as one of the major pollutants of the water and as well as a major Biogeochemical problem in many countries that have historic or current mining activity. It is the prevalence of the mining waste water which is highly acidic in nature basically rich in heavy metals (iron sulphides). This heavy metal reacts with the atmospheric oxygen, moisture and acidophilic iron-oxidizing bacteria, resulting as sulfuric acid, dissolved iron and precipitation of ferric hydroxide. There are so many Primary, Secondary, and other sources to produce the Acid Mine Drainage. Acid Mine Drainage effects various aquatic ecosystem by increasing the amount of net acidity and depleting the amount of oxygen in the water bodies which is unsuitable for marine aquatic life. The toxic heavy metals or contaminants in soil and water disbalance the food chain. Conventional technologies use for the treatment of AMD include various physiochemical methods, which involve excessive use of chemical and methods, which limestone Channel designed in abatement of AMD by facilitating reduction of metals, sulphates which generates the alkalinity. Biological treatment has emerged as efficient and eco-friendly. Sulphate Reducing Bioreactor method is used by the involve of microbes as bacteria and fungi. Thus, Biotechnological approaches can prove an asset in developing techniques that can treat the AMD water in an eco-friendly way.

Keywords: Weathering process, Yellow-boy, Open limestone channel, Aerobic and anaerobic wetlands, Sulphate reducing bacteria.

1. Introduction

Acid drainage problem is associated with the mining. It is an anthropogenic point source of pollution that affects many mines impacted ecosystems around the world both aquatic and terrestrial. The contaminants released by mining activities can help lasting effects on downstream aquatic environment if not properly managed. Acid mine drainage refers to metal reach sulphuric acid solutions released from mine tunnels, open piles and waste rock piles. Similar solutions are produced by the drainage of some coastal wetland resulting in the formation of acid sulphate soils. It is a worldwide problem, which leads ecological destruction in water sheds and the contamination of human water sources by sulphur dioxide and heavy metals like arsenic, copper, lead etc.

Acid Mine Drainage or Acid Rock drainage (Figure 1) is the outflow of acidic water which has a very acidic flow after being in contact of sulphur air and metal. Simply we can say that AMD is a natural of contaminated runoff formed by a chemical reach between air, water and rocks containing sulphur bearing minerals like pyrite. Acid mine drainage typically Heels pH values ranging from 2 to 4 however extreme size such as iron mountain in California have produced pH values as low as 3.6. Acid Rock drainage occurs when sulphide ores are exposed to the atmosphere which can be enhanced through milling processes where oxidation reaction are initiated.

Figure 1: Acid mine drainage (USGS 2019)

It also occurs naturally by Rock weathering processes. It exacerbated why large-scale earth disturbances characteristics of mining and other large construction activities. Metal rich drainage can also occur in mineralized areas that have not been mined. Neutral to alkaline mine drainage is also common in areas where the surrounding geologic units contain carbonate rocks to buffer acidity. Metals that were once part of the host Rock are solubilized and exacerbate the deleterious effect of low PH on terrestrial and aquatic receptions. Concentration of common element such as Cu, Zn, Al, Fe and Mn all dramatically increases in in nature with low pH. Metals that were once part of the host Rock are solubilized and exacerbate the deleterious effect of low pH on terrestrial and aquatic receptions. Since large masses of sulphide minerals are exposed quickly during the mining and milling processes the surrounding environment can often not attenuated the resulting low pH condition. The increased soil excavation of mining activities for other accelerates AMD formation. Conventional technologies for treatment of AMD include various physical chemical methods which involves excessive use of chemical and capital.

Acid mine drainage (Figure 1) has been identified as the largest environment liveability facing the Canadian Mining industry and is estimated at $2 to $5 billion dollars. In response to the challenge presented by integration of AMD. Technology and Technical descriptions in this article have been kept simple so as the provide a review that can be used by a wide audience.

2. Sources of acid-mine drainage

There are many to sources of AMD. They are primary sources and secondary sources.

2.1. Primary Sources: During exploration, operation, and closure of mine from the mines' –

- **Dewatering system:** Mine dewatering is the action of removing groundwater from a mine. When a mine extends below the water table groundwater will, due to gravity, infiltrate the mine workings.

- **Tailing disposal:** The predominant method of tailings disposal is by pumping and sub-aerial deposition of an aqueous slurry (typically at 30–45% initial solids concentration by mass and an initial gravimetric moisture content, w, of 233–122%) to a surface TSF. The tailings may be discharged from a single pipe outlet or from a number of reduced diameter spigots off the main perimeter pipeline.
- **Waste heap:** It accumulated mass of solid materials exploited in the course of exploitation of, or together with, mineral raw materials and separated therefrom by physical methods.

2.2. Secondary sources: Effluents coming out from (a) Treatment sludge pounds, (b) rock cuts, (c) stockpiles, (d) concentrated spins along roads and (e) emergency ponds.

2.3. Other Sources: Mining of (a) gold, (b) silver, (c) copper, (d) iron, (e) zinc, (f) lead and (g) coal.

3. Chemistry of acid mine drainage

Whenever any surface mining activities expose the ore bodies to an oxidising environment, the constituent minerals being not in equilibrium with the oxidising environment initiates a complex series of chemical weathering reactions spontaneously. The rate of these reactions is much greater than the natural weathering processes and this accelerated rate of reaction contributes in release of more amount of damaging quantities of acids, metals etc. into the environment.

3.1 Factors controlling the rate of acid generation

A. pH
B. Temperature
C. Oxygen content of the gas phase, if saturation is less than 100%
D. Oxygen concentration in the water phase
E. Degree of saturation with water
F. Chemical activity of Fe^{3+}
G. Surface area of exposed metal sulphide
H. Chemical activation energy required to initiate acid generation
I. Bacterial activity
J. Other factors include waste rock dump permeability. Dumps with high permeability have high oxygen access which contributes to the higher chemical reaction rate.

Acid mine drainage results from the oxidation of sulphide minerals which are present in the ore bodies and the surrounding rocks. The various iron sulphide minerals which mostly contribute to the AMD formation are such as pyrite (FeS_2), chalcopyrite (FeS.CuS) and pyrrhotine (FeS).
Oxygen (from air or dissolved oxygen) and water (as vapour or liquid) when come in contact with the sulphide minerals react with them and cause the chemical oxidation reactions and thus produces sulfuric acid.

Overall chemical reactions associated with pyrite are as follows:

Reaction 1: Pyrite is initially oxidized by atmospheric oxygen in the presence of water and produces ferrous iron (Fe^{+2}), sulphate and hydrogen ions(acidity).

$$2FeS_2 + 7O_2 + 2H_2O \rightarrow 4Fe^{2+} + 4SO_4 + 4H^+$$

Reaction 2: It is the rate determining step. Here the ferrous iron gets oxidized and converts into ferric iron.

$$4Fe^{2+} + 7O_2 + 2H_2O \rightarrow 4Fe^{3+} + 2H_2O$$

Thiobacillus ferrooxidans acts as a catalyst in this reaction which may accelerate the oxidation of ferrous iron into ferric iron by a factor of 106:1. Reaction rates are strongly increased by microbial activity (e.g., *Acidithiobacillus* sp. or *Leptospirillum* sp.)

Reaction 3: In this step, hydrolysis of Fe (III) takes place with the release of additional acidity. Also, solid iron (III) hydroxide (ferrihydrite) precipitates, if the Ph level becomes greater than 3.5 (Ph > 3.5).

$$2Fe^{3+} + 12H_2O \rightarrow 4Fe\,(OH)_3 + 12H^+$$

Yellow boy: If the Ph level of the acid mine drainage raises above 3, either due to its contact with freshwater or neutralizing minerals, the iron (III) ions which was previously soluble gets precipitated out as iron (III) hydroxide. It is a yellow – orange solid colloquially known as yellow boy.

Reaction 4: It is a cyclic and a self – propagating step. Here all the additional pyrite (from steps 1 and 2) are oxidised by Fe (III) ions. Iron is the oxidizing agent here and not the oxygen.

$$FeS_2 + 14Fe^{3+} + 8H_2O \rightarrow 15Fe^{2+} + 2SO_4^{2-} + 16H^+$$

Overall reaction:

$$4FeS_2 + 15O_2 + 14H_2O \rightarrow 4Fe\,(OH)_3 + 8H_2SO_4$$

The sulphuric acid produced in these reactions increases the solubility of other sulphide minerals in the solid surfaces. Ferric iron in the acid solution also oxidises the metal sulphides. The reaction is as follows –

$$MS + 2Fe^{+3} \rightarrow M^{+2} + S + 2Fe^{+2}$$

Here MS = metal sulphide (galena, sphalerite, etc.)

Aluminium, copper, lead, zinc, manganese, nickel are common metals which are found in AMD. AMD may also leach uranium, thorium and radium from mine wastes and tailings associated with uranium mining operations. Metals which are in the form of carbonates, silicates, and oxides often get mobilised aided by biological catalysts.

3.2 Factors controlling the quality of acid mine drainage

Acid mine drainage (AMD) has been a detrimental by-product of coal mining for many years. The formation of acid drainage is a complex geochemical and microbially mediated process. The acid load ultimately generated from a mine site is primarily a function of the following factors:

3.2.1. Microbiological controls

The conversion of ferrous iron to ferric iron is largely catalysed by the presence of a bacterial species known as Thiobacillus ferroxidans. This is because the bacteria can oxidize the hydrogen sulphide being produced during acid dissolution of sulphide minerals producing sulfuric acid and thus increases the rate of sulphide mineral dissolution. These bacteria and several other species which are involved in the pyrite weathering are widespread in the environment and increase the conversion rate by a factor of hundreds to as much as one million times. The bacterial activity is Ph dependent and they become more active with optimal conditions and Ph range between 2–3. AMD environments are acidic environments that contain various types of metals such as Zn, Al, Cd, Cu, Mn and As due to increased solubility of minerals and a range of pH, thus the microbial community may be diverse, having specific gene expression pathways and adaptations that the micro-organisms use for their survival. Many microbes live under a range of conditions such as chemolithoautotrophic, chemomixotrophic, or chemoheterotrophic and can oxidize iron sulphide minerals. These organisms may also have some capability for metal resistance.

3.2.2. Depositional environment

Paleoenvironments under which coal bearing rocks formed can be classified as freshwater, brackish and marine. Rocks formed in brackish water conditions are generally most prone to acid production. Paleoenvironment is a controlling factor in the inherent distribution of pyrites and carbonates.

3.2.3. Acid /Base balance and reaction rates

The quality of acid mine drainage depends on two competing processes, i.e., acid formation from pyrite oxidation and production of alkalinity due to dissolution of carbonates and basic minerals.

The rate of reaction can be slow or enhanced depending on the mass balance between minerals producing acid and alkali. Thus, the relation between the acidic and basic minerals and the resultant drainage quality is as follows –

- In the presence of low pyrite and low base content, the drainage may contain low levels of acids, or maybe non-acid. It may also contain low concentrations of dissolved metals.
- In the presence of low pyrite and high base content, the drainage is alkaline with low concentrations of dissolved metals.
- In the presence of high pyrite and low base content, the drainage is acidic with high concentrations of dissolved metals.
- In the presence of high pyrite and high base content, the drainage is usually alkaline, occasionally acid, with high concentrations of dissolved metals.
- The conditions that mostly contribute to acid formation are presence of high level of pyrite contents with little base material.

3.2.4. Lithological controls

The physical properties of a rock, such as porosity, and presence of accessory minerals also effects the overall chemical weathering process. For example- pyrite sandstones release its acid

load rapidly but argillaceous rocks take longer time to release the acid. Also clays and other silicate minerals present as accessory minerals may dissolve, lead to formation of new minerals, or attenuate the acid and alkaline weathering products.

3.2.5. Mineralogical controls

Pyrite occurs in several different morphological forms and has a large range of grain sizes (from microscopic to several inches). Framboids and other fine-grained pyrites have a large surface area and therefore are much more chemically reactive than the coarse-grained pyrites. This fact reflects that the chemical reactions occur at the surface of the mineral.

3.2.6. Minesite hydrological conditions

Hydrology of the mining area is an important factor for determining the quality of acid mine drainage. In the absence of percolating waters, the acid salts that are produced from the limited available moisture may reside within the spoil, but in the presence of excess moisture, the acid weathering products get dissolved and transported with the water moving through the material. The ground-water discharge chemistry varies depending on two factors –

- Degree of flushing and time since the last precipitation event.
- The water table position within the spoil also effects the acid mine drainage quality.

Thus, various biological, chemical and physical factors interact to control and even influences the quality of acid mine drainage.

4. Effects of acid mine drainage

4.1. Chemical impacts of AMD

AMD adversely effects various aquatic ecosystems such as river and stream ecosystems by increasing acidity and depleting the amount of oxygen in the water bodies. It increases the biochemical oxygen demand (BOD) and chemical oxygen demand (COD) due to the input of large amount of pollutants in the water body. The greater these values are, the more rapidly the oxygen is being depleted in the water body. This means that less amount of oxygen is available to the aquatic plants and animals. Reduction in Ph due to increasing acidity also results in destruction of the bicarbonate buffering system.

It also increases the rate of weathering of minerals due to which various toxic elements and heavy metals such as Al^{+3}, Fe^{+3}, Mn^{+2}, Zn^{+2} etc. get released into the stream. It thus results in the increase in concentration of soluble metals and particulate metals in the water body. Also, at low pH levels, heavy metal release from soil colloids increases. Due to precipitation of Fe $(OH)_3$, a bright orange colour of water and rocks appears.

4.2. Physical impacts of AMD

It increases sedimentation which leads to more adsorption of metals onto the sediment and reduces the turbulence and increases the laminar flow. It also increases the turbidity which leads to reduction in photosynthesis due to decrease in light penetration.

4.3. Biological impacts of AMD

AMD reduces the Ph level and oxygen content of the water bodies due to which the water in these rivers and streams become unsuitable for sustaining the aquatic life. AMD also leads to clogging of interstitial pore space in coarse aquatic substrate habitat due to more sedimentation and thus results in substrate modification. It also reduces the primary productivity and thus harms various biological resources and becomes a cause of death and elimination of various aquatic plants. It also leads to change in channel hydraulics.

Moreover, it also increases the stress on other biota or organisms which are dependent or associated with aquatic habitats. These organisms become more prone to various health disorders such as respiratory, behavioural and reproduction related problems. It creates a disbalance of osmoregulation and an acid – base failure in these organisms. It also makes them more susceptible to acute and chronic toxicity leading to death of some sensitive species.

4.4. Ecological impacts of AMD

It has various ecological impacts such as it results in habitat modification and niche loss for various organisms. They face loss of food source or prey and various species are eliminated due to lack of food.

It also leads to bioconcentration and bioaccumulation i.e., the toxic heavy metals or contaminants in soil and water enters the food web and gradually gets accumulated in the body of the organisms (plants, fish, livestock, and humans through the process of eating and being eaten). These toxic elements pass from one trophic level to another within a food web and thereby their concentration increases gradually in the higher level of organisms, leading to various heath disorders and abnormalities in these organisms. These leads to food chain modification which adversely effects our ecosystem.

4.5. Impact on fishes

When fishes directly get exposed to metals and H+ ions through their gills, they become prone to impaired respiration due to chronic and acute toxicity from the metals. Through ingestion of contaminated sediments and food items, fishes may also get exposed to metals indirectly. A common weathering product of sulphide oxidation is the formation of iron hydroxide Fe $(OH)_3$ precipitate, found in streams that are affected by AMD. Iron hydroxides and oxyhydroxides may physically coat the surface of stream sediments and streambeds destroying the aquatic habitat, diminishing the availability of clean gravels used for spawning, and reducing the food items for the fishes such as benthic macroinvertebrates. The waters that are affected by AMD may have a low pH as 2.0 to 4.5, levels which are harmful and toxic to most forms of aquatic life such as fishes as low pH conditions alter gill membranes or change gill mucus resulting in death of the fishes due to hypoxia. It may also lead to the impairment of hemeostatic electrolyte and osmotic mechanisms.

4.6. Impacts on human resources

It corrodes pipes, pumps, bridges, etc. Also, it degrades the drinking water supplies and makes it unfit for human consumption. It also does harm to the fisheries.

5. Remedies of Acid Mine Drainage

5.1. Chemical Treatment

Calcium Oxide - It is mainly used for many of the metals present in the solution to precipitate as hydroxide and carbonates. It is alkaline in nature so that when it is added with the acid mine drainage water the pH level of the water is increased. It has the lowest material cost and is the safest and easiest way to handle.

Anhydrous Ammonia -The Anhydrous Ammonia is used to raise the pH level of the water quickly. It should be injected into flowing water at the entrance of the pond to ensure good mixture as ammonia is lighter than the water. The ammonia is extremely soluble and reacts rapidly at gaseous state. It behaves like a strong base and can easily raise the pH level of the receiving water.

Figure 2: Aerobic constructed wetlands (WESA 2016)

5.2. Passive Treatment /Biological Treatment

5.2.1 Constructed Wetlands: There are so many functions in Acid Mine Drainage like to remove or dissolved heavy metals is done by the wetland plants. There are different types of wetlands. They are as follows –

- **Aerobic Wetlands –** Aerobic wetlands are mainly constructed for the treatment Mine waters which are net alkaline in nature. If there is insufficient alkalinity in the mine water to prevent a significant fall in pH as a result of these reactions. The oxidation of ferrous iron and hydrolysis of the ferric iron are subsequently the main remediative reaction that occurs within them, which is a net acid generating reaction.

$$4Fe^{2+} + O_2 + 4H^+ \rightarrow 4Fe^{3+} + 2H_2O \qquad \text{(i)}$$

Aerobic wetlands are relatively shallow systems that operate flow to control the oxidizing conditions (Figure 2).

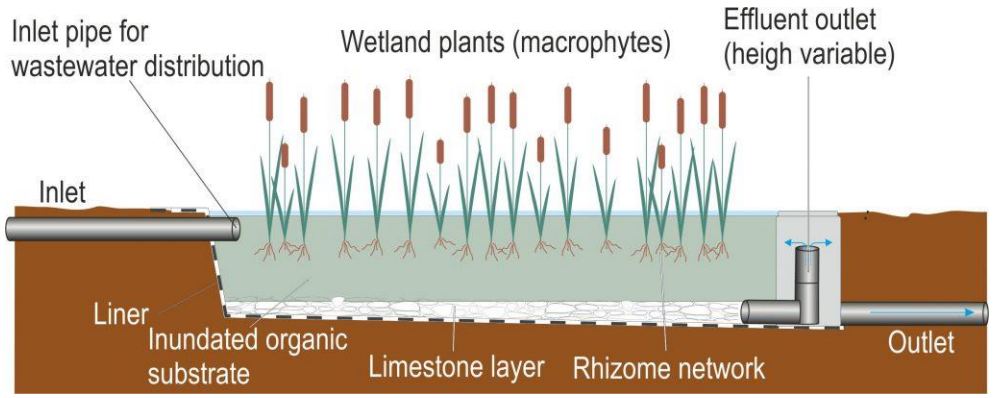

Figure 3: Schematic diagram of anaerobic wetlands

- **Anaerobic Wetlands -** Anaerobic wetlands are mainly used to improve the water quality in the wetlands by the filtration process of suspended and colloidal materials by an adsorption of metals to the soil substrate or other organic based substrates (Figure 3).

Metal-Laden waters and net acidic waters are treated by anaerobic wetlands. They can be used only if a large enough area of land is available. A limestone layer overlain by an organic compost layer are the main constituent of Anaerobic Wetlands, filtration process of suspended and colloidal materials.

For the construction of the wetlands are efficient when the effluent is low in its acidity loading, but often show reduced efficiency and even fail under high acid loading.

5.2.2 Treatment of Acid Mine Drainage using the construction of wetlands

Treatment of Acid Mine Drainage is challenge because of its persistent nature. Traditional treatment methods based to neutralize with alkalinity reagents are not ideal because they require a substantial investment of resources and a continual oversight. In Recent time, construction of wetlands has been proposed as a long-term treatment. Over 1000 wetlands have been constructed in the eastern United States for the treatment of Coal Mine Drainage. To construct wet and AMD consist of a series of clay-lined cells layered with limestone and organic substrate (compact wetland). The actual purpose of this scheme to diffuse the alkalinity from underlying layers and often are not adequate to full neutralize acidity.

Many types of organic substrates like mushroom compost, manure compost, hay mixtures and decomposed wood these products have been incorporated into the wetlands construct for AMD treatment to stimulate the mainly sulphate-reducing bacteria. In addition to SRB bacteria like *Clostridium sp.* and *Acidiphilium sp.* plays a vital role in wetlands sediment.

The highly demand in constructing wetlands to focus on design criteria or measurements to treat efficient through influent and effluent monitoring. Therefore, the main theme of this

wetland to characterized the sediment column for the treatment of AMD. So, there are some objectives of this treatment –

The first objective of this wetland is to determine the minerology of Ochre precipitation and also to determine the rates of mineral transformation in the sediment column of Carbondale wetlands minerals like hydrosulphate like ferrihydrite [$HFe_5O_8H_2O$] and Schewertmanite [$Fe_8O_8(OH)_6SO_4$] are efficient sorbents of the contamination of trace metals and oxyanions and effectively remove them from solution and the second objective is to evaluate the effects of the seasonal changes in pore water chemistry and mineral formation transformation process on the distribution of metals with depth in the sedimentary column.

And lastly, is to profile bacterial community composition in the Carbondale sediment column in relation to basic pore water chemistry. As wetlands are designated as well as provide an environment for the development of beneficial microbial communities.

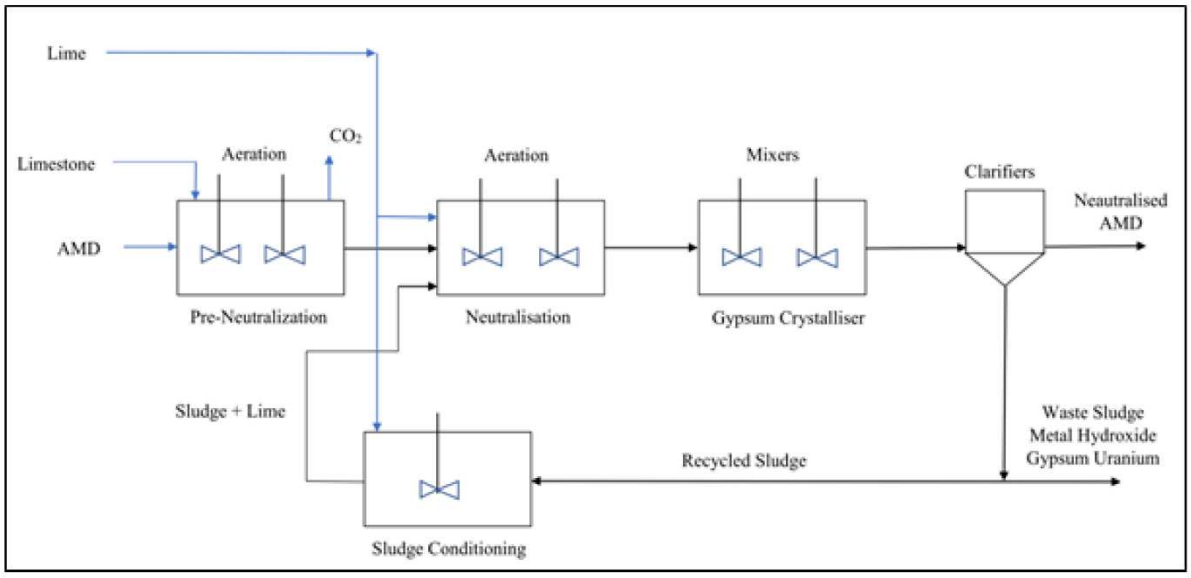

Figure 4: Reclamation of the water and synthesis of gypsum and limestone by open limestone channel. (Thaisani et al. 2021)

5.2.3 Open Limestone Channel

To increase the alkalinity of the water with the limestones open limestone channel are consistently used as the long channels or ditches (Figure 4). Acid mine drainage is treated by limestone dissolution where the acid water flows by the limestone bed. Open Limestone Channel is determined by the flow rate, influent acidity concentration, channel slop and this information will dictate the weight of limestone, the cross-sectional area and length of the channel. The quantity of time that the limestone is with the contact of Acid Mine Drainage water is main and is a property of influent acidity and flow. The ideal limestone size is 15-30 cm in diameter. One of the primary design factors is to have a steep enough slope and too large that the limestone particle size to prevent iron, aluminium hydroxides from plugging up limestone pores.

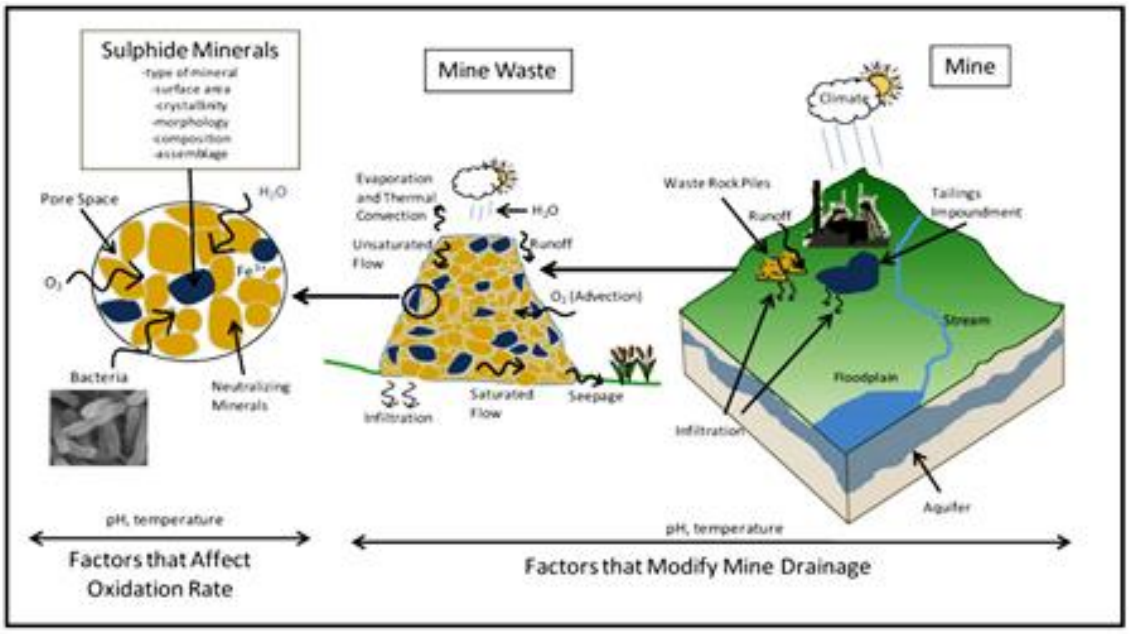

Figure 5: Soil Cover system design for mine waste (Hatari 2017)

5.2.4 Soil Covers

Soil covers are mainly consumed for granular earthen materials placed over mine wastes. The objective matters of a soil cover are variable (Figure 5). It includes –

i. Dust and erosion control.

ii. Chemical stabilization of oxygen.

iii. Contaminant release control through improved quality of runoff water and control of infiltration.

iv. Provision of a growth medium for the establishment of sustainable vegetation.

5.3.1 Sulphate Reducing Bacteria (SRB)

The actual purpose of using SRB in AMD treatment is to produce sulphides reduction for metal sulphide precipitation while generating Alkalinity. The chemical employ of SRB remediation mainly associates with microbially mediated sulphur reduction with organic matter oxidation. It also involves the chemical reduction of metal (Me) (Figure 6).

There are some metals which precipitate as metal sulphide. They are cadmium, copper, iron, lead, mercury, nickel and zinc. Besides this the metal like manganese, iron, nickel, copper, zinc, cadmium, mercury and lead may also removed to some extent by co-precipitation with the reaction of other metal sulphide. Again, SRB species have been found that can reduce some metals in a more insoluble form, such as the Uranium$^{(VI)}$ reduction to Uranium$^{(IV)}$ reduction. Sulphate reduction consumes the acidity which raises the pH level. This increase of pH level helps to this above reaction of precipitation and also creates competent conditions to this precipitation of this metal hydroxides.

Because oxygen, Nitrate, Manganese and Iron reduction all dedicate more energy per equivalent than sulphate, Anaerobic conditions are required, and the oxidation reduction

potential (ORP) must be less than –200mv to permit SRB to stay and to occur sulphate reduction. In the reduction of iron to ferrous state these redox conditions are also worthy, that will precipitate with sulphide.

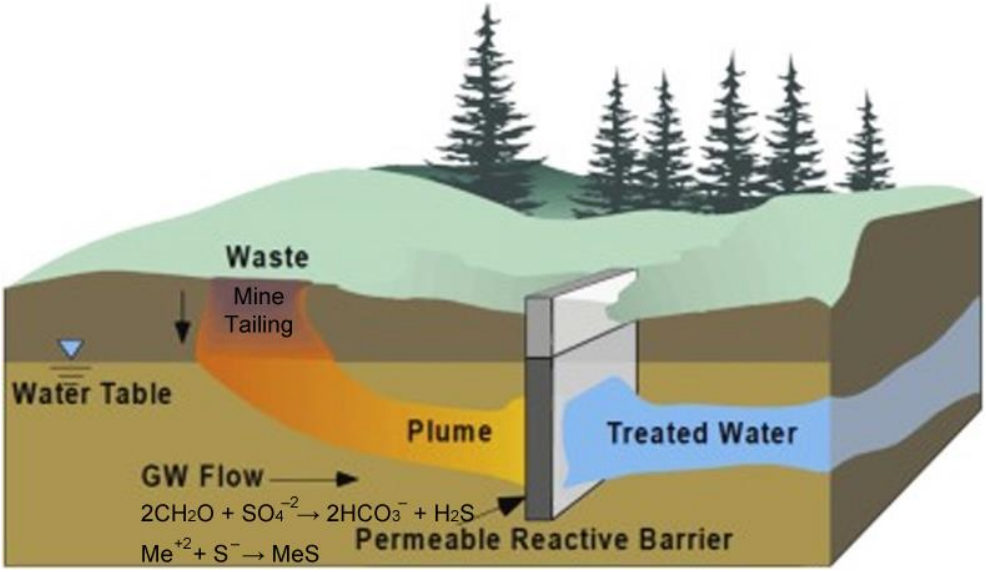

Figure 6: Acid mine drainage remediation (Rad & Fazlali 2020)

5.3.2 Biological Characteristic of SRB

SRB are mainly nominated for anaerobic respiration that uses sulphate as terminal electron acceptor. They are subdivided into the following four taxonomic groups –

1. The S-Proteobacteria subdivision contains gram (–) mesophilic SRB which included the genera *Desulfovibrio*, *Desulfomicrobium*, *Desulfobulleus*, *Desulfobactor*, *Desulfobacterium*, *Desulfococcus*, *Desulfosarcina*, *Desulfomonile*, *Desulfohema*, *Desulfobotulus*, *Desulfoarculus*. All these bacteria have optimum growth temperatures ranging from 20° – 40°C. This group is diverse with varieties of shape and physiological traits represented.
2. The gram (+) spore forming SRB are mainly represented by the genus *Desulfomaculum* and form heat resistant endospores. This species raises in the temperature range to group 1.
3. The bacterial thermophilic SRB group contains. the genera of thermo *Desulfobacterium*, *Desulfovibrio*. These species have optimum growth at 65° – 70°. and inhabit high temperature environments such as geothermal vents.
4. Archael thermophilic SRB growth at temperature above 80°C, have been found only in marine hydrothermal vents. These species SRB belong to the genus Archeoglobus.

Sulphate Reducing Bacteria inhabitant of a variety of sulphate rich in reducing environments. SRB have been found in lacustrine and wetland sediments, cattle rumens and in geothermal vents in a high amount. Their presence is also competent in human-impacted environments such as rich paddies paper mills and streams influenced by AMD. To stimulate bioremediation, an SRB source such as cow manure or organic substrate from one of the environments listed above is generally added to for passive treatment systems.

An anoxic, reducing environment is one habitat requirement to thrive sulphate reducing bacteria. Substrate temperature, pH and AMD chemistry may also impose limits and have been the subject of laboratory and in the field studies.

- **Substrate**: Sulphate reducing bacteria generally made on Simple carbon compounds such as organic acids or alcohols, serve as electron donors for the reduction of sulphate, when the carbon source is used as organic matter, other heterotrophic bacteria must break it down into simple carbon particles. BTech and pilot studies using the intended carbon source and AMD may be treated as critical calculation for determining the sulphate-reduction rates and design efficient full-scale systems.

- **Temperature:** When the temperature is low the activity of the reaction rates of the SRB becomes slow down. SRB functions effectively at 6°C, the lowest temperature tested (Tsukamoto et.al 2004). Cold-adapted species are able to function at temperatures as low as 4°C (Higgins et.al 2003)

- **pH:** To take the benefit for tolerating acid in bacteria they are used to treat acidic drainage. It shows that SRB can thrive through a wide range of pH conditions, but become less active below a certain pH. Acid-tolerating strains of SRB have characterized and isolated and their introduction to AMD treatment systems may improve performance. Furthermore, the precipitation for effective metal a high level of pH may be required.

5.3.3 AMD Chemistry

Whether passive SRB treatment is sufficient for the treatment of a particular AMD stream also depends on its chemistry. Up to a point, higher concentrations to higher metal precipitation rates. Under these conditions, potential metal precipitation can be calculated from sulphate reduction rates and kinetics of reaction. Though, batch studies showed that higher metallic concentration could slow bacterial population growth, decrease sulphate reducing capacity, and ultimately cause death.

Lesson from coal mining: Passive treatment technologies including sulphate reducing bacteria have been used to treat AMD from coal mines for over 20 years. The process which generates AMD are the same for both types of mines, like coal mines, most hard rock mines have potential to generate high acidity, sulphates and metals, particularly iron, manganese and aluminium.

The major categories for passive treatment involving SRB are constructed anaerobic wetlands, SAPS, sulphate reducing bioreactors, permeable reactive barriers and organic (amendments). These treatments of SRB systems or their precursors have been used at coal mine sites.
Therefore, in this way we can know the history of passive treatment at active or abandon coal mine sites.

6.Conclusion

One of the most serious environmental contamination issues connected to mining is the acid mine drainage. Acid mine drainage greatly influences water quality and has environmental impacts. Thus, it is necessary to address this global issue as soon as possible. The discharge of acid mine water causes direct impact on water environment and indirectly on human health. There are several techniques to avoid the generation of acid mine drainage. Each of them is effective for a different situation. Iron-oxidizing bacteria and archaea play a crucial role in AMD production by speeding up the normally slow oxidation reaction, which encourages pyrite disintegration and causes a rapid buildup of ions near the flow channel.Using a system approach a number of new procedures have been developed to successfully characterize, manage and rehabitate AMD generating mine sites and to protect surface and groundwater from environmental damage. The importance of an interactive protocol with their management objective and procedures is vital to successful rehabilitation of such sites and long-term protection of the environment.

ACKNOWLEDGMENTS

We are very thankful to our professor Dr. Kaushik Kiran Ghosh for encouraging us to pursue with this topic.

REFERENCES

[1] Hatari (2017) Soil cover system design for mine waste dumps. Hatari Labs, updated on: March 17, 2017. Available at: https://hatarilabs.com/ih-en/soil-cover-system-design-for-mine-waste-dumps. Accessed on: 07-11-2021.

[2] Higgins, J.P., Hard, B.C. and A. Mattes, 2003. Bioremediation of rock drainage using sulphatereducing bacteria. Proceedings of Sudbury 2003: Mining and Environment, Sudbury, Ontario, May 25-28, 2003.

[3] Rad P.R. and Fazlali A. (2020) Optimization of permeable reactive barrier dimensions and location in groundwater remediation contaminated by landfill pollution. Journal of Water Process Engineering, Vol.35, June 2020, 101196. DOI: 10.1016/j.jwpe.2020.101196.

[4] Thisani S.K., Kallon D.V.V. and Byrne P. (2021) Review of Remediation Solutions for Acid Mine Drainage Using the Modified Hill Framework. Sustainability, 13(15), 8118; DOI: 10.3390/su13158118

[5] Tsukamoto T.K, Killion H.A and Miller G.C (2004) Column experiments for microbiological treatment of acid mine drainage: low-temperature, low-pH and matrix investigations. Water Research, Volume 38, Issue 6, March 2004, Pages 1405-1418.

[6] USGS (2019) Mine Drainage. Water Resources Mission Area. Published on: February 28, 2019, Available at: https://www.usgs.gov/mission-areas/water-resources/science/mine-drainage, Accessed on: 07-11-2021.

[7] WESA (2016) Constructed Wetlands May Be Key To Tackling Acid Mine Drainage (Environment & Energy, 90.5 WESA), Published on July 21, 2016 by Noah Brode, Available at: https://www.wesa.fm/environment-energy/2016-07-21/constructed-wetlands-may-be-key-to-tackling-acid-mine-drainage. Accessed on: 07-11-2021.

Ocean Salinity

Kathashree Kundu[1], Monisha Halder[2] and Ritu Sau[3]
Students of 3rd Semester Geology Honours Course
[1] *kathashreekundu2001@gmail.com*, [2]*monishahalder02@gmail.com*
[3]*ritusaujnv100@gmail.com*

Abstract: Salinity determines many aspects of the chemistry of natural water along with its biological processes. It also governs the physical characteristics like heat capacity and density of water as it has the power of conductivity. Ocean currents have a significant impact on salinity in marginal seas with open sea contact, and it also varies horizontally as well as vertically. In the emergence of ocean currents, variations in ocean salinity becomes a significant factor. Fluctuation in levels of salinity can affect marine organisms which are adapted to prevailing concentrations of salts in oceanic water.

Key Words: Salinity, Salt, Palaeosalinity, Flora, Fauna, Climate.

1. Introduction

Salinity is the saltiness or amount of salt dissolved in a body of water. As we know salt are compounds like sodium chloride, magnesium sulphate, potassium nitrate and sodium bicarbonate, which can be formed by the weathering of rock evaporation of ocean water and formation of sea ice. Salinity is used for determination of the density of sea water and comprises a major effect on the freezing point of sea water, and heat capacity. It is generally expressed in grams per kilogram (g/kg) or parts per thousand.

In the open ocean salinity of surface water is controlled primarily by the balance between evaporation and precipitation. As a result, highest saltiness is found in the so called subtropical central gyre regions centerer at about 20° to 30° North and South. Where evaporation is extensive but rainfall is minimum. The highest surface saltiness is found in Red Sea.

2. Causes

Ocean salinity is mainly caused by rain washing mineral ion from the land into the water. Carbon dioxide in the air dissolve into rain water making it slightly acidic. When rain falls, it weathers rock with releasing minerals, salts that separate into ion.

The ions are carried by run-off and ultimately reach the ocean. Under water Volcanoes, salt domes and thermal vents on the sea-bed can also release salt into the ocean. (Table I, Prothero & Schwab, 2014).

Sodium chloride, make up over 90% all the ions found in the sea water. Around 3.5% of the weight of sea water comes from dissolved salts. The tendency of components to remain in the solution is called as Residence time. It is measured in Years and calculated by dividing total mass of an ion in sea water by its annual flux. Ions having long residence time are not metabolized by organism. The principal condition that favours the inorganic precipitation of

these ions require isolation of sea water settings. The short residence time means the ease with which these ions are either metabolized by organism and incorporated into shells, or extracted inorganically. Ions with medium residence time such as potassium, magnesium must be extracted by slower, more complex process.

Table 1: Relative Abundance of Dissolved Ions in Seawater

	Total Dissolved Solids (%) (Salinity = 35,000 ppm or 3.5%)
Bicarbonate $(HCO_3)^-$ and carbonate $(CO_3)^{2-}$	0.4
Calcium (Ca^{2+})	1.2
Amorphous silica (H_4SiO_4)	<0.01
Sulfate $(SO_4)^{2-}$	7.7
Chlorine (Cl^-)	55.0
Sodium (Na^+)	0.6
Magnesium (Mg^{2+})	3.7
Potassium (K^+)	1.1
Iron $(Fe^{2+}$ and $Fe^{3+})$	<0.01
Aluminum $Al(OH)_4^-$	<0.01
Nitrate $(NO_3)^-$	<0.01
Total	**99.7**

3. Salinity in different Ocean

Horizontal Distribution of Salinity: The Salinity for normal open ocean ranges between 33 to 37.

High Salinity Regions: In the land locked Red Sea, it is as high as 41. In hot and dry regions, where evaporation is high, the salinity somewhere reaches 70.

Comparatively, *low Salinity Regions:* In the estuaries (enclosed mouth of a river where fresh and saline water get mixed) and the Arctic, the salinity fluctuates from 0-35, seasonally (fresh water coming from ice caps).

Pacific Ocean:

- The salinity variation in the Pacific Ocean is mainly due to its shape and large areal extent.

Atlantic Ocean:

- The average salinity of the Atlantic Ocean is around 36–37.
- The equatorial region of the Atlantic Ocean has a salinity about 35.
- Near the equator, there is heavy rainfall, high relative humidity, cloudiness and calm air of the doldrums.
- The Polar areas experience very little evaporation and receive large amounts of fresh water from the melting of ice. This leads to low levels of salinity, ranges between 20 and 32.
- Maximum salinity is observed between 20°N and 30°N and 20°W-60°W. It gradually decreases towards the north.

Indian Ocean

- The average salinity of Indian Ocean is 35.
- The low salinity trend is observed in the Bay of Bengal due to influx of river water by the river Ganga.
- On the contrary, the Arabian sea shows high salinity due to high evaporation and low influx of fresh water.

Marginal Seas

- The North Sea, in spite of its location in higher latitudes, records higher salinity due to more saline water brought by the North Atlantic Drift.
- Baltic sea records low salinity due to influx of river water in large quality.
- The Mediterranean Sea records higher salinity due to high evaporation.
- Salinity is, however very low in Black Sea. Due to influx of enormous fresh water from water from river.

Inlands Seas and Lakes

- The salinity of the inland seas and lakes are very high because of the regular supply of salt by the rivers falling into them.
- Their water becomes progressively more due to evaporation.
- For instance, the salinity of the Great Salt Lake, the Dead Sea and the Lakevan in Turkey is 220, 240 and 330 respectively.

4. Salinity Distribution in Ocean

Surface winds drive currents in the upper Ocean. Deep below the surface, however, ocean circulation is primarily driven by changes in seawater density, which is determined by salinity and temperature. In some regions such as the North Atlantic near Greenland, cooled high- salinity surface waters can become dense enough to sink to great depths. The oceans store more heat in the uppermost 3 meters than the entire atmosphere.

Thus density- controlled circulation is key to transporting heat in the ocean and maintaining Earth's climate. Excess heat associated with the increase in global temperature during the last century is being absorbed and moved by the ocean. In addition, Studies suggest that seawater is becoming fresher in high latitudes and tropical areas dominated by rain, while in sub-tropical high evaporation regions, waters are getting saltier. Such changes in the water cycle could significantly impact not only ocean circulation but also the climate in which we live.

Sea-surface salinity plays an important role in thermohaline ocean circulation. The research team, led by Jacqueline Boutin of LOCEAN[1] and Nicolas Reul of Ifremer[2], have generated the longest and most precise satellite sea-surface salinity global dataset to date. Spanning nine

[1] Laboratoire d'Océanographie et du Climat
[2] Institut Français de Recherche pour l'Exploitation de la Mer

years, the dataset is based on observations from the three satellite missions that measure sea-surface salinity from space: ESA's SMOS[3] and the US SMAP[4] and Aquarius missions.

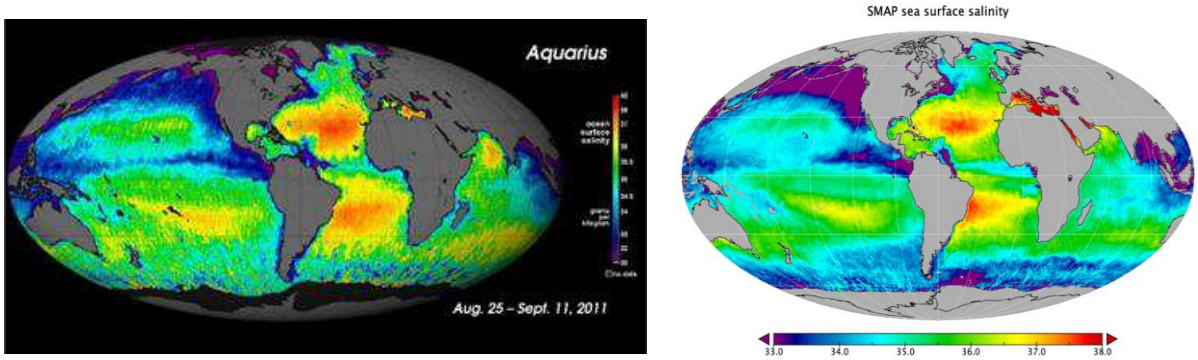

[A] [B]

Figure 1: Salinity distribution in oceans a. August 2011 b. June 2021

Figure 1 is a composite of the first two and a half weeks of data since Aquarius became operational on August 25, 2011. The numerical values represent salt concentration in parts per thousand (grams of salt per kilogram of sea water). Yellow and red colours represent areas of higher salinity, with blues and purples indicating areas of lower salinity. Areas coloured black are gaps in the data. The average salinity on the map is about 35.

The map reveals predominantly well-known ocean salinity features, such as higher salinity in the subtropics, higher average salinity in the Atlantic Ocean compared to the Pacific and Indian Oceans, and lower salinity in rainy belts near the equator, in the northernmost Pacific Ocean and elsewhere. These features are related to large-scale patterns of rainfall and evaporation over the ocean, river outflow and ocean circulation. Other important regional features are clearly evident, including a sharp contrast between the arid, high-salinity Arabian Sea west of the Indian subcontinent, and the low-salinity Bay of Bengal to the east, which is dominated by the Ganges River and south Asia monsoon rains.

5. Change of Salinity through time

It is known that average sea levels have been risen over the past century, and that global warming is to blame. And climate change has an effect on saltiness or salinity of oceans. This is an important question because big shifts in salinity could be warning that more severe droughts and floods are on their way or even that global warming is speeding up.

When the climate was cold, more water was locked up in ice sheets and glaciers — which caused an oscillation of ocean salinity from 34.7‰ to 36‰. Now, new research suggests that the amount of salt in seawater is varying in direct response man - made climate change. Climate change could be responsible for rises in salinity that have been recorded in the sub -

[3] Soil Moisture and Ocean Salinity (SMOS) mission of European Space Agency
[4] Soil Moisture Active Passive, or SMAP, is an Earth satellite mission of US Govt.

tropical regions of the Atlantic Ocean, areas of latitudes immediately north and south of tropics. Three major factors influence salinity (salt concentration) in ocean waters:
Precipitation, evaporation and winds. Precipitation brings freshwater into the ocean, diluting its salt concentration.

Evaporation of ocean water and formation of sea ice both increase the salinity of ocean. However, these "Salinity rising" factors are continually counterbalanced by process that decrease salinity such as the continuous input of fresh water from rivers, precipitation of rain and snow, and melting of ice. The saltiness of ocean is the result of several natural influences and processes, water from rivers entering the ocean is just one of these factors. But over time, as rain felt to the earth and ran over the land breaking up rocks and transporting their minerals to the ocean, the oceans become saltier.

6. Palaeosalinity

Palaeosalinity can be determined from oxygen isotope data of foraminifera reflect the geochemistry of the water during that time. It is based on the changes in isotope fractionation factor with temperature between sea water and CaCO3 and the change in the isotopic composition of sea water through evaporation and freshwater input. The oxygen isotope of sea water and salinity both increase in evaporation and decrease with higher precipitation and run off.

The relation is: $S = S^* + (\Delta\delta^{18}O_F - a - b\Delta T)/c$
Where S = past local salinity,
S*= present salinity,
$\Delta\delta^{18}O_F$ = the measured deviation between modern and past $\delta^{18}O_F$ values of forams,
a= variation of global sea water $\delta^{18}O_{sw}$,
b= slope of $\delta^{18}O_F$ Vs temp. ΔT=local temp. variation, c= slope of δ18Osw Vs salinity relationship.

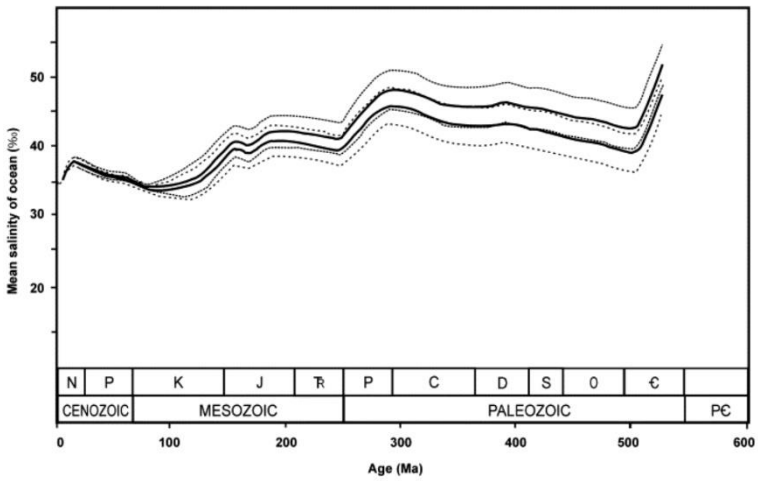

Figure 2: Change of salinity through time (Hay et al. 2006)

Figure 2 shows the overall decline through Phanerozoic (Hay et al, 2006). These changes have had important effects on ocean circulation and on plankton levels and possibly contributed to the explosion of complex life in the Cambrian, 541–520 million years ago.

7. Role of Salinity into Flora

Salinity is a major abiotic stress limiting growth and productivity of plants in many areas of the world due to increasing use of poor quality of water for irrigation and soil salinization. Plant adaptation and tolerance to salinity stress involves complex physiological traits, metabolic pathways and molecular or gene networks. A comprehensive understanding on how plants respond to salinity stress at different levels and an integrated approach of combining molecular tools with physiological and biochemical techniques are imperative for the development of salt-tolerant varieties of plants in salt affected areas. Recent research has shown various adaptive responses to salinity stress at molecular, cellular, metabolic and physiological levels, although mechanism underlying salinity tolerance are far from being completely understood. This paper provides a comprehensive review of major research advances on biochemical, physiological, and molecular mechanisms regulating plant adaptation and tolerance to salinity stress.

8. Role of Salinity into Fauna

Along with climatic aridification and rising sea levels, are increasing salt concentrations in inland freshwater and costal habitats, which produces severe negative economic and biological effect. Contrarily fresh water input mainly caused by mainly irrigated agriculture in arid landscapes, are diluting naturally saline rivers estuaries and salt marshes, with harmful effects. At levels above or below the isosmotic point of organism internal fluids, salinity can disrupt metabolism and water balance. Therefore, aquatic organisms have evolved different intra and extracellular osmoregulation mechanism to control osmotic and dehydration stress in the face of salinity changes in external environment. However, organisms' osmoregulation capacities might be insufficient to deal with anthropogenic salinization.

9. Climate changed through salinity

First, along with temperature, they directly affect seawater density (salt water is denser than freshwater) and therefore the circulation of ocean currents from the tropics to the poles. These tropics concentrate the salt in the water left behind in the North Atlantic, causing salinity to increase. Evaporation moves fresh water from the ocean into the atmosphere and increases the ocean salinity; precipitation puts freshwater into the ocean and reduces its salinity. Consequently, salinity changes integrate effects over broad areas and provide an excellent indicator for water cycle change. The warming climate is altering the saltiness of world's ocean. The water cycle is the worldwide phenomenon of rain water falling to the surface, evaporating back into the air and falling again as rain. The wetter parts of the world are getting wetter and the drier parts drier. The researchers know this because the saltier parts of the ocean are getting saltier and the fresher parts, fresher. Records showed that the saltier parts of the ocean increased salinity – or their salt content – by 4 percent in the 50 years between 1950 and 2000. If the climate warms by an additional 2 or 3 degrees, the researchers

project that the water cycle will turn over more quickly, intensifying by almost 25 percent. The movement of heat around the globe is important for maintaining earth as a habitable place. As the climate warms, the ocean's capacity to store heat decreases, affecting the water cycle, global circulation and other physical properties (PNAS April 19, 2016 113 (16) 4278-4283; first published April 4, 2016).

10. Conclusion

Scientific analysis suggests that global warming is changing precipitation patterns over the planet. Higher temperatures increase evaporation in sub-tropical zones; the moisture is then carried by the atmosphere towards higher latitudes (towards the poles), and by the trade wind across Central America to the Pacific, where it provides more precipitation. This process concentrates the salt in the water left behind in the North Atlantic, causing to increase. Salinity measurements taken since the 1950s indicate global trends of saline areas of the ocean becoming saltier, and freshwater areas becoming fresher.

ACKNOWLEDGEMENT

We would like to express our thanks and gratitude towards our mentor and teacher Smt. Asima Kar, Department of Geology, Jogamaya Devi College who guided and encouraged us throughout the article.

REFERENCES

[1] Hay W.W, Migdisov A., Balukhovsky A.N., Wold C.N., Flögel S. and Söding E. 2006. Evaporites and the salinity of the ocean during the Phanerozoic: Implications for climate, ocean circulation and life. *Palaeogeography, Palaeoclimatology, Palaeoecology* 240, 3–46.

[2] Cullum J., Stevens D.P. and Joshi, M.M. 2016. Importance of ocean salinity for climate and habitability. *Earth, Atmospheric, and Planetary Sciences*, 113(16), 4278–4283.

[3] Prothero D.R. and Schwab, F. 2014. Sedimentary Geology, An Introduction to sedimentary rocks and Stratigraphy, 3rd Edition. W. H. Freeman, London, 500p. ISBN: 9781429231558

Weblinks

[1] http://www.nasa.gov/aquarius. Accessed on 18.02.2022.

[2] http://www.conae.gov.ar/eng/principal.html Accessed on 18.02.2022.

Ocean Thermal Energy Conversion System

Nandita Misra[1], Ipsita Mondal[2], Raniria Mitra[3]
Students of 5th Semester Geology Honours Course
[1]*nanditamisra2019@gmail.com*, [2]*ipsitamondal22295@gmail.com*, [3]*riarani2000@gmail.com*

Abstract: Planet Earth is divided into two major parts: land and oceans. About 29% of Earth's surface is covered by continents and islands. The remaining 71% is covered by water mostly by oceans, seas, deltas, gulfs, rivers, and lakes. Our planet contains enormous amounts of natural resources and energy potential, but due to the growing population it constantly increases the demand of natural resources and energy to survive. Most commonly used mineral resources are fossil fuels which cause global warming. Though Earth provides us with fossil fuels, they are also a limited source of energy. Thus comes the idea of OTEC- Ocean Thermal Energy Conversion.

Key Words: OTEC, Open Cycle, Close Cycle, Heat Exchanger, Platform Design

1. Introduction

Like solar technology, the ocean thermal energy conversion (OTEC) concept has been known for years. Jacques-Arsène d'Arsonval first proposed the idea in 1881. Ocean Thermal Energy Conversion (OTEC) is a system which converts heat energy into electricity by using the temperature difference between warm water at the ocean's surface and the cold ocean water of the depths. The OTEC cycle operates in a tropical area where water depth is about 1000 m and at 20°C. The tropical zone lies between the Tropic of Cancer above and the Tropic of Capricorn below the equator. The sea water in this zone of the earth is warmed by the sun's rays daily and receives about 10,000 times the energy consumed by all mankind in that same 24hours period. The cold water mentioned above generally originates from the Arctic and Antarctic circle. The water originating from the poles is heavier because of its cold temperature than the warm water which originated from the Tropical area. This is the reason that the cold water sits close to the bottom of the sea. Since the deep, cold water has existed there for millions of years, hardly no energy has been utilised. The only energy source that is practically unbounded, sustainable, and so far, the only one that is big enough to displace fossil fuels is OTEC. The operation of OTEC does not release any greenhouse gases into the atmosphere while it is in operation. By hydrolysing seawater, we may make hydrogen and oxygen using the energy generated by OTEC.

2. Applications of OTEC

OTEC was primarily thought of as the means of generating electric power from the warm and cold ocean water but gradually we utilize the concept of OTEC which serves a broader perspective of work. The major applications of OTEC are as follows:

- **Energy generation**
  Energy generation plays a major role in OTEC. The main methods used for power generation are:

- Closed cycle method
- Open cycle method
- Hybrid cycle method

An open-cycle plant can be used to produce desalinated water, which can be used for irrigation and human consumption. A closed-cycle OTEC plant can also act as a chemical treatment plant. An OTEC plant can also be employed for pumping deep seawater.

Figure 1: Ocean Thermal Energy Conversion

- **Marine farming**

OTEC operation brings up cold ocean water from the depths of the ocean. This cold ocean water has two qualities that make it a valuable resource for the cultivation of marine organisms. First of all, it is free of pollutants and organisms created by humans that might harm marine life. Second, the water is roughly 4°C, which allows for the creation of an ecosystem similar to the seafloor and the cultivation of species like lobsters, salmon, trout, oysters and clams are possible. These are not indigenous to tropical waters but can flourish there. OTEC structures function as an artificial reef, giving fish, benthic algae, and sessile and motile invertebrates a new habitat. The organisms that live on the structure can find food and refuge in this artificial unit, which could also serve as a landmark for fish that are passing through. Standing stocks of nekton and benthic organisms will rise as a result of enhanced local production and the attraction of species from the nearby waters. Studies on artificial habitats could be used to determine how large a fish community might grow around an OTEC plant.

Figure 2: Marine Farming

- **Fresh Water Production**

  This application of OTEC is often cited as being the most important, in parallel with energy generation and in future scenarios, it may be the motivating factor behind the development of OTEC. The high through-put rate (450m^3 per second for a 100MW open cycle plant) means that fresh water can be generated at rates compared to municipal requirements. In areas where is lack fresh water, such islands in the South Pacific, initial studies indicate the OTEC generated fresh water is cheaper than that generated by other means.

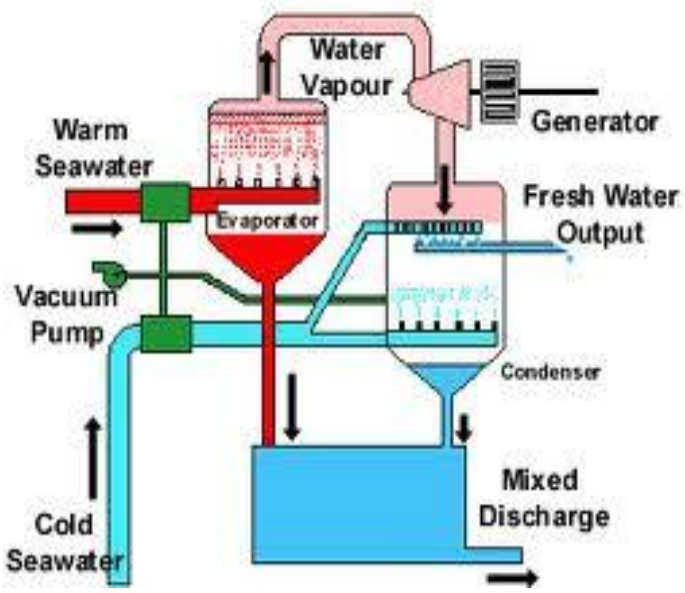

Figure 3: Fresh water production

- **Refrigeration and air conditioning**
  The cold water can be utilized to create cold storage space, as well as for air-conditioning. The laboratory at the Natural Energy Laboratory is air-conditioned by passing the cold sea water through the heat exchanger. Similarly, small-scale applications would be appropriate among the tropical Pacific islands. Aquaculture Enterprises, the wholesaler of wild Maine lobsters being shipped to Japan and will use the cold sea water as an economical substitute for refrigeration.

- **Other Applications and Benefits of OTEC**
  It is proved that a single OTEC unit sited in a carefully chosen site can result in a range of benefits. After being used to generate electricity, it could be passed through an air conditioning system, and then either used for a range of marine farming applications or used to produce fresh water. The concept of a "multi-purpose OTEC centre" has been suggested by the Japanese OTEC group. The design and construction of such a centre would probably need a consortium of companies in a range of industries, with the various applications being mutually beneficial. It is suggested that a useful addition to a multi-purpose OTEC centre would be a research and development centre aimed at the environmentally safe exploitation of the ocean's resources.

3. OTEC Technology

An Ocean Thermal Energy Conversion plant is mainly a heat engine that uses the temperature difference between the warm water of the sea surface and cold water of deep sea to produce electricity and the temperature difference can be used to generate power.

In 1881, the technology for OTEC was first proposed by Jacques d'Arsonval. In 1930 Jacques d'Arsonval's student Georges Claude built the first open cycle OTEC plant in Cuba.

With a proper design, ocean thermal energy is a potential source of renewable energy. An OTEC system contains 3 basic components

A. An energy supply source
B. A power generation system
C. A possible desalination system

The warm water from the surface is pumped through an evaporator which contains a working fluid. The vaporized working fluid drives a turbine or generator. The vaporized fluid is turned back to a liquid in a condenser which is cooled with cold, deep ocean water which is then pumped. OTEC systems using seawater as the working fluid. It can use the condensed water to produce desalinated water.

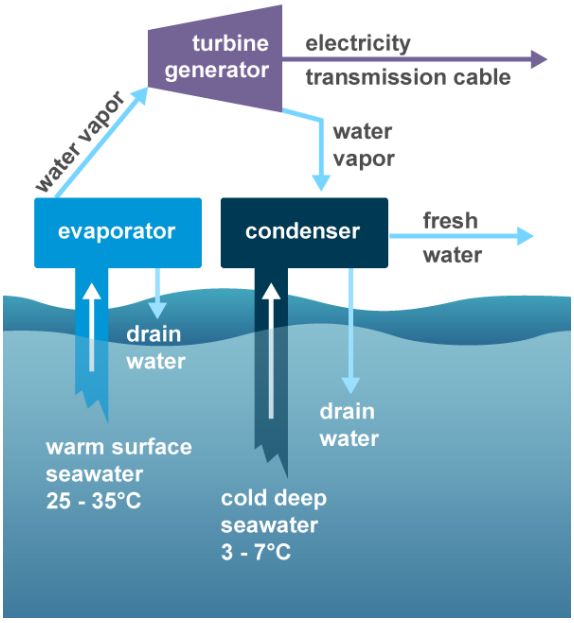

Figure 4: Working Principle of OTEC (EIA 2021)

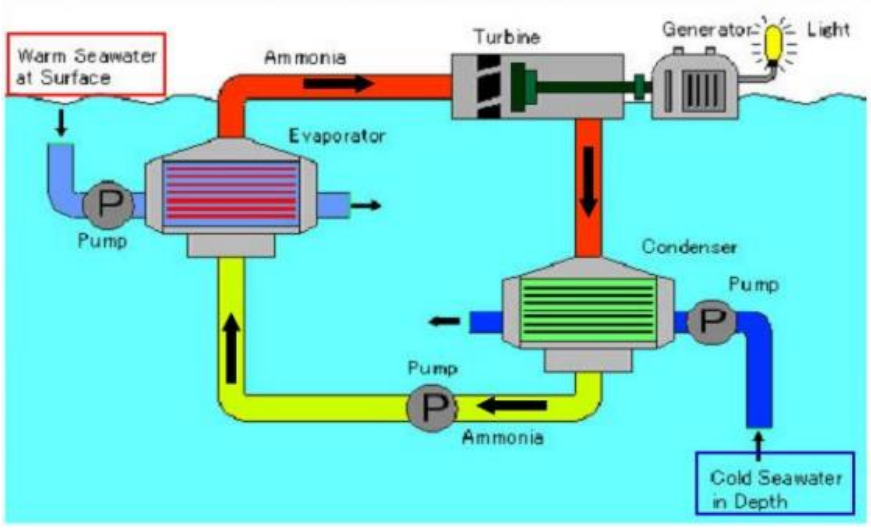

Figure 5: Ocean Thermal Energy Conversion system

Ocean thermal energy conversion power systems are basically divided into two types,

1. Open Cycle
2. Closed Cycle

3.1 Open Cycle: This system utilizes the warm surface water as working fluid. The surface warm water is pumped into a vacuum chamber where it is flash evaporated and the resulting steam drives a turbine, combined to a generator and then is condensed (using deep sea cold seawater pumped to the surface) to produce desalinated water. So, the open cycle formed of the following steps:

- Flash evaporation of a fraction of the warm surface seawater by reduction of pressure below the saturation value corresponding to its temperature.
- Expansion of the vapor through a turbine used for generating power.

- Heat transfer to the cold deep seawater thermal sink resulting in condensation of the working fluid.
- Compression of the non-condensable gases (air released from the seawater streams at the low operating pressure) to pressures required to turn them away from the system.

In open cycle flash evaporation is a prominent feature and it involves complex heat and mass transfer processes.

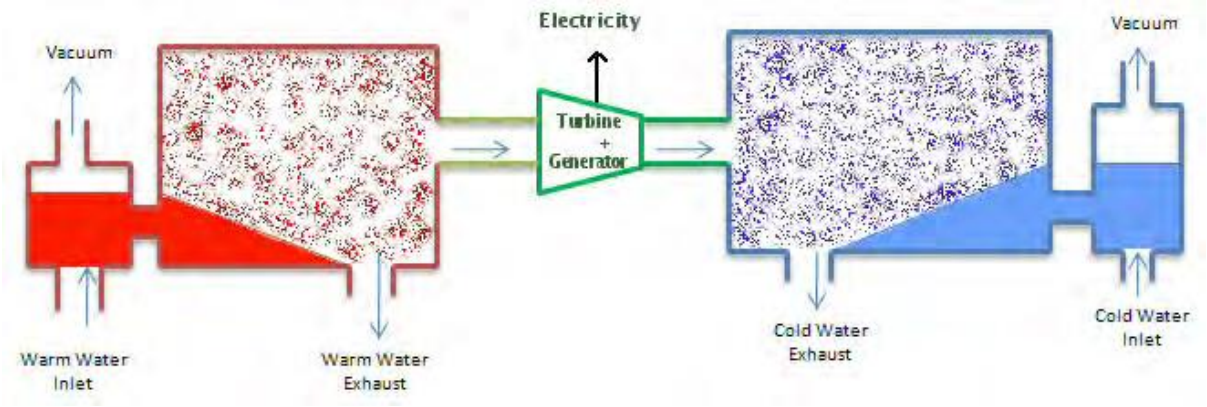

Figure 6: Open-Cycle OTEC System (CRRC 2009)

3.2 Closed Cycle: The closed- cycle OTEC power plant was the first OTEC cycle proposed by d'Arsonval in 1881. The system contains a working fluid, like ammonia or ammonia - water mixture. The ammonia fluid is pumped into the evaporator where fluid is vaporized and turn moves a turbine. Closed-cycle plants operate on a cycle which is called Rankine cycle.

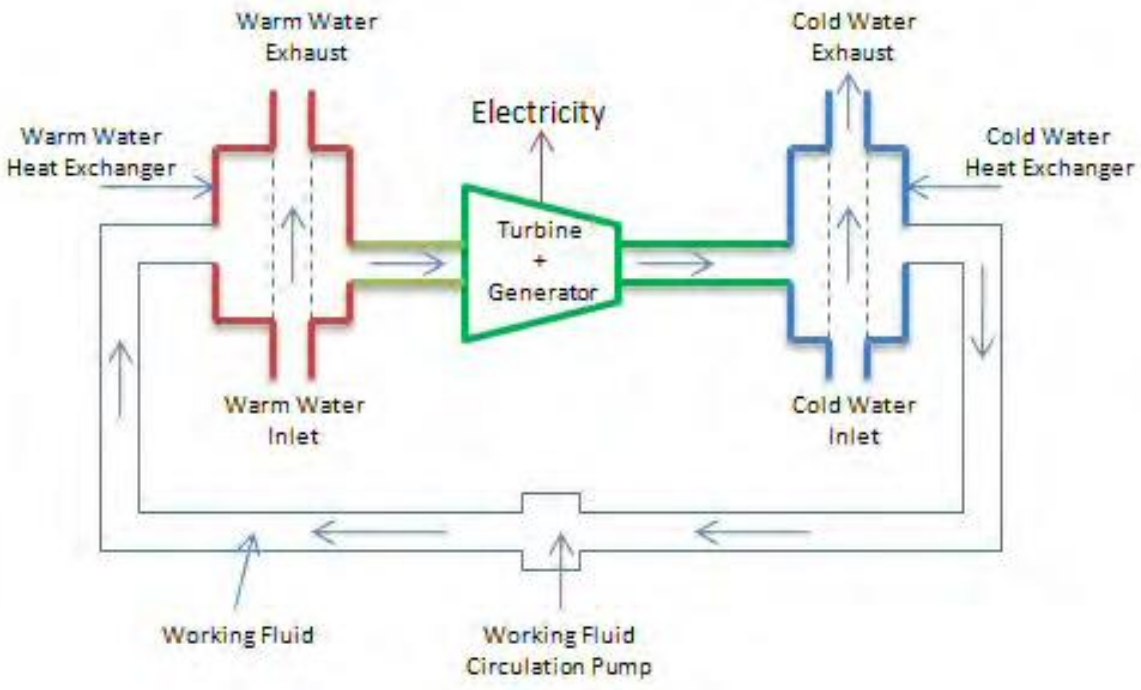

Figure 7: Closed-Cycle OTEC System (CRRC 2009)

Rankine cycles, are able to produce non-zero net power due to the fact that less energy is required to increase the pressure of a liquid then it is able to be recovered when the same fluid spread as a vapor. It is for this reason that phase changes are important when producing energy this way.

The advantages of using a closed-cycle system are, it is more compact than an open-cycle system and designed to produce the same amount of power. The closed-cycle can also be designed utilizes already existing turbo machinery and heat exchanger designs. The operation of a closed-cycle OTEC plant, using anhydrous ammonia as working fluid, is imitated with the saturated Rankine cycle. Fig. 7 shows a simplified flow diagram of the Closed Cycle-OTEC cycle.

Hybrid Design OTEC: The system is yet to be tested but uses principles of both the closed and open cycle OTEC system to get maximum efficiency. The hybrid cycle uses both seawater and other working fluid, usually ammonia. The fresh water is firstly flashed into steam, similar to the closed- cycle and this occurs in a vacuum vessel. In that same vessel the ammonia is evaporated through heat exchange with the warm surface sea water. The ammonia physically mixed with the warm seawater in a two phase, two- substance mixture. After that the evaporated ammonia is separated from the steam and re-condensed into the closed loop cycle. The phase change of the vapor turns a turbine which produces energy.

Common processes for the hybrid-OTEC are: The system uses hydraulic turbines and vapor turbines

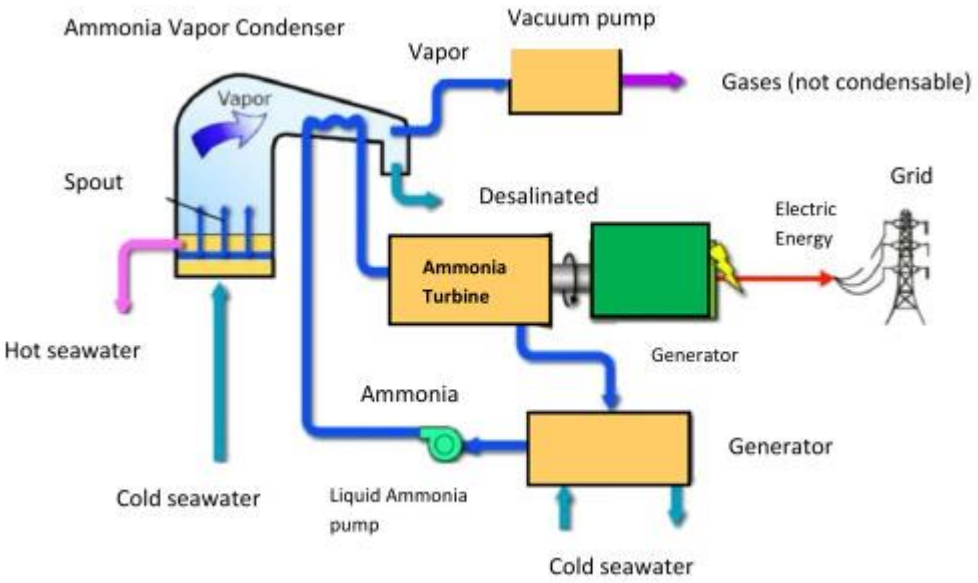

Figure 8: Hybrid Cycle OTEC System

4. Research on OTEC

4.1 Energy utilisation

Earlier researches on OTEC technology were carried out with the main focus on investigating its probability to produce sustainable energy and promoting its possibility to replace

hydrocarbons as major energy sources in future. As a renewable energy, OTEC uses the temperature difference between the warm surface sea waters of the tropical oceans (228°C–248°C) and the cold water stored at deep water (48°C–88°C) to convert solar energy to mechanical and electrical energy (Avery 2001, Lennard 2004). The greater the temperature difference, the greater the avail of the OTEC power plant. Hence, the sea site with huge temperature difference is an important requirement for an OTEC platform to operate. The OTEC power plant was designed in a way that it can transmit energy to the shore by submarine cables through a shore-side electrical grid system. The DC transmission cable is preferable as it would reduce transmission losses for power plants located 30 km or more than 30 km offshore as claimed by Marland (1978). The generated electricity from the OTEC power plant has been explored for many applications, such as production of hydrogen from water through the electrolysis process (Ikegami et al. 2002) and the hydrogen could then be liquefied and transported to land (Avery et al. 1985). The electrolytically-formed hydrogen and oxygen could also be used as feedstocks for methanol production (Pelc and Fujita 2002).

Production of OTEC methanol include the transportation of coal to the OTEC power plant where the coal is oxidised, using oxygen and steam to produce carbon monoxide. The process is followed by the reaction of the carbon monoxide with the added electrolytic hydrogen to yield methanol (Avery et al. 1985). The OTEC methanol offers an essential alternative to future dependence on the dwindling petroleum resources as it could be produced from an abundant source of coal as well as natural gas (Avery et al. 1985). The hydrogen which is generated could also be used to produce ammonia (for fertiliser and chemicals) by combining with nitrogen from the open air. The ammonia obtained via electrolytically-produced hydrogen appeared to be effective economically and environmentally as compared to their counterparts produced from coal. It could also be effective to nations that do not have an abundant or assured supply of natural gas or oil, the generated ammonia could also be used for hydrometallurgical process to extract metal from the ocean mines.

Another effective use of the OTEC power is in bauxite mining and refining for aluminium production at tropical sites, such as in Jamaica and Indonesia (Fuller 1978, Crews, 1997). Water supplies are a problem in these countries because of deforestation and poor maintenance of treatment plants. The electricity which is generated from the OTEC plant could be used to power the reverse osmosis desalination process (Kumar et al. 2007) in order to produce fresh water for the mining industry as well as for other purposes. The OTEC desalination plant is very economical as compared to the land-based desalination plant in producing both water and electricity. Suitable places for the shore-based OTEC are also found in the tropical islands which have limited sources of fossil fuels such as Maldives. The distilled water produced as a by-product of generating electric power in the OTEC plant can be used to support their tourism industry. Researchers from the University of Hawaii have also investigated the advantage of using OTEC for agricultural purposes by burying an array of cold-water pipes (CWPs) in the ground to reproduce cool weather growing conditions that are not found in tropical areas. Such a system could help producing strawberries and flowers throughout the year in the tropical countries. The cold ocean water obtained from the OTEC plant could also be used to make a cold storage. (Takahashi and Trenka 1992). The cold

storage is used as an economical substitute of refrigeration in the aquaculture industry. Economic studies on the new development of air-conditioning by using cold seawater have indicated that such technology is economically effective for metropolitan and resort application.

The OTEC power plant and subsystems proposed by the Committee on Investigation of New Power Generation Methods (Kamogawa 1972) in Japan could also use the nutrient-rich cold water discharged from the plant for the production of marine culture. For this purpose, two OTEC power plants were placed in the offshore of Osumi Islands and Toyama Bay which are rich in pelagic fish eggs and fish larvae (Kamogawa 1980). These OTEC power plants were found to be well suited in these two places due to its ability to generate power and marine products continuously. The extraction of cold water with a temperature of about 48°C from the deep sea also make possible the reproduction of the seafloor environment which is efficient for cultivation of organisms such as lobsters, oysters, abalone, and macro- and micro- algae, deep nutrient-rich seawater for mariculture and nuclear power plant cooling in Taiwan.

4.2 Platform design

The design of the OTEC platform is based on a number of consideration, it depends on the weight and volume of the components on the structure as well as the operating sea conditions, other factors like motion response due to environmental loading force, to improve its seakeeping performance, forces induced in the cold-water pipe (CWP), the ability to efficiently support the heat exchangers, energy conversion equipment and auxiliary equipment for closed cycle operations, relatively easy construction and maintenance, life cycle costs involved, and the most optimal size for commercial applications. Several configurations for the surface platform/power plant have been investigated, including semisubmersibles, spar buoy shapes, ship-like forms, and sphere or disk shaped buoys. The simplest form being the rectangular barge type such as the first MINI OTEC plant and the Sea Solar Power Inc.'s OTEC power plant (United Engineers and Constructors Inc 1975).

Various designs of the OTEC platform and mooring systems have been considered by researchers over the past few decades. From their platform studies, the larger the plants were the more cost-effective from the standpoint of power production efficiency versus size. Large plants also keep down the platform motions and resulting stresses induced in the cold-water pipe. However, large size also has its limitations in the form of it's construction, transportation and deployment, particularly for platform and cold-water pipe. Keeping in mind these size considerations, a compromising selection favoured size distribution of approximately 100-400 MW for commercial size applications involving the mainland power grid. Another interesting OTEC Plant is the Grazing OTEC Plant Ship which is equipped with a propulsion system that has been proposed and designed by the Applied Physics Laboratory of Johns Hopkins University. This OTEC plant is able to 'roam' the Pacific Ocean and the Atlantic Ocean in order to seek for a high temperature differential. As the operating conditions are located at the hurricane belt and subjected to iceberg impact, the OTEC platform has to be designed against these environmental loads.

The OTEC tugboat concept was later proposed for the same purpose but without the need to install a propulsion system. The 100 MWe dOmeTEC power plant (Kleute et al. 2009) was proposed by the students from the Delft University of Technology for the island of Curacao. The power plant is dome shaped and the cheapest way to protect the OTEC system from harsh environment conditions was concluded by making it a floating dome. The domeTEC design also incorporates an innovative 'airlift' pump system, where it allows air to be injected to the fluid in order to aerate the fluid and reduce its density. As a result, liquid could flow upwards due to the increase in pressure difference over the inlet of the pipe. The 'airlift' pump system is more robust and is able to increase its efficiency by 20– 30% as compared to the conventional pumps. A jacket-spar (J-spar) type of OTEC power plant was introduced by Srinivasan (2009) from Deepwater Structure. Since commercial OTEC platforms will be of a similar size to those designed by the petroleum industry, the designs and accomplishments of that industry will play an important role in development of OTEC structures. However, it is realized that many commercial applications, such as those required for islands may require power levels an order of magnitude lower.

Based on size the platform studies revealed that the spar and ship/barge were the preferred platform configurations, and were subsequently used in conceptual designs for a 10 – 40 MW pilot plant. A concrete barge design with an articulated concrete CWP has been developed for the grazing plant-ship concept; and a steel spar design with an articulated steel CWP. A few oil storage and production platforms approximate to the size necessary for OTEC. However, long-term operating experience with even these platforms is still very limited.

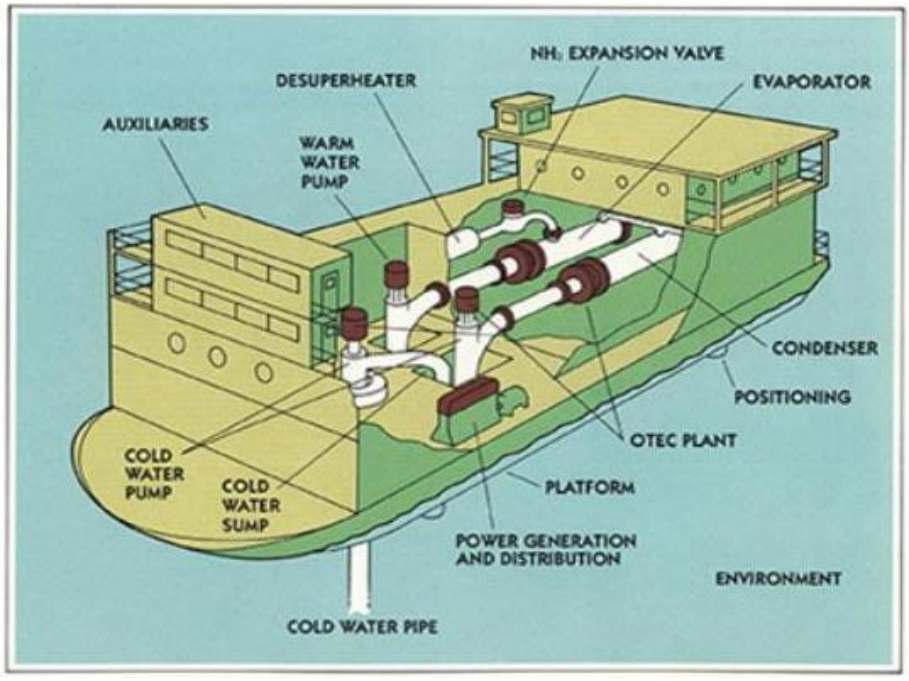

Figure 9: Platform Design of OTEC

4.3 Mooring system

Offshore OTEC platforms/plants require deep-water mooring systems, for generating electricity and transmitting power to shore by transmission cable. Such mooring systems are required to limit the movements of the platform with coupled cold-water pipe, and to minimize flexure in the electrical cable used for power transmission. The size of these platforms ranges from about 70,000 tons for a 40 MW plant, to about 500,000 tons for a 400 MW Commercial Plant. Site selection for a moored OTEC power plant requires many considerations including: proximity to shore to minimize electric power delivery costs, accessibility of an adequate cold-water source, sea floor terrain profile to avoid going aground with the cold-water pipe, sea floor conditions for mooring, and overall environmental loading conditions. Platform movements are influenced by many factors, especially its impact on transmission cable and mooring system design, operating life and costs. The design life of OTEC plant mooring systems is based on a 30-year expected plant life with some replacements permitted provided there are no significant disturbance in power generation. Though there are deep-water mooring systems in existence, little experience relates to long life requirements.

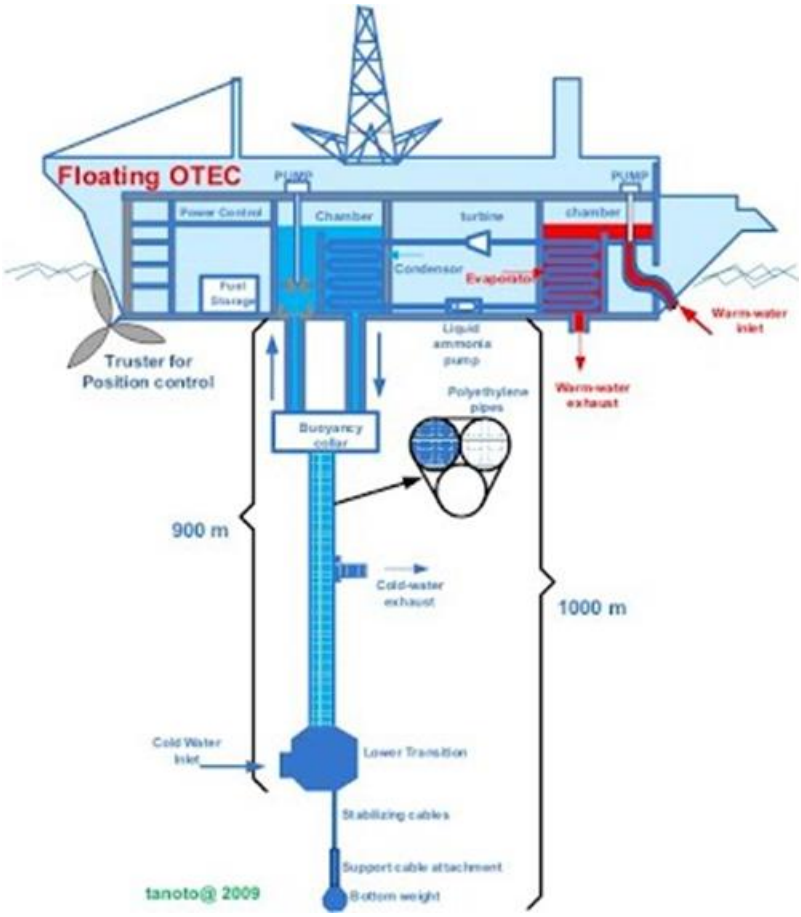

Figure 10: Mooring system of OTEC (TMI 2021)

Several methods for estimating this force have been formulated; still further investigation is required. A number of mooring concepts were considered in the conceptual design studies. Components such as chain, anchors, winches, and windlasses are not considered off-the-shelf

items and quality assurance for the intended usage may not be as expected. A much better way of predicting wave drift forces is preferable, to reduce the seaway loads to a realistic minimum. When subject to environmental forces, the platform, cold-water pipe and transmission cable are all in motion and they are interacting so the degree of coupling needs to be more accurately estimated, and a better method for predicting the dynamic response of the total system is sensible. Plans such as obtaining fatigue test data on wire rope, chain and other mooring system components. Sea-floor engineering investigations should be made at the planned sites to obtain data on soil properties and seafloor stability for anchoring design. Future investigations are aimed at obtaining better understanding of the effects of environmental forces on the dynamic function of a moored OTEC plant.

4.4 Heat exchangers

The heat exchanger system is one of the most important components of the closed-cycle OTEC plants which are currently being developed. Its function is to evaporate and condense the working fluid using the warm and cold seawater. The heat exchanger system is the most costly part of an OTEC, so the cost effectiveness involves reliability and maintainability, using available biofouling control methods. The major cost of the OTEC power plant lies in the heat exchanger. The capital cost of the heat exchangers has been estimated to be one-fifth to two-fifths of the total cost of the plant, dependent upon configuration and material. The assurance of reliability and maintainability has a major impact on life-cycle economics. Several types of heat exchanger designs have been suggested. The most common heat cycle suitable for OTEC is the Rankine cycle using a low-pressure turbine. Two main types of the Rankine cycle heat exchanger are used in the OTEC, i.e., the closed Rankine cycle process and the open Rankine cycle process. Most of the research studies on OTEC heat exchangers focused on the closed cycle heat exchanger due to its energy efficiency. The closed-cycle system uses working fluid with low boiling point to rotate a turbine. The working fluid is vaporised by heat exchanged with the warm surface water and the vapour used to drive the power turbine/turbo-generator. The vapour is then condensed by heat exchanged with cold sea water after driving the power turbine/turbo generator.

On the other hand, the open cycle used the vacuum flash vaporisation of warm water to drive a low pressure steam turbine. Such a system was initially used in the OTEC plant by Claude in 1930. This system avoided the necessity of transmitting enormous quantities of heat through the inevitably dirty walls of the immense boilers which would result in the loss of efficiency. This remains a major problem faced by the modern versions of the OTEC (Marland 1978). To increase the efficiency of the open cycle heat exchange, an improved version of the open cycle heat exchanger which used a steam lift water pump and a foam lift concept was later developed by Beck (1975) and Zener and Fetkovich (1975), respectively. The steam lift water pump and foam lift were used to raise the warm water into a vacuum, where the vapour and liquid were separated at some elevation, with the vapour passing to a condenser and the liquid falling down to drive a hydraulic turbine (Marland 1978). In order to reduce the impact of released non-condensable gases during the vacuum flash-evaporation process, a pre-deaeration chamber should be installed below the flashing chamber so that gas molecules could be removed before entering the steam turbine. Such design will result in a

net gain of efficiency as well as the environmental benefits of discharging oxygenated water. Besides that, it could prevent the discharge of carbon dioxide and other greenhouse effect gases to the atmosphere.

The closed-cycle system has advantages over the open-cycle because of the use of ammonia as the working fluid which has less uncertainty in its detail design phase. The open cycle is however less expensive than the closed cycle and the evaporator is designed to produce distilled water since water is used as the working fluid. This has prompted engineers to combine the features of both closed and open cycle systems in the OTEC plant which resulted in a hybrid cycle system. This allows the intake of warm seawater into a vacuum chamber where it is flash-evaporated into steam, similar to the open-cycle evaporation process. The steam vaporises the working fluid of a close-cycle loop which is then used to drive a turbine to produce electricity.

Another two basic types are shell and tube systems, and plate and fin systems. The largest heat exchangers constructed to date have tube surface areas of about 500,000 sq. ft. A 400 MW OTEC will require 40 times that, or about one square mile of heat exchanger surface area. Materials for OTEC heat exchangers include copper-nickel alloys, stainless steel alloys, aluminium alloys and titanium. Copper--nickel alloys have been the standard material for marine heat exchangers and seawater piping systems for many years. Though this material is relatively inexpensive and abundant, it is not compatible with ammonia which is the principal working fluid in closed-cycle designs. However, aluminium remains suitable at-sea, closed ammonia cycle operation and is subject to complex corrosion mechanisms. Titanium is also a good candidate material for evaporators and condensers because operating experience indicates good resistance to pitting, stress, and intergranular corrosion can be achieved. Titanium is compatible with ammonia and has high strength for its weight. The useful life of titanium heat exchangers has been predicted to be approximately 30 years. Welding and joining techniques for titanium on very large, complex structures, have not been satisfactorily demonstrated. High cost and limited supply would prohibit large-scale use of the material in the near future but long range development for OTEC application may make it more economical.

So far, there is no obvious best cost-effective material for the heat exchangers. However, titanium appears to be the most technically acceptable material. Only design and testing of the heat exchanger over a substantial period of time will determine the most reliable and cost-effective material. The major findings from the heat exchanger technology area are:

[1] enhanced surfaces may be used effectively on the tube side (power-fluid side) of shell-and-tube heat exchangers;
[2] on-line mechanical cleaning systems (brushes and circulating balls) are leading candidates for microfouling control in circular tubes, and work well on single tube tests;
[3] chlorination and copper alloys or antifoulant cladding on the tube sheet are being considered for macrofouling control;
[4] material selection for ultimate commercialization remains the dominant question in heat exchanger design.

Further work is required to control macrofouling. The range of possible heat transfer tube materials has increased. In addition to titanium, several stainless steel alloys offer high corrosion resistance. Copper--nickel claddings, copper alloys and special aluminium claddings have shown promise for continued corrosion evaluation. Trade-off studies have shown that less expensive materials such as aluminium and plastics of shorter life may be economically feasible. Further development efforts will be necessary to develop cost-effective heat exchangers for mainland commercial OTEC application. The following is a listing of technical areas where further improvements may be achieved. (1) Lower life cycle cost heat exchangers, (2) Efficient and environmentally acceptable techniques of mechanical tube cleaning. (3) Benefits and costs of chlorination, within the limits imposed by environmental regulation. (4) Cleaning methods for corrugated plates or non-circular water channels. (5) Effective brush or ball cleaning systems in water, side enhanced tubes. (6) Effective ultrasonic cleaning techniques. (7) Vertical tube, thin-film evaporators under sea conditions. (8) Ammonia-water chemistry requirements versus material type, and the effects of corrosion due to ammonia leakage.

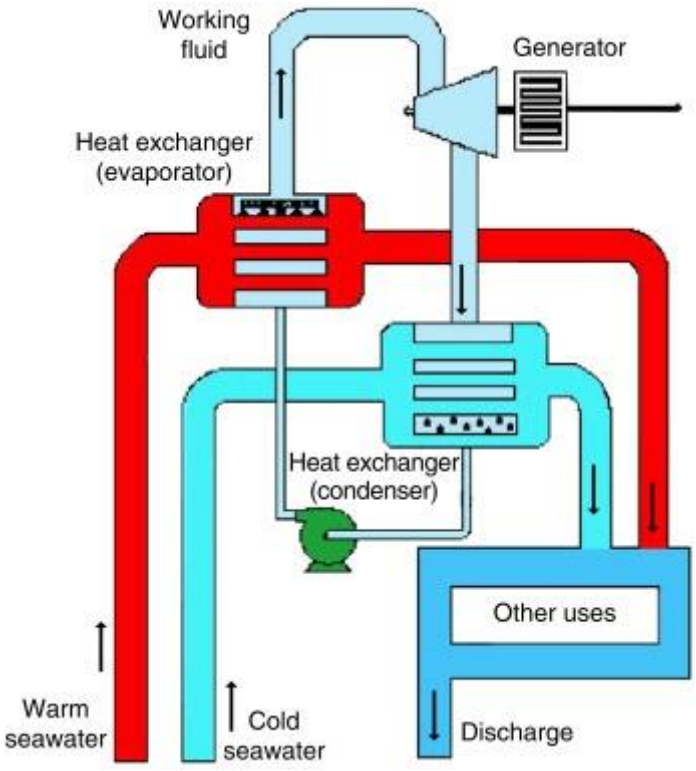

Figure 11: Heat exchanger system of OTEC

5. Environmental Impact And Impacts of Artificial Upwelling

The installation of the OTEC power plant in the ocean can cause a significant impact on the environment. As one of the most benign power production technologies, the OTEC does not produce radioactive waste and does not involve any release of noxious pollutants to the environment. The building materials for the OTEC plant such as steel, concrete and aluminium are also benign to the environment. Nevertheless, on closer examination of the

OTEC design, the handling of hazardous substances, such as ammonia, halocarbon and hydrocarbon (propane and isobutene) as the working fluid, would cause environmental problems if leakage occurs. As these substances are easily soluble in water, it is harmful to marine life and could damage the marine ecosystem. The release of the power plant's effluent (such as chlorine and other chemicals that are used to clean water passages in the power plant) and the discharge of biocide which is required for macrofouling control would cause encroachment of nearshore organisms and commercially important species. A potentially dramatic application of the upwelled sea water might be in enhancing global greenhouse warming, according to some researchers. Rising levels of Carbon dioxide in the atmosphere have led to proposals for the construction of large open-ocean farms for cultivating carbon-dioxide-consuming macroalgae, using nutrient-laden upwelled sea water, and thereby reducing the amount of that gas now being released. While the upwelled water contains naturally-occurring Carbon dioxide there is conjecture that it may be possible to combine the deep water nutrients and Carbon dioxide, with selected materials and, through a managed biological growth mechanism, remove additional Carbon dioxide, from the atmosphere.

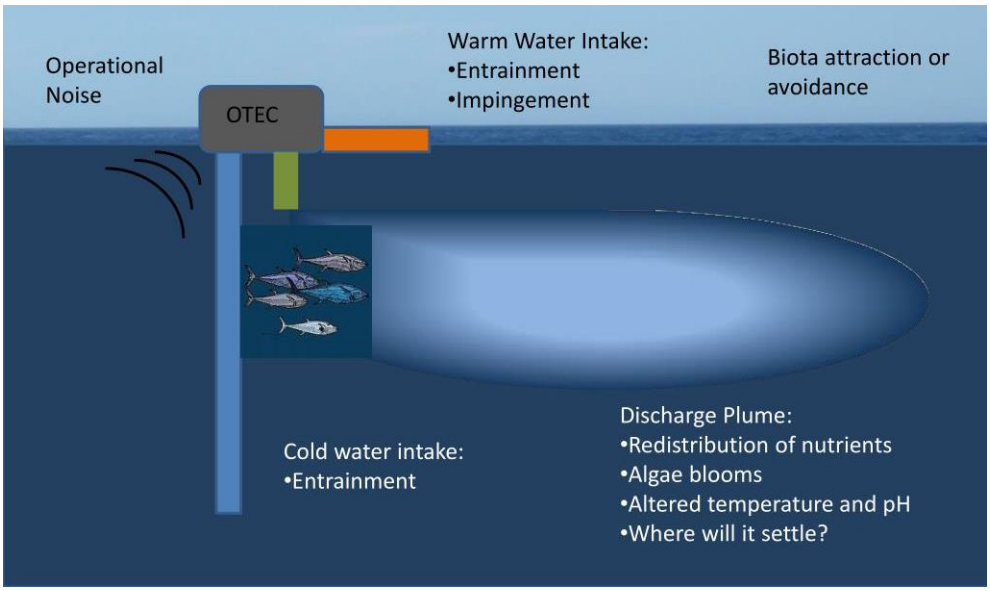

Figure 12: Environmental Impact Of OTEC

6. Present status of OTEC

Nearly 15 years of research and development on OTEC systems have create a wealth of data on the scientific and technical aspects of this technology. An extensive bibliography has been compiled by the Korea Ocean Resource Research and Development Institute. 21 Research is to refine knowledge about OTEC and the construction of planned small experimental plants and pilot-scale commercial plants in the next few years is expected to lead to widespread commercialization of OTEC by the year 2000. This work has also led to the conclusion that the key to commercial success of OTEC will rely not only on the generation of electricity but will depend on also other attributes of OTEC, especially the capability of producing fresh water and the potential for using cold deep sea water for air conditioning, mariculture, and other applications.

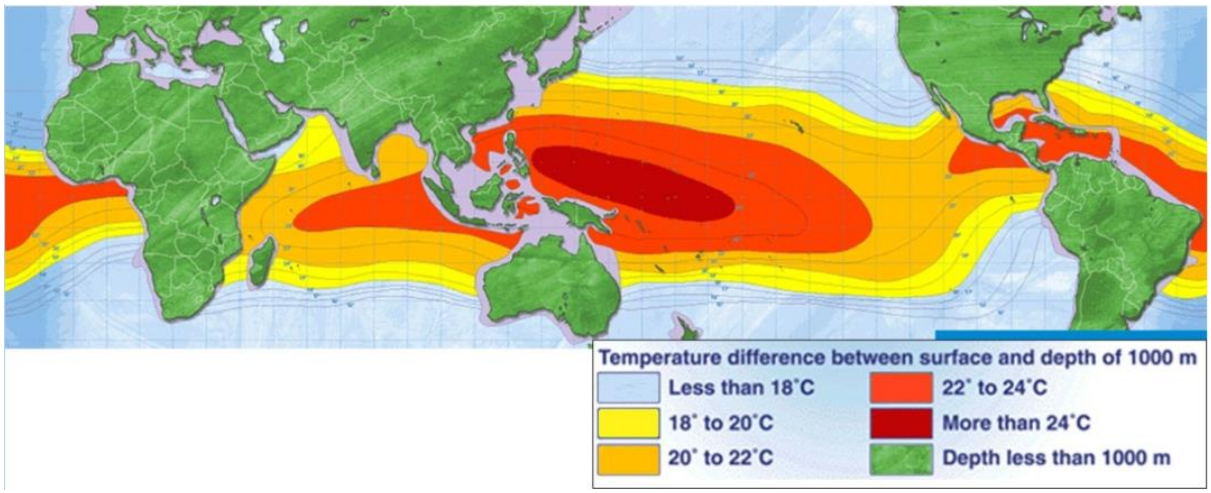

Figure 13: Distribution of ocean temperature gradients in excess of 20°C (TMI 2021)

7. Global Scenario

- The United States

  The US government does not appear to have a well postulated policy with regards to the renewable energies and OTEC in particular. In 1990, funding for OTEC was $4mn, which dropped to $3mn by the following year and is now maintained at roughly this level. On the positive side, the US has the engineering and industrial base which will help to develop and OTEC programme and it remains true that a huge proportion of OTEC expertise is in the US. Large company involvement will obviously help in development of OTEC.

- Japan

  The Japanese OTEC programme have reached a standstill as the government's interest in renewable energy appears to have diverted to what it sees as more viable forms (fuel cell, solar). Japanese industry's plans of obtaining $100mn funding from the Overseas Development Agency to build a prototype OTEC plant and associated facilities looks unlikely to materialise in the future, given both Japan's current recession and the low priority afforded OTEC by the Japanese government. The Japanese OTEC industry has recently initiated research to try to determine why OTEC has not been successful in Japan, and determine how to more closely match the technology with the market place. This is a step in the right direction. Japan, as the US, certainly has the engineering expertise to commercialise OTEC, and Japanese companies excel at bringing technology to the marketplace.

- Taiwan

  Currently Taiwan represents the closest fit between technology and market, regards to OTEC as an energy source in the near future.

Currently the U.S. leads the world in the development of OTEC technology. The Pacific islands are expected to be the initial market-entry point for open-cycle OTEC system due to the huge cost of power generation by diesel fuel, the demand for potable water, and the socio-

economic benefits of this technology. L. Dunbar (1981) surveyed 98 nations and territories with direct access to the OTEC thermal resource within their 200-nautical-mile Exclusive Economic Zones.

A market assessment of 67 free market, developing nations and U.S. territories was also conducted to know the potential for OTEC. The study assessed the OTEC source, technology, market, barriers, and incentives to implementation. The results indicate the significant market potential for OTEC in most of the countries surveyed if the resource is within two nautical miles of shore. In southeast Asia in PICHTR surveyed 26 sites and the Pacific to determine OTEC potential in 1987. Total demand for power projected for these sites over the year 1987 was 2,953 MWe for the year 2000 and a cumulative total of 24,898 MWe by the year 2015. In 2015, this would represent a demand for about 250 plants of 10 MWe in size. The market of OTEC in the Pacific countries depends on many factors. In particular, the fresh water and mariculture components of the system give rise to six Pacific Island governments to request PICHTR to conduct feasibility studies of the technology for their island. Even the availability of a renewable, clean source of energy does not seem to be as effective as the potential benefits of derivable from fresh water and the mariculture potential.

Figure 14: OTEC-Desalination lab at NIOT (National Institute Of Ocean Technology), India

8. OTEC Development in India

In India the recent OTEC project is being developed in Andaman and Nicobar Islands a picture of Andaman OTEC project is given in the slide. These OTEC plants are set up to power a desalination plant. The power expected to be generated is under 200 kW. It is in the design phase currently and is likely to be commissioned in early 2019. India is geographically well-placed to generate ocean thermal energy, with around 2000 kms of coast length along the South Indian coast, where a temperature difference of above 200°C is available throughout the year. The total OTEC potential around India is estimated as 180,000 MW, considering 40% of gross power for parasitic losses. OTEC holds promise for a large country like India with a long coastline. Ocean thermal energy conversion uses the temperature difference between cooler deep and warmer shallow or surface seawaters to run a heat engine

and produce electricity. It is a system with base load electricity generation. OTEC is one of the continuously available renewable energy resources. "The current OTEC project is being set up to power a desalination plant. The power expected to be generated is under 200 kW. It is in the design phase currently and is likely to be commissioned early 2019,"

9. Conclusion

OTEC holds promise as a sustainable way to meet global energy needs, while reducing climate impact. This technology is successful in areas that are in need of resources like clean drinking water and sustainable agriculture, in addition to energy needs. Despite being an old technology, OTEC is yet to be commercialized. It is however a fast-gaining ground with new projects on the horizon and intensive research. OTEC IS technically feasible with the investment of considerable financial and technical resources. This is important in order to ease the pressure on fossil fuels resources and also to provide a cheap and uninterrupted power supply to the tropical regions where the countries are underdeveloped. The major hurdle that needs to be overcome is the inefficiency of OTEC, but its continuous source of energy somehow nullifies the disadvantage of inefficiency. OTEC is the technology that offers the near terms potential in being useful to the world.

ACKNOWLEDGMENTS

We are very thankful to our professor Dr. Kaushik Kiran Ghosh for encouraging us to pursue with this topic.

REFERENCES

[1] EIA 2021. Hydropower explained: Ocean thermal energy conversion. Available at: https://www.eia.gov/energyexplained/hydropower/ocean-thermal-energy-conversion.php. Accessed on: 07-11-2021.

[2] Etemadi A., Emdadi A., AsefAfshar O. and Emami Y., 2011. Electricity Generation by the Ocean Thermal Energy, *Energy Procedia*, V.12, pp.936–943.

[3] Faizon. M and Ahmed, M.R.., On the ocean heat budget and ocean thermal energy conversion, *International Journal of Energy Research*, V.35(13), pp.1119 – 1144.

[4] Takahashi P.K. and Trenka A. 1992. Ocean thermal energy conversion: Its promise as a total resource system, *Energy*, V.17(7), pp.657–668.

[5] Tanner D. 1995. Ocean Thermal Energy Conversion: Current Overview and Future Outlook, *Renewable Energy*, V.6(3), pp.367–373.

[6] TMI, 2021. OTEC Overview. Available at: https://sites.google.com/site/otecmooringsinc/otec-principle. Accessed on: 07-11-2021.

[7] Wang C.M., Yee A.A., Krock H. and Tay Z.Y. 2011. Research and developments on ocean thermal energy conversion, The IES Journal Part A: Civil & Structural Engineering, V.4(1), pp.41–52.

[8] Wikipedia 2021. Ocean thermal energy conversion. Available at: https://en.wikipedia.org/wiki/Ocean_thermal_energy_conversion. Accessed on: 07-11-2021.

[9] Yamada N., Hoshi A., and Ikegami Y. 2008. Performance simulation of solar-boosted ocean thermal energy conversion plant. *Renewable Energy*, V.34(7), pp.1752–1758.

Geometry and Composition of Laccolith

Aparajita Mukherjee[1], Srija De[2] and Sukanya Chaube[3]
Students of 3rd Semester Geology Honours Course
[1]*aparajitamukherjee03@gmail.com*, [2]*deysrija901@gmail.com*
[3]*schaubegeology@gmail.com*

1. Introduction: Intrusive and Extrusive Rocks and Their Formation

Igneous rock forms when hot, molten magma solidifies. The melt originates deep within the Earth, and tends to rise upward due to the density difference between the magma and the surrounding rocks. If the ascending magmatic fluid reaches the Earth's surface and extrudes, it is called lava, which solidifies to form the extrusive igneous rocks like basalt, rhyolite etc. The extrusive igneous rocks, also known as volcanic rocks are solid products of cooling of lava and the pyroclastic materials ejected from the volcanoes. (Etymology of *extrusive; Extrusive (Adj.), "of or pertaining to extrusion or that which has been extruded," in Geology a rock that has been thrust out of the earth by volcanic activity, 1816, from Latin 'extrus'*). On the other hand, if the magma cannot reach the surface of the earth, it solidifies at a depth to produce intrusive igneous rocks like granite, gabbro etc. (etymology of *intrusive; 1400, "usurping", from Latin intrus -, Geological sense "thrust in out of regular place" is form 1826*).

On the basis of their depth of occurrence intrusive igneous rocks are subdivided into plutonic and hypabyssal. Plutonic rocks are relatively large sized intrusions with medium to coarse grained texture that form at moderate to great depth; Like- Gabbro, plutonic equivalent of basalt. Hypabyssal rocks are relatively small sized intrusions with fine grained texture that form at shallower depth. (>one kilometer). Like-Dolerite, hypabyssal equivalent of basalt.

2. Classification of Igneous Emplacements: Intrusive igneous bodies are divided into two classes **(**Bose 1997):

2.1. Discordant Intrusive Body: If an intrusive rock body is not parallel to the pre-existing country rocks, and crosscuts the latter, it is called a 'discordant intrusion'. Examples are dyke, cone sheets etc.

2.2. Concordant Intrusive Body: If an intrusive rock body is parallel to the structures of the country rock in which it occurs, it is called a 'concordant intrusion'. Examples are sills, lopoliths, laccoliths etc.

2.3. Intrusive Igneous Settings

2.3.1. Dyke – A tabular intrusion of rock that cross cuts across the layering of country rock. Example: A typical example is the Dolerite dyke swarm, described as Newer Dolerite Dykes, traversing the Singhbhum granite body in eastern India.

2.3.2. Sill – A nearly horizontal table-top shaped tabular intrusion that occurs between the layers of country rock. Example: Passage of Deccan lavas to sills has been noted in Satpura hills.

2.3.3. Laccolith – If the spreading rate of magma between the strata is low, the intrusion of magma accumulates locally and thus form a dome shaped body. If it's convex upward then called Laccoliths. Example: Sitampundi complex in South India.

2.3.4. Lopoliths – They are large concordant saucer shaped intrusion and have broadly a geometry opposite to that of Laccoliths (i.e., convex download). Example: Bushveld complex in South Africa

2.3.5. Pluton – An irregular of blob shaped intrusion; can range in size form tens of m across to tens of km across.

2.3.6. Batholith – A vast composite, intrusive igneous rock body up to several hundred km long and 100 km wide, formed by the intrusion of numerous plutons in the same region. Example: The Bhongir Fort batholiths in India.

2.3.7. Xenolith – A relict of wall rock surrounded by intrusive rock when the intrusive rock freezes.

3. Geometry of Laccoliths

A laccolith is a concordant intrusive body with a flat base and domed (convex) top – that is a mushroom-shaped body.

When the magma is relatively viscous, the supply of magma from depth is generally greater than the rate of it's lateral spreading. The magma therefore accumulates locally, and lift the overlying country rocks in the form of a dome. The magma body thus solidifies in a plano-convex form like a mushroom, with an arched upper surface and a flat lower surface, to form a laccolith.

They form at shallow depth mostly within 3 km of the Earth's surface. They are commonly emplaced in relatively flat-lying stratified country rock.

On erosion, an upright laccolith will produce a central oval outcrop pattern on ground surface, the body of course may be associated with a number of annular lenticular smaller satellite laccoliths.

Gilbert (1877) studied both laccolith and sills in the same region (Henry Mountains), but sills always had areal extents of less than 1 km^2 where laccoliths were greater than1 km^2.From this he concluded that sills were the forerunners of laccoliths, but that they required a minimum area before they exerted sufficient force to dome upward the overlying rocks.

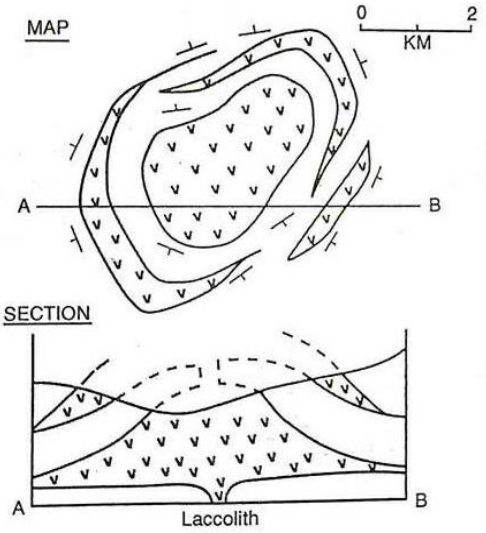

Figure 1: Map and Section view of Laccolith (Bose 2019).

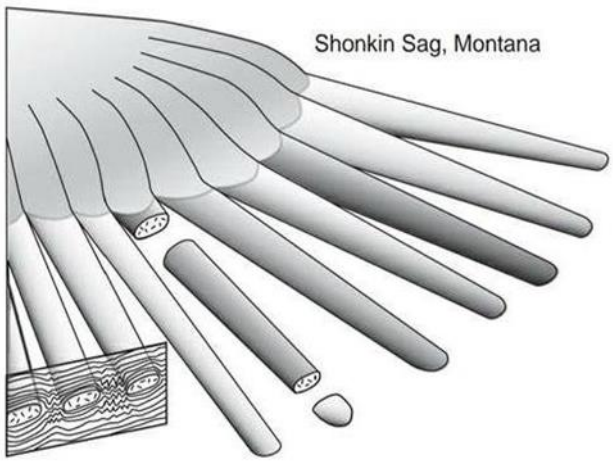

Figure 2: Laccolith in three-dimensional view (Philpotts & Ague 2019)

If the spreading rate of magma is low or the magma is relatively viscous, the magma accumulates locally and lifts the cover rocks in the form of a dome. Thus, laccolith is created. They are commonly formed from magmas with intermediate silica contents, those with moderate viscosity. But examples ranging in composition from basaltic to rhyolitic are known. SiO_2 content; commonly 55-65 wt. % and intermediate in Fe, Mg, Ca, K, Na.

5. Comparison of Laccoliths with Other Intrusive Bodies

5.1. Comparison with Sills and Dykes

Geometry:

- As sill and dykes have great lateral extension than their thickness, their two surfaces are approximately parallel to each other. The two parallel surfaces are again parallel to the intruded country rock for those of sills.
- To form a dome, the overlying country rocks tend to bent upward. So, the two boundary surfaces of laccoliths are non- parallel to each other.

Petrography

- Sills and dykes are commonly composed of basaltic magma with low silica contents. For the low viscous nature of basaltic magma, it can flow easily to travel a long distance.

Near the surface of the earth magma enters into the fractures to form dykes and at depth magma intrudes along the plane of weakness to form sills.

- Laccoliths are generally composed of magma with intermediate silica contents i.e., rhyolitic to andesitic magma. For the high to moderate viscosity of those magmas (yield strength of about 100 pascal) it can't spread too far laterally and therefore produce a dome shaped top surface.
- Dykes are generally formed near the earth surface. For their great lateral extension and closeness to surface favours magma to cool down rapidly forming mainly fine-grained crystals. Besides, as sills form at depth, in spite of having a lateral extension the environment favours to form medium to coarse grain crystals.
- Laccoliths contain coarse grained rocks especially at their flat base than those of sills because of their variances of thickness.

Table 1: Comparison of laccoliths with sills and dykes.

Property	Sills and Dykes	Laccolith
Geometry	Two parallel boundary surfaces	Non- parallel boundary surfaces
Composition	Basaltic magma	Rhyolitic to andesitic magma
Texture	Magmas cool down rapidly forming mainly fine-grained crystals in Dyke. As sills form at depth, favours to form medium to coarse grain crystals.	Laccoliths contain coarse grained rocks especially at their flat base than those of sills because of their variances of thickness.

5.2. Comparison With Lopoliths

Composition

- Laccoliths are formed from rhyolitic to andesitic magma with intermediate viscosity while lopoliths are formed from basaltic or more mafic magmas with low viscosity and low silica content.

Shape

- If the spreading rate of magma is low or the magma is relatively viscous (andesitic to rhyolitic) the magma can accumulate locally and pushes the overlying rock upward to form a dome. Here in the case of laccoliths the magma consolidated in a form of mushroom with arched roof and a flat base.
- On the other hand, lopoliths are large concordant saucer shaped intrusive body. So, they have a geometry of inverted laccolith.
- Laccoliths make space for themselves by doming upward the overlying country rocks while lopoliths make room for themselves by bowing down the base rocks as lopoliths are large enough to affect the entire crustal thickness of any region.
- Lopoliths are of much larger dimension than laccoliths.

Table 2: Comparison of Lopolith and Laccolith

Property	Lopolith	Laccolith
Composition	Basaltic magma	Rhyolitic to andesitic magma
Shape	Large concordant saucer shaped intrusive body (inverted laccolith)	Mushroom shaped with arched roof and a flat base.
Emplacement	Makes room by bowing down the base rocks	Make space by doming upward the overlying country rocks

5.3. Comparison with Batholith

Depth

- Laccoliths form at shallow depths, mostly within 3 km of the earth's surface while batholith is a plutonic igneous body, formed at (Greek '*bathys*': deep).

Shape

- Batholith is a large irregular mass of intrusive igneous rock with no particular shape whereas laccolith is a mass of igneous rock found within strata which forces the overlaying strata upwards and forms dome shape.

Composition

- Batholiths are made of relatively low-density rocks, ranging in composition from quartz diorite to granite, with granodiorite being most abundant. Proterozoic batholiths are made of anorthosite with a low density than surrounding rocks whereas Laccoliths are composed of magma with intermediate silica content, ranging in composition form basaltic to rhyolitic.

Table 3: Comparison of Batholith and Laccolith

Property	Batholith	Laccolith
Depth	Forms at greater depth.	Forms at shallow depths (within 3 km).
Shape	Large irregular mass of intrusive igneous rock.	Mushroom shaped with arched roof and a flat base.
Composition	Low density rocks, ranging from quartz diorite to granite, with granodiorite being most abundant.	Composed of magma with intermediate silica content, ranging in composition form basaltic to rhyolitic.

6. Possible Models of Laccolith Emplacement

6.1. The Model of Gilbert (1877) for Laccolith Emplacement

This model considered a laccolith as a piston-like body that lifted the overlying rock along a ring fracture, as shown in Figure 3.

The force *F* lifting the overlying country rocks of laccolith:

$$F=\pi r^2 P_m \qquad \text{(Equation 1)}$$

Where P_m = the pressure in the magma on the upper surface of laccolith r = radius of the laccolith, if its upper surface is approximated as a circle.

F would be opposed by the weight of the overlying rocks W.

If the overlying country rocks have a thickness T and density ρ_c, then

$$W=\pi r^2 T\rho_c g \qquad \text{(Equation 2)}$$

But $T\rho_c g$ is the lithostatic pressure at depth T. Therefore,

$$W=\pi r^2 P_l \qquad \text{(Equation 3)}$$

Where P_l is the lithostatic pressure.

In lifting the overlying rocks, magma also has to overcome the frictional resistance along the ring fracture resulting from its shear strength τ.

This stress acts on the surface area of the ring fracture and gives a resisting shear force S.

$$S= 2\pi rT\tau \qquad \text{(Equation 4)}$$

Gilbert argued that for a laccolith to be able to lift the overlying rocks, the lifting force of the magma must be equal to or greater than the sum of the forces resulting from the weight and shear strength of the overlying rocks. Therefore,

$$\boldsymbol{F = W + S}$$

Or, $\pi r^2 P_m = \pi r^2 P_l + 2\pi rT\tau$

Or, $(P_m - P_l)r = 2T\tau$ (Equation 5)

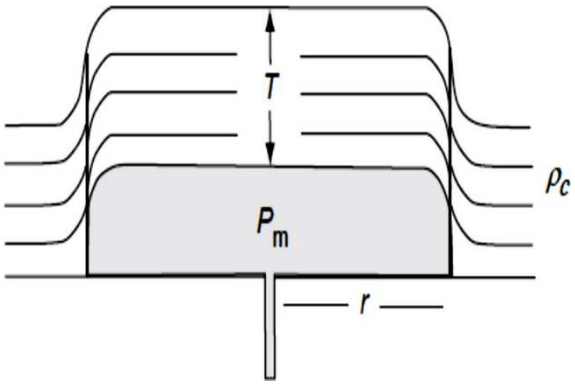

Figure 3: The Model of Gilbert (1877) for Laccolith Emplacement: The laccolith is considered as a piston-like body that lifts the overlying country rocks along the ring fractures.
T = Thickness of the overlying country rocks, ρ_c = Density of the overlying country rocks, P_m = the pressure in the magma, r = radius of the laccolith. (*After Philpotts& Ague, 2009)*

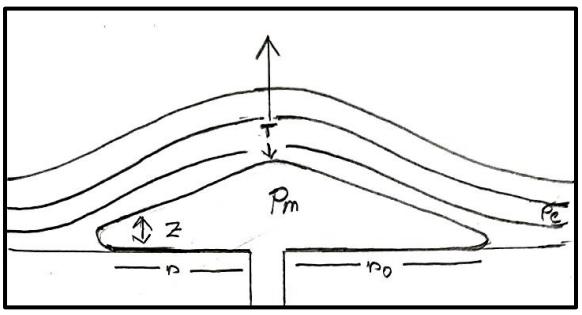

Figure 4: The model of Pollard and Johnson (1973) for Laccolith emplacement. Laccolith acts like a lever, extend from the conduit to left end point and from conduit to right end point as shown in the Figure 4 (ρ_c = Density of overlying rocks, P_m = Pressure of Magma, T= Thickness of overlying rocks, r_o= Effort arm of the lever, r= Distance from the conduit to the point of height Z)

Implications of the Equation 5, derived from the model of Gilbert (1877):

1. A minimal radius is necessary for a laccolith to overcome the shear strength of the overlying rock.
2. The radius of laccoliths increases with increasing depth of emplacement.

We cannot expect Equation 5 to give a precise description of the parameters governing laccolith formation. It does formation. It, consider the force necessary to bend the overlying rocks or the pressure necessary to intrude the magma between the two contacts, regardless of the amount of lifting.

6.2. The Model of Pollard and Johnson (1973) For Laccolith Emplacement

- Pollard and Johnson had considered that the intrusion of a sill acts like a lever where the vertical upward force is applied at the point of magma influx, the fulcrum is at the leading end of the intrusion and the load may be assumed as concentrated at the centre of the mass. Therefore, the lever is a second-class lever (Figure 4).
- At the initial stage when the sill in very small in size, the mechanical advantage is also small as the effort arm is small i.e., the distance from the point of magma influx to the leading end of the sill. Therefore, the magma simply flows laterally uplifting the overlying rocks.
- With the increase in size of the sill, at a critical stage of growth the overlying country rock can be bent to make room for the intrusion rather than being uplifted. Thus, the upward convex shape occurs to form a laccolith. The depth of magma emplacement and the physical properties of the magma along with the country rock are the controlling factors of the extent to which the sill will expand before the critical stage of laccolith formation.

According to Pollard and Johnson's (1973) model, a laccolith in any given vertical section can be considered as a combination of two levers, one extending from the conduit to left endpoint, and the other from conduit to right endpoint. It is shown in Figure 4.

On the left-hand side, the vertical upward force is applied at the conduit. The fulcrum is at the left endpoint and the load maybe assumed as concentrated at the centre of mass of this portion.

Similarly at the right-hand side another lever may be considered.

They gave an equation to calculate the height of the laccolith (z) at the point which is at "r" distance from conduit. The equation is given below –

$$z = \frac{3(P_m - \rho_c g T)}{16BT^3}(r_0{}^2 - r^2)^2$$

where,

p_m =The pressure in the magma

ρ_c = Density of overlying rocks

T =Thickness of overlying rocks

r_0 = radius of the intrusion; effort arm of the lever
r = distance from the conduit to the point of height 'z'; (difference between the lengths of the effort arm and the load arm of the lever)
B =elastic modulus of overlying rocks, which is defined as $E/(1 - v_2)$,
(E being Young's modulus and v Poisson's ratio)

Implications of the Equation given Model of Pollard and Johnson (1973)

1. Pressure difference of the magma, $(P_m - \rho_c gT)$ which is the effective to uplift the overlying rocks and the load pressure $(\rho_c gT)$ of the overlying rocks try to sink the roof.
2. With increasing $(r_0^2 - r^2)$ i.e., the length of the lever arm, the height (z) to which the roof can be lifted will increase, due to the increase of mechanical advantage.
3. The height to which the overlying country rock can be lifted (also = z) is inversely proportional to its thickness (T) and elastic modulus (B). Therefore, as either of those factors decrease, the height increases.

The equation given in the model of Johnson and Pollard (1973) uses the simplifying assumption that the country rock overlying the laccolith is displaced by flexure only. But in nature, there may be extensive faulting and peripheral vertical dyke intrusion associated to laccolith emplacement along with flexure, which are not considered in this model. The shape of a laccolith thus cannot be described completely by this model.

7. Conclusion

7.1. Limitations of the Model of Gilbert

Equation does not describe precisely the governing parameters. It does not consider the force necessary to bend the roof rocks. It does not consider the pressure necessary to intrude the magma between the two contacts.

7.2. Limitations of the Model of Johnson and Pollard

Equation cannot describe completely the shape of a Laccolith. It considers only simple flexing (bending)of roof rocks. It does not consider faulting and dyke intrusion along laccolith margins.

Scopes for Further Investigations: Formulation of new model that considers both bending of roof rocks, and marginal faulting and dyke intrusion.

ACKNOWLEDGEMENT

We would like to express our special thanks of gratitude to respected professor Bhaskar Ghosh and other respected professors of our department who bestowed us with the golden opportunity to do this wonderful project on the topic Geometry and Composition of Laccolith

which also helped us in doing a lot of research. We got a vivid knowledge about the topic we dealt with.

REFERENCES

[1] Bose, M.K. 2019, Igneous Petrology, 2nd Edition, The World Press Private Limited

[2] Gilbert, G.K. (1877). Report on the Geology of the Henry Mountains. Washington, DC: U.S. Geographical and Geological Survey of the Rocky Mountain Region (Powell), 160p.

[3] Johnson, A.M., and Pollard, D.D. (1973). Mechanics of growth of some laccolithic intrusions in the Henry Mountains, Utah: I. Tectonophysics, 18, 261-301

[4] Philpotts, A. R, Ague. J.J, 2019. Principles of Igneous and Metamorphic. 2ndEdition, Cambridge University Press.

[5] Winter, J.D., 2014. Principles of Igneous and Metamorphic Petrology. 2nd Edition, Pearson Education Limited.

Viscosity of Magma

Ankita Samaddar[1], Debadrita Nag[2] and Tanushri Bera[3]
Students of 5th Semester Geology Honours Course
[1]samaddarankita93@gmail.com, [2]debadritanag@yahoo.co.in
[3]tanushribera13@gmail.com

Abstract: Viscosity of magma is the measure of the resistance of magma to gradual deformation by shear stress. Magma is considered to be non-Newtonian fluid in general. It depends on various factors like silicate structure or polymorphism, temperature, pressure, density, volatile content and crystallinity. Due to difference in viscosity of magma different types of volcanoes, pyroclastic materials and intrusive bodies are formed.

Keywords: Viscosity, Magma, basalt, rhyolite, andesite

1. Introduction to Viscosity

Viscosity is defined as the measure of the resistance of a fluid to gradual deformation by shear stress. In other words, viscosity describes a fluid's resistance to flow.

1.1 Viscosity Formula

Viscosity is measured in terms of ratio of shearing stress to the velocity gradient in a fluid.

$$\eta = \frac{(shear\ stress)}{(shear\ rate)}$$

Where, η is viscosity

1.2 Unit of viscosity

As we know that, the dimensional unit of viscosity is $\eta = \frac{F}{A}\frac{dx}{dv}$

Hence, η = dynes × cm / cm^2 ×cm sec^{-1}. Therefore, we can write as,
η = dynes cm^{-2} sec or the viscosity units are, dynes sec cm^{-2}.

This quantity is known as 1 Poise.

f = m × a

$$\eta = \frac{(m \times a \times dx)}{(A.dv)}$$

Hence, η = g cm^{-1} s^{-1}

Therefore, η = 1 poise. In S.I. units,

$\eta = \frac{F}{A}\frac{dx}{dv}$ = (N×m)/(m^2×ms^{-1})

Therefore, we can write, η = N m^{-2} or Pas

1 Poise = 1 g cm^{-1}sec^{-1} = 0.1 kg m^{-1} s^{-1}

Unit of viscosity- The dimensions of viscosity are force × time ÷ area. The unit of viscosity is newton-second/metre^2. It is usually written as pascal-second in SI unit.

1.3 Types of viscosity

There are 4 types of viscosity

1.3.1 Dynamic viscosity:

Dynamic viscosity is the force needed by a fluid to overcome its own internal molecular friction so that the fluid will flow. In other words, dynamic viscosity is defined as the tangential force per unit area needed to move the fluid in one horizontal plane with respect to other plane with a unit velocity while the fluid's molecules maintain a unit distance apart. Dynamic viscosity is also referred as absolute viscosity in the field of fluid mechanics.

Shear stress can be expressed

$$\tau = \mu \frac{dc}{dy} = \mu\, \gamma \qquad (1)$$

Where,

τ = shearing stress in fluid (N/m^2)

μ = dynamic viscosity of fluid (N s/m^2)

dc = unit velocity (m/s)

dy = unit distance between layers (m)

$\gamma = \frac{dc}{dy}$= shear rate (s^{-1})

Equation (1) is known as the Newton's Law of Friction.

Equation (1) can be rearranged to express Dynamic viscosity as

$$\mu = \tau \frac{dc}{dy} = \frac{\tau}{\gamma} \qquad (1b)$$

1.3.2 Kinematic viscosity: When the dynamic viscosity is divided by the density of the fluid, the viscosity is called kinematic viscosity and it is usually observed under the Newtonian force. It is gained by keeping the temperature same for both viscosities. It is measured in square meters over seconds in the International System of units. The SI unit is poise and it is represented by a symbol V. This type of viscosity is generally seen in *Newtonian fluid*.

The kinematic viscosity formula is expressed as,

$\nu = \mu/\rho$

Where

μ= absolute or dynamic viscosity, = Pa×S= kg/(m×s)

ρ = density = kg/m^3

Therefore, kinematic viscosity = (kg/(m×s)x10^{-3})/ (kg/m^3)= m^2/s×10^{-6}

1.3.3 Extensional viscosity: .Extensional viscosity is a viscosity coefficient when applied stress is extensional stress. It is often used for characterising polymer solutions.

1.3.4 Apparent viscosity: The apparent viscosity is, the shear stress divided by the speed that the fluid takes to deform by the presence of non-linear behaviour. The relationship between the viscosity and shear rate also refers to the apparent viscosity. This type of viscosity is measured by dividing shear stress by shear rate which is directly affected by the shear rate for non-Newtonian fluids. It remains constant for *Newtonian fluids*.

1.4 Newton's Law of Viscosity

Newton's law of viscosity states that "shear stress is directly proportional to velocity gradient"

$$\tau = \mu \frac{du}{dy}$$

Where

μ is the constant of proportionality known as viscosity

τ = shear stress =F/A

$\frac{du}{dy}$ = Rate of shear deformation

2. Newtonian and Non-Newtonian fluid

When viscosity of a fluid is the measure of a fluid's ability to resist flow and only varies in response to changes in temperature or pressure, that fluid is said to be Newtonian. Generally, a Newtonian fluid tends to take the shape of its container. Under constant temperature and pressure conditions, the viscosity of a Newtonian fluid is the ratio between the shear stress that builds within the fluid to resist its flow and the shear rate applied to the fluid to induce flow; the viscosity remains the same for all shear rates applied to the fluid.

The fluid that does not follow Newton's law of viscosity, i.e., has constant viscosity independent of stress is called a non-Newtonian fluid. In non-Newtonian fluids, viscosity changes with rate of deformation or shear strain.

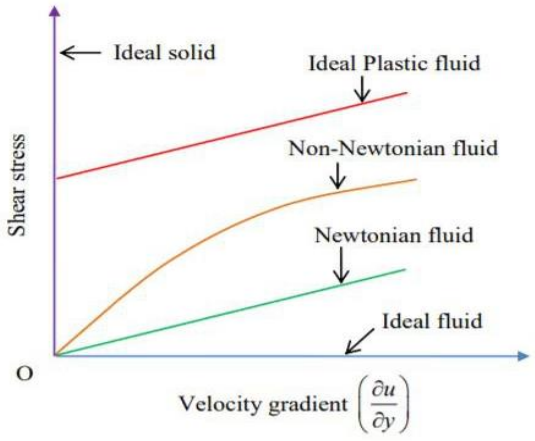

Figure 1: Graph showing Newtonian and non-Newtonian fluid (TutorialsTips 2020)

3. Definition of Magma

Magma is a molten or partially molten rock from which igneous rocks form. It is made up of silicate liquid, although carbonate and sulphide melts occur as well. Magma migrates either at depth as well as at the Earth's surface. When it is ejected outside it is called lava. There are 3 types of magma - Basaltic, Andesitic and Rhyolitic.

4. Whether Magma a Newtonian or Non-Newtonian fluid

Magma is considered to be a non-Newtonian fluid in general that is, the relationship between strain rate and shear stress cannot be described by a linear dependency. Basaltic magma though treated as a quasi-Newtonian liquid, still has observations of non-Newtonian behaviour. With a method a strong shear rate dependency of viscosity in a wide range of temperature for molten basaltic magma was found. The properties of the molten phase as the cause are indicated by temperature-viscosity dependency. An in-depth knowledge of the rheological properties of lava is required by Lava flow models. Lavas are non-Newtonian at their typical eruption temperatures. These occur due to the formation and destruction of crystal networks and bubble deformation during shear. Using analogue fluids with bubble concentrations <20% the effects of bubbles are investigated experimentally in this contribution. Magma is typically a multiphase suspension which consists of silicate melt, crystals and gases. The relative proportion of these three phases significantly influences the magma rheology, and therefore the eruption is dynamic. Then at low gas and crystal volume fractions, magma can be considered to behave as a Newtonian fluid, where the viscosity n_o is constant. However, at moderate crystal and gas fractions, the apparent viscosity of the suspension n_s is function of the shear stress and strain rate ε, such that $n_s = \sigma_s/\varepsilon$.

5. Factors Affecting Viscosity of Magma

5.1 Silicate structure and polymorphism: The basic fundamental structural unit of all silicate minerals is the silicon tetrahedron where one silicon atom is surrounded by four oxygen atoms (each at the corner of a regular tetrahedron). Oxygen atoms can be linked in variety of ways with these SiO4 tetrahedron. The ability of a specific chemical composition to crystallize in more than one form is called polymorphism. This normally occurs due to change in temperature or pressure or both.

Melts have a short range of structural order where tetrahedrally coordinated Si and Al cation are surrounded by 4 O anion and octahedrally bonded cations such as Ca and Fe^{2+} surrounded by 6 O anion. There can be little change in the degree of order in the molecular structure of the melt relative to the crystalline silica because the entropy of melting of the crystalline silica is relatively small. Short range order is roughly similar to crystalline state, whereas long range order is evident where symmetric crystal lattice absent.

Viscosity is the most important dynamic property of magma or melt which depends on their molecular structure. It is determined largely by its chemical composition which controls it degree of polymerization. Highly polymerized melts are more viscous. Depolymerization of magma due to increase in some components can reduce viscosity i.e., increase in small proportion of dissolved water or fluorine can depolymerize the magma.

Water free (dry) rhyolitic magma is nearly completely polymerized, has no non bridging O_2 virtually so they are highly viscous. Mineral content of groundmass of rhyolitic magma is generally quartz and plagioclase, with lesser amounts of orthoclase, biotite, amphibole (augite), pyroxene (hornblende), and glass whereas phenocrysts is of plagioclase and quartz, often with amphibole and/or biotite, sometimes orthoclase. The mineral assemblage is predominantly quartz, sanidine, and plagioclase.

In basaltic magma as the silica content is low, the abundance of Fe, Mg, Ca is high resulting in increase in number of non bridging oxygens (NBO). Increase in NBO makes the bonds weaker and making it less viscous. Olivine and augite are the most common porphyritic minerals in them; porphyritic plagioclase feldspars are also found. Basaltic lavas are frequently spongy or pumiceous and the steam cavities become filled with secondary minerals such as calcite, chlorite, and zeolites. Common minerals in basaltic magma include olivine, pyroxene, and plagioclase. Basaltic magma promotes the growth of large crystals like pegmatites, but crystal growth is prevented in rhyolitic magmas, which usually are quenched as glass.

Andesitic magma is rich in plagioclase feldspar and amphibole minerals. Quartz and pyroxene minerals may be absent or present in small quantities and small amounts of micamay be present as biotite or muscovite. Andesites contain crystals composed primarily of plagioclase feldspar and pyroxene (clinopyroxene and orthopyroxene) and lesser amounts of hornblende. Peridotite will produce andesitic melts during partial melting under hydrous conditions.

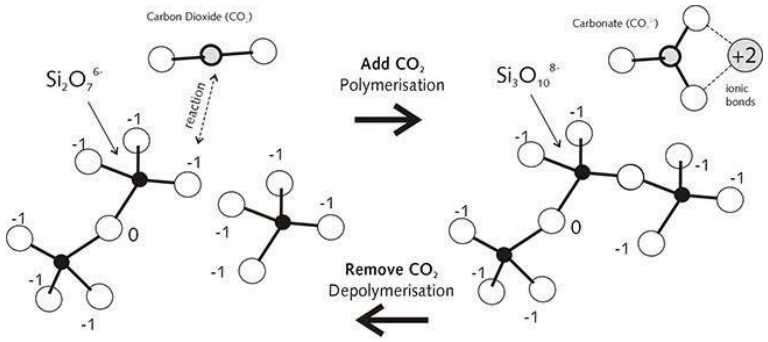

Figure 2: Polymerisation and depolymerisation of silicate structure (Alexstrekeisen 2021)

5.2 Temperature: Temperature has a significant influence on viscosity. The higher is the temperature, the lower is the viscosity as viscosity is an exponential function of temperature (according to Arrhenian model of viscosity). The Arrhenian equation is –

$$\eta(T) = \eta(o)exp\left(-\frac{E}{RT}\right)$$

Where, $\eta(o)$ = viscosity under standard temperature and condition
E = Activation energy
R = Universal gas constant
T = Temperature

The impact of increase in temperature of magma reduces the cohesive force which results in decrease in viscosity. Similarly with decrease in temperature of magma, their cohesive force increases making it more viscous.

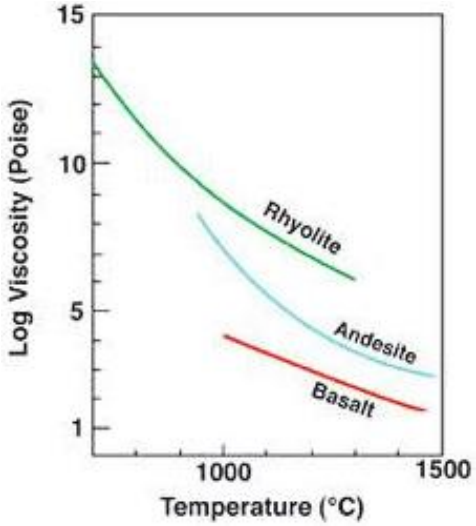

Figure 3: Temperature effecting viscosity of different types of magma (Volcanocafé 2014).

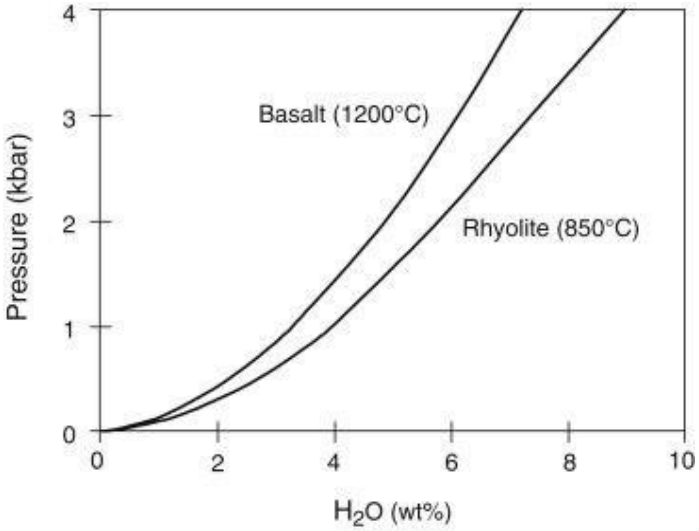

Figure 4: Pressure effecting viscosity of different types of magma (Wallace et al. 2015).

5.3 Pressure: The direct influence of pressure on magma viscosity is much less than chemical composition and temperature. Higher pressure promotes solution of more water in the magmas, which depolymerizes the magma and lowers the viscosity. Lower pressure restricts solution of water in the magmas, which polymerizes the magma making it more viscous.

5.4 Density: Density (ρ) and viscosity (μ) of hydrous silicate magmas are two geologically important physical properties that determine their migration through the Earth's mantle and crust. Changes in density and viscosity affect buoyant ascent potential and ease of flow. In natural environments density and viscosity change in response to changing pressure (P), temperature (T) and composition (X) along a flow path. Then by analysing the pressure, temperature and composition, how fast magma can flow through inside the earth can be determined.. Densities of common magmas near the surface of earth vary from 2.3 – 3.0 Mgm^{-3}. The bulk densities of magma are intermediate between solid igneous rocks and pure magmatic liquids because most magmas are mixtures of liquid and crystals. Magma being compressed under higher pressures at high depth has higher density. But if the increased

pressure is the result of high amount of dissolved water, the resulting change in magma composition decreases the density significantly.

5.5 Volatile content (CO_2 and H_2O): The combination of viscosity and volatile content determines whether a volcanic eruption will be violent or quiet. The volatiles diffuse very easily through silicate magmas, mainly if polymerization is low. Volatile content and viscosity are directly proportional to each other. Lower the volatile content lower will be its viscosity. In less viscous magma the volatiles can escape easily through it resulting decrease in its volatile content. Whereas in high viscous magma the volatiles could not escape through the magma resulting increase in volatile content.

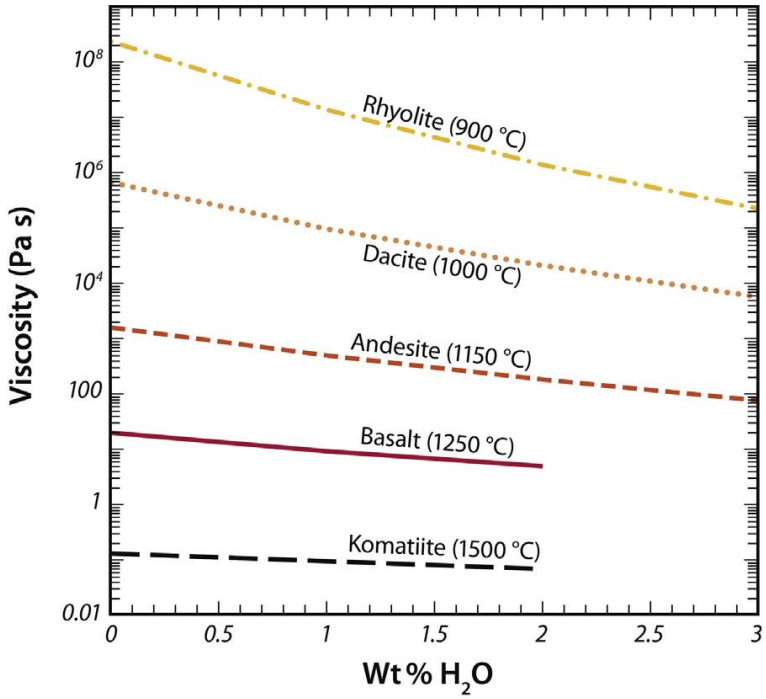

Figure 5: Effect of volatile content on viscosity of magma (Lesher & Spera 2015)

5.6 Crystallinity/grain size: The viscous magma opposes diffusion of ions by inhibiting crystallisation. Silica content of magma is directly related to viscosity of magma as SiO_4 and AlO_4 complexes form linkages to produce a dense network. Thus, viscous magma results in formation of fine-grained rock like rhyolite. The less viscous rock has a wider time span for crystallization so it results in formation of coarse-grained rock like diorite. The low viscosity of magma permits initiation of process of formation of euhedral phenocrysts within magma itself. The relative deformable phase volume of magma is decreased by phenocryst. The mechanical interactions between phenocrysts have a strong effect on bulk magma rheology so it increases magma viscosity. The phenocryst bearing magmas develop a yield strength and strain rate dependent viscosity so it become non-Newtonian. The magma viscosity decreases with increasing strain rate when the phenocryst content is fixed.

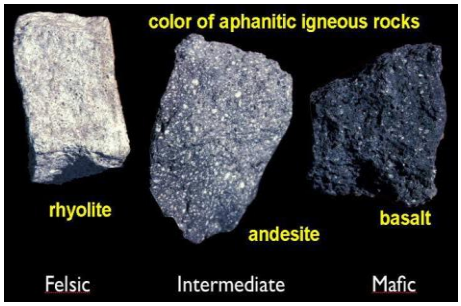

Figure 6: Different type of Igneous rock

Table 1: Different types of Magmas

Magma type	Solidified Rock	Chemical Composition	Temperature	Pressure	Polymorphism	Volatile content	Viscosity
Basaltic	Basalt (Coarse grained)	45 – 55% SiO_2, high in Fe, Mg, Ca, low in K, Na	1000°C–1200°C	100–200 MPa	Depolymerized	Low	Low
Andesitic	Andesite (Medium grained)	55 – 65% SiO_2, intermediate in Fe, Mg, Ca, Na, K	800°–1000°C		Moderately polymerized	Intermediate	Intermediate
Rhyolitic	Rhyolite (Fine grained)	65 – 75% SiO_2, low in Fe, Mg, Ca, high in K, Na	650°C–800°C	800 MPa	Completely polymerized	High	High

7A 7B 7C

Figure 7: A–Basaltic magma, B–Andesitic magma, C–Rhyolitic magma (Scientia 2021)

6. Effects of magma viscosity

6.1 Volcanic landforms: The geological processes that form volcanos and act on them after they have formed control volcanic landforms. Thus, a given volcanic landform will show the characteristic of the type of material it is made up of, which depends on the prior eruptive behaviour of that volcano itself.

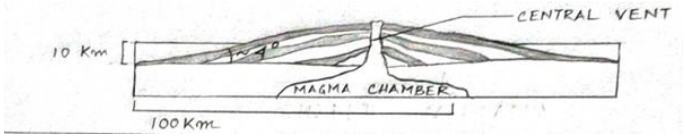

Shield volcano

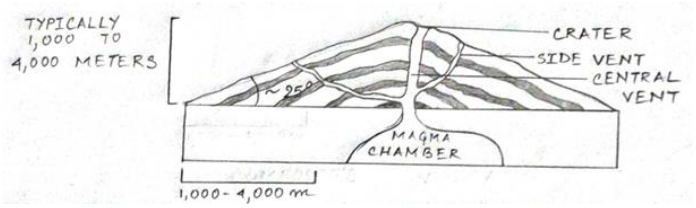

Composite volcano

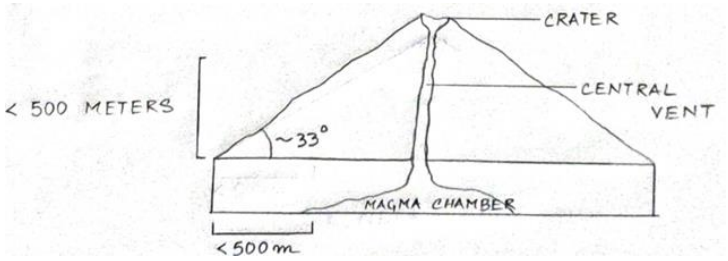

Cinder cone

Figure 8: Types of volcanoes

6.2 Types of volcanos: There are mainly 3 types of volcanos – shield volcano, stratovolcano or composite volcano and cinder cone.

6.2.1 Shield volcano: A shield volcano is characterized by gentle upper slopes (about 5°) and somewhat steeper lower slopes (about 10°). They are composed almost entirely of relatively thin lava flows built up over a central vent. Most of them are formed of low viscosity basaltic magma that can flow downslope easily from the summit vent.

6.2.2 Stratovolcano or composite volcano: A composite volcano is characterized by steep upper slopes (about 30°) and somewhat gentle lower slopes (about 6°-10°). Most of them are formed of high viscosity rhyolitic magma that do not travel far downslope from the summit vent. They are usually more explosive than shield volcanoes due to its higher viscosity magmas erupted from these volcanoes. Stratovolcano show interlayering of lava flow and pyroclastic material so it is called composite volcano.

6.2.3 Cinder cone: Cinder cone is characterized by steep slope (between about 25 and 35o). They are formed of low to moderate viscosity of basaltic to andesitic material. They are small volume cones consisting predominantly of ash and scoria that result from mildly explosive eruptions.

Table2: Types of Volcanoes

Name of volcano	Slope of the volcano	Composition	Explosive/ Non explosive
Shield volcano	gentle upper slopes (about 5°) and somewhat steeper lower slopes (about 10°)	low viscosity basaltic magma	Non explosive
Stratovolcano	steep upper slopes (about 30°)	high viscosity rhyolitic	Explosive

	and somewhat gentle lower slopes (about 6-10°).	magma	
Cinder cone	steep slope (between about 25 and 35°)	low to moderate viscosity of basaltic to andesitic material	Mildly explosive

6.3 Pyroclastic material: When the magma has high gas content and high viscosity then the gas will expand in an explosive way and break the liquid into clot that can fly through the air and cool along the path through the atmosphere. Alternatively, the solid pieces of rock that once formed, the volcanic edifice blasts out. All these fragments are considered to be as pyroclasts. Loose fragments of pyroclasts are called tephra. Pyroclastic flow and explosive eruptions associate with highly viscous lava. They can be classified into bomb, block, lapilli or ash depending on size.

- Blocks: They are angular fragments which were solid during ejection
- Bombs: They are solid fragments with an aerodynamic shape which indicates that it is liquid during ejection.
- Lapilli: They are unconsolidated volcanic fragments that are ejected during explosion.
- Ash: They are dissolved gases in magma that escaped violently in atmosphere.

Table3: Classification of Tephras and pyroclastic rocks

	Tephra and Pyroclastic rocks	
Average particle size (mm)	Unconsolidated material (Tephra)	Pyroclastic rock
>64	Bombs or blocks	Agglomerate
2-64	Lapilli	Lapilli tuff
< 2	Ash	Ash tuff

7. Emplacement and crystallization of magma

Igneous bodies are formed as a result of solidification of magma. When magma is cooled at depth it forms intrusive bodies or plutonic bodies called plutons. The intrusion of magma affects the surrounding rock and vice-versa. It causes hydrothermal alteration or the surrounding rocks may get metamorphosed by it. When magma comes in contact with surrounding rocks it cools rapidly near the contact forming chilled margins.

Viscosity determines the action of magma. Mafic magma being less viscous will flow easily to the surface whereas felsic magma being more viscous does not flow easily. Most felsic magma stays deeper in the crust and cools down to form intrusive igneous rocks such as granite and granodiorite. The felsic magma gets stuck within the magma chamber as it is too viscous to move through it. The magma chamber begins to build pressure when dissolved gases get trapped by thick magma. On the basis of forms mode of emplacement of magma, igneous bodies can be divided into intrusive rock bodies and extrusive rock bodies.

7.1. Intrusive Rock bodies: An igneous rock bodies that form by magma crystallization by slow cooling below the surface of the Earth at considerable depth.

7.2. Extrusive Rock bodies: An igneous rock bodies that being derived from magma (molten silicate material) poured out or ejected at Earth's surface.

Intrusive Rock bodies are further subdivided into plutonic (at moderate to great depth large intrusions are formed) and hypabyssal (near the Earth's surface small intrusions are formed).

7.1.1 Sill: Sills are thin tabular sheets of magma which occur parallelly along the bedding surfaces that enclose them. They are two dimensional bodies with contact walls more or less parallel and have relatively narrow width. Thickness is maximum near the eruption vein and it decreases away from the vein. They usually vary in thickness from few centimetres to several metres. They are formed when magma intrudes between the bedding plane of country rocks, forming a horizontal or gently-dipping sheet of igneous rock. Their spreading capacity mainly depends on the viscosity of magma and basic magma being more hot and more fluid usually occur as sill. Often occur in clusters which are regionally distributed forming swarms or belts.

7.1.2 Laccolith: If the viscosity of magma is relatively high as a result the spreading rate is low, the magma accumulates locally and lifts the cover rock in the form of a dome. A laccolith is thus formed as the magma body accumulates in the form of a mushroom with arched roof and flat floor. It often occurs in clusters or swarms. If an upright laccolith is eroded, a central oval outcrop pattern on the ground surface will be produced; the body may be associated with a number of annular lenticular smaller satellite laccoliths and sills. Example: Sitampundi complex, South India.

7.1.3 Lopolith: Lopoliths are large concordant intrusions which are saucer shaped having a contrast geometry to that of laccolith i.e., concavity upward. Lopoliths are of much larger dimensions than laccoliths. They are formed when basic magmas are emplaced under calm condition showing evidences of slow cooling. Development of prominent layers can be seen and the layers may be of different mineralogy and section. Largest lopolith- Bushveld complex in South Africa covering an area of about 66,000 sq. kms.

7.1.4 Dyke: Dykes are tabular or sheet like discordant intrusions which crosscut the planer surfaces of country rocks. It is formed when magma intrudes vertically or at an angle into a line weakness cutting across bedding planes which eventually cools and solidifies at a very slow rate there. The overlying rocks may collapse when an emplaced magma comes closer to the surface, producing caldera. Dykes vary in texture and composition which can range from diabase or basaltic to granitic to rhyolite, but basaltic composition mainly occurs on a global perspective. Usually, they occur in clusters with regional distributions and are described as swarms or belts. Annular fractures filled by intruded magma is often associated with such

collapse. These arcuate systems of sheet intrusions are described as ring dykes. It is Usually, described as ring complex or central complex when a variety of dyke rocks constitute such a ring system.

7.1.5 Batholith: A batholith is a large mass of intrusive igneous rock which is formed when the magma cools beneath the earth's surface, forming a rock structure that extends at least one hundred square kilometres across and to an unknown depth. Batholiths are almost always made mostly of felsic or intermediate rock types, such as granite, quartz monzonite, or diorite.

7.1.6 Bysmalith: Bysmaliths are more or less vertical and cylindrical discordant bodies that crosscut adjacent sediments and are bounded by steep faults. They are commonly associated with the mountain-building or orogenic processes, and are typically composed of granites or granodiorites. It is formed when highly viscous magma is injected so that the lateral spreading along the bedding plane will be very less, thus the intruding magma acquires a cylindrical shaped body.

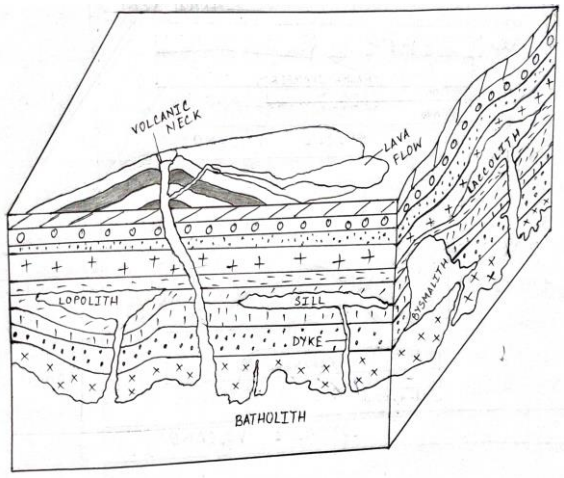

Figure 9: Forms of igneous bodies

8. Change of rock texture in response to magma viscosity

8.1 Pearlitic cracks: The texture that represents conchoidal fracture system consisting of numerous curving cracks roughly concentric around closely spaced centres is called pearlitic cracks. It is formed by the rapid cooling of viscous lava or magma. It is generally developed in microscopic scale in acid glasses (rhyolitic or dacite) called pitchstone.

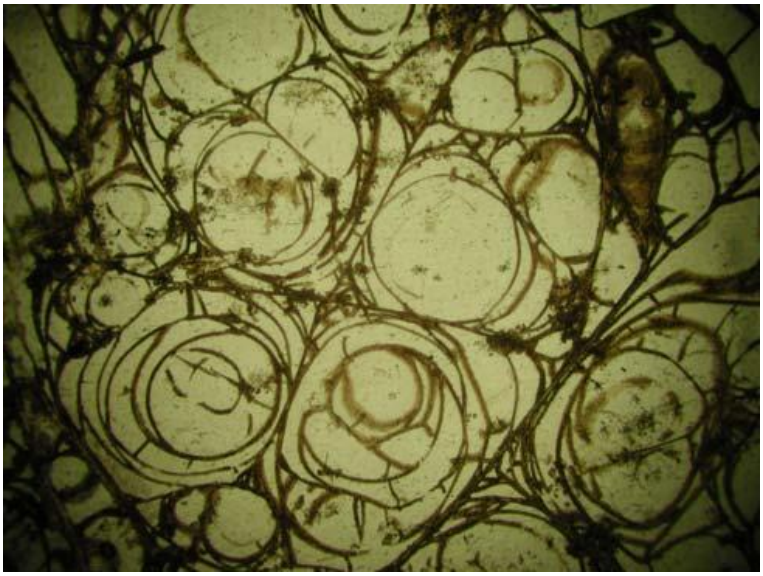

Figure 10: Pearlitic cracks (Rotella & Simandl 2010)

8.2 Spinifex texture: Spinifex texture is the most diagnostic fabric of ultramafic lavas, such as Precambrian komatiites, The texture consists of bunches cress-crossing arrays of highly elongated olivine crystals (many cm long but less than a cm thick). It results from rapid growth of olivine (with simple structure) in a very low viscosity magma and not by slow cooling.

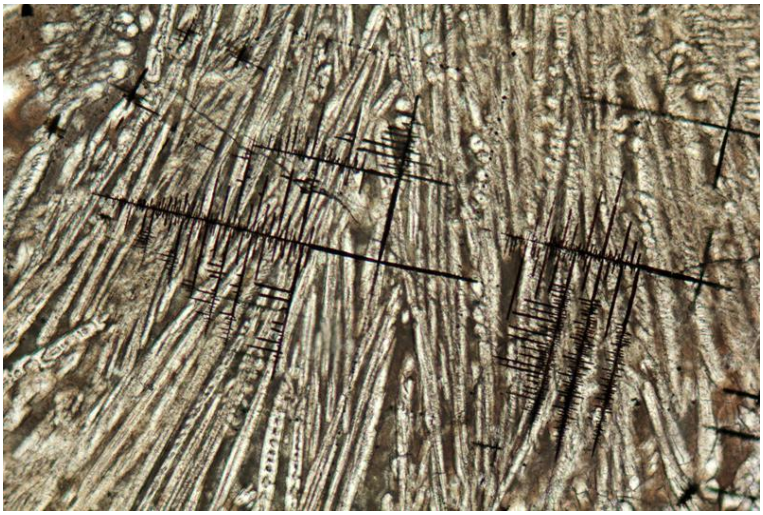

Figure 11: Spinifex texture (Alexstrekeisen 2021)

8.3 Glassy texture: The texture of a rock in which it looks like a block of (coloured) glass, with no visible mineral crystals is called glassy texture. It forms due to rapid cooling of magma so that that no crystals could form. The high silica (SiO_2) concentrations found in rhyolitic rocks causes a rock to form a glass much more easily than it would in low silica rocks such as basalt. Thus, the rate of cooling of a basaltic and rhyolitic lava flow could be the same, but the rhyolitic flow would form a glass because it is packed with silica.

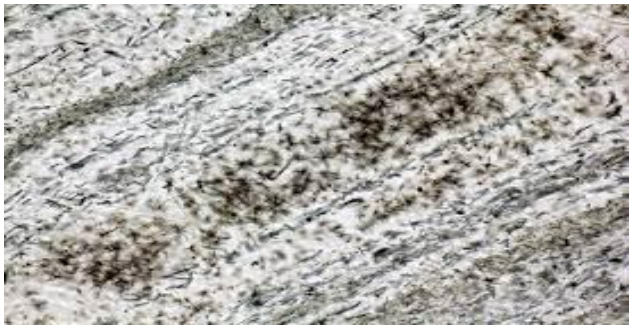

Figure 12: Glassy texture

8.4 Trachytic texture: The texture of a rock where the groundmass contains little volcanic glass and consists predominantly of minute tabular crystals, namely, sanidine microlites are called trachytic texture. The microlites are parallel, forming flow lines along the directions of lava flow and around inclusions. This texture occurs in rocks that are rich in alkalis; hence the vitreous mass of the rocks has a relatively low viscosity. It is especially characteristic of trachytes and rocks similar to trachytes. . Macroscopic trachytic textures which are visible with the naked eye are sometimes called trachytoid textures.

Figure 13: Trachytic texture

9. Conclusion

Viscosity is defined as the measure of the resistance of a fluid to gradual deformation by shear stress. Magma being a non-Newtonian fluid also has viscosity. Viscosity of magma depends on factors such as polymorphism of silicate structure, temperature, density, pressure, volatile content, crystallinity and grain size etc. Thus, we come to the conclusion that magma with less viscosity is depolymerized, has low density, low pressure, low volatile content, high temperature and the opposite is true for highly viscous magma. Viscosity of magma influences the types of volcanoes formed around the world and the pyroclastic materials ejected from them. Types of volcanoes include mainly shield volcano, stratovolcano and cinder cones and they have low, high and intermediate viscosity respectively. Forms of

igneous bodies also depend on the viscosity of magma such as low viscosity basaltic magma results in formation of sill, lopolith, and dyke; high viscosity rhyolitic magma results in formation of laccolith, bysmalith whereas intermediate viscosity andesitic magma results in formation of batholiths.

ACKNOWLEDGEMENT

We would like to express our gratitude to our mentor Prof. Keya Bandyopadhyay for her sincere guidance and valuable suggestions.

REFERENCE

[1] Alexstrekeisen (2021) Spinifex texture. (*Website*) Available at: https://www.alexstrekeisen.it/english/vulc/spinifex.php. Accessed on: 09-11-2021.

[2] Alexstrekeisen (2021) Holohyaline texture. (*Website*) Available at: https://www.alexstrekeisen.it/english/vulc/holohyaline.php. Accessed on: 15-11-2021.

[3] Alexstrekeisen (2021) Trachytic texture. (*Website*) Available at: https://www.alexstrekeisen.it/english/vulc/trachytic.php. Accessed on: 15-11-2021.

[4] Alexstrekeisen (2021) Volcanic Rocks. (*Website*) Available at: https://www.alexstrekeisen.it/english/vulc/index.php. Accessed on: 07-09-2021.

[5] Auckland (2021) Rhyolite. (*Website: The University of Auckland*.) Available at: https://rocksminerals.flexiblelearning.auckland.ac.nz/rocks/rhyolite.html. Accessed on: 09-11-2021.

[6] AZoNetwork (2013) How does Temperature Change Viscosity in Liquids and Gases? Updated on: Sep 23, 2013. Accessed from: https://www.azom.com/article.aspx?ArticleID=10036. Accessed on: 02-09-2022.

[7] Britannica (2022) Magma. Updated on: Apr 05, 2022. Accessed from: https://www.britannica.com/science/magma-rock. Accessed on: 02-09-2022.

[8] Britannica (2018) Silicate Mineral. Updated on: Aug 17, 2018. Accessed from: https://www.britannica.com/science/silicate-mineral. Accessed on: 02-09-2021.

[9] Britannica (2022) Polymorphism. Accessed from: https://www.britannica.com/science/mineral-chemical-compound/Polymorphism. Accessed on: 02-09-2021.

[10] Britannica (2021) Basalt. (*Website*) Available at: https://www.britannica.com/science/basalt. Accessed on: 09-11-2021.

[11] Britannica (2021) Classification of volcanic and hypabyssal rocks. (*Website*) Available at: https://www.britannica.com/science/igneous-rock/Classification-of-volcanic-and-hypabyssal-rocks. Accessed on: 09-11-2021.

[12] Britannica (2021) Discover why some volcanic eruptions are more explosive, like at Mount Pinatubo in contrast to Kilauea. (*Website*) Available at:

https://www.britannica.com/video/182702/magma-role-components-eruptions-flow-explosiveness-rate. Accessed on: 07-09-2021.

[13] Best, M.G., 2003. Igneous & Metamorphic Petrology. Blackwell, Oxford, UK, 729p.

[14] Bose M.K., 2017. *Igneous petrology* 2nd edition; World Press, Calcutta. 358p

[15] CSCScientifi (2020) What is the Difference Between Dynamic and Kinematic Viscosity? Written by Art Gatenby; Last updated on: Oct 19, 2020 7:30:00 AM (*Website*) Available at: https://www.cscscientific.com/csc-scientific-blog/whats-the-difference-between-dynamic-and-kinematic-viscosity?hs_amp=true. Accessed on: 13-09-2021.

[16] CorrosionPedia (2020) Dynamic Viscosity. Available at: https://www.corrosionpedia.com/definition/5323/dynamic-viscosity. Accessed on: 09-11-2021

[17] Course Hero (2021) Magma Composition. (*Website*) Available at: https://www.coursehero.com/study-guides/geophysical/magma-composition/. Accessed on: 09-11-2021.

[18] GeeksforGeeks (2022) Dynamic Viscosity Formula, Last updated on Apr 04, 2022 Available at: https://www.geeksforgeeks.org/dynamic-viscosity-formula/. Accessed on: 12-09-2021.

[19] Girty G.H. (2009) Perilous Earth: Understanding Processes Behind Natural Disasters, ver. 1.0, June, 2009. Department of Geological Sciences, San Diego State University. Available at: http://www.sci.sdsu.edu/visualgeology/naturaldisasters/Chapters/_Chapter2Volcanoes.pdf Accessed on: 12-09-2021.

[20] GuidanceCorner (2021) Types of Viscosity. (*Website*) Available at: https://guidancecorner.com/types-of-viscosity/. Accessed on: 12-09-2021.

[21] Hack A.C. and Thompson A.B. (2011) Density and Viscosity of Hydrous Magmas and Related Fluids and their Role in Subduction Zone Processes; Journal of Petrology 52(7 & 8): 1333–1362. doi:10.1093/Petrology/Egq048

[22] Hale A.J., Wadge G. and Mühlhaus H.B. (2017) The influence of viscous and latent heating on crystal-rich magma flow in a conduit. *Geophys. J. Int.* **171:** 1406–1429.

[23] King, H.M. (2021) Andesite. (*Website*) Available at: https://geology.com/rocks/andesite.shtml. Accessed on: 09-11-2021.

[24] Lesher, C.E., Spera, F.J., 2015. Thermodynamic and Transport Properties of Silicate Melts and Magma. In: Sigurdsson, H., Houghton, B., Rymer, H., Stix, J., McNutt, S. (Eds.), The Encyclopedia of Volcanoes, pp. 113–141. ISBN: 9780123859389

[25] Nelson S.A. (2017) Volcanoes and Volcanic Eruptions. Course Material (EENS/1110 Physical Geology) Tulane University. Last updated on Aug 26, 2017 (*Website content*) https://www2.tulane.edu/~sanelson/eens1110/volcanoes.pdf. Accessed on: 12-09-2021.

[26] Philpotts and Auge 2009 Principles of Igneous and Metamorphic Petrology 2nd edition. Cambridge University Press. 684p. ISBN: 9780521880060

[27] PITT (2021) Glassy Textures. (*Website*) Available at: https://sites.pitt.edu/~cejones/GeoImages/2IgneousRocks/IgneousTextures/6Glassy.html. Accessed on: 05-11-2021.

[28] Reddit (2021) Is Lava a non-Neutonian fluid? (*Website: r/askgeology*) Available at: https://www.reddit.com/r/askgeology/comments/8w3qir/is_lava_a_nonneutonian_fluid/. Accessed on: 13-09-2021.

[29] Rotella M. and Simandl G. (2010) Marilla Perlite – Volcanic Glass Occurrence, British Columbia. *In Industrial Minerals with emphasis on Western North America*. pp.263–272. Available at: https://www.researchgate.net/publication/237619193. Accessed on: 09-11-2021.

[30] Scientia (2021) Andesitic Magma. (*Website*) Available at: https://scientiafantastica.wixsite.com/scientiafantastica/single-post/2017/12/06/andesitic-magma. Accessed on: 07-09-2021.

[31] Scientia (2021) Andesitic Magma. (*Website*) Available at: https://scientiafantastica.wixsite.com/scientiafantastica/single-post/2017/12/06/andesitic-magma. Accessed on: 07-09-2021.

[32] Scientia (2021) Rhyolitic Magma. (*Website*) Available at: https://scientiafantastica.wixsite.com/scientiafantastica/single-post/2017/12/02/rhyolitic-magma. Accessed on: 07-09-2021.

[33] SlideShare (2021) Intrusive topography. (*Website*) Available at: https://www.slideshare.net/venkateshsambandan/intrusive-topography. Accessed on: 02-09-2021.

[34] SlideShare (2021) Igneous rocks. (*Website*) Available at: https://www.slideshare.net/gauravhtandon1/igneous-rocks-27236143. Accessed on: 03-09-2021.

[35] USGS (2015) EarthWord: Batholith. Last updated on: September 7, 2015 (*Website*) Available at: https://www.usgs.gov/news/earthword-batholith. Accessed on: 03-09-2021.

[36] Saint Clair Systems (2017) Measuring the Different Types of Viscosity with Viscometers. Posted by Mike Bonner; Last updated on: Nov 30, 2017 3:01:00 PM (*Website*) Available at: https://blog.viscosity.com/blog/measuring-the-different-types-of-viscosity-with-viscometers. Accessed on: 13-09-2021.

[37] TutorialsTips (2020) Volcanocafé (2014) Magma properties and Lava Fragmentation – in simple words. (Website) Available at: https://volcanocafe.wordpress.com/2014/05/29/magma-properties-and-lava-fragmentation/. Accessed on: 07-11-2021. Last updated on: October 20, 2020 (*Website*) Available at: https://tutorialstipscivil.com/civil-topics/types-of-fluid/. Accessed on: 07-09-2021.

[38] Wikipedia (2021) Dike (geology). (*Website*) Available at: https://en.wikipedia.org/wiki/Dike_(geology)#Magmatic_dikes. Accessed on: 06-09-2021.

[39] Wikipedia (2021) Rhyolite. (*Website*) Available at: https://en.m.wikipedia.org/wiki/Rhyolite#. Accessed on: 09-11-2021.

[40] USGS (2021) Glossary – Andesite. (*Website*) Available at: https://volcanoes.usgs.gov/vsc/glossary/andesite.html. Accessed on: 09-11-2021.

[41] Volcanocafé (2014) Magma properties and Lava Fragmentation – in simple words. (*Website*) Available at: https://volcanocafe.wordpress.com/2014/05/29/magma-properties-and-lava-fragmentation/. Accessed on: 07-11-2021.

[42] Volcanocafé (2014) Magma properties and Lava Fragmentation – in simple words. (*Website*) Available at: https://volcanocafe.wordpress.com/2014/05/29/magma-properties-and-lava-fragmentation/. Accessed on: 07-11-2021.

[43] Wallace P.J., Plank T., Edmonds M., Hauri, E.H. (2015) Chapter 7 - Volatiles in Magmas, in Sigurdsson H. (editor): The Encyclopedia of Volcanoes (2nd Edition), Academic Press, pp.163-183. ISBN 9780123859389, doi:10.1016/B978-0-12-385938-9.00007-9. Available at: https://www.sciencedirect.com/science/article/pii/B9780123859389000079

[44] Wallace P.J., Plank T., Edmonds M., Hauri, E.H. (2015) Chapter 7 - Volatiles in Magmas, in Sigurdsson H. (editor): The Encyclopedia of Volcanoes (2nd Edition), Academic Press, pp.163-183. ISBN 9780123859389, doi:10.1016/B978-0-12-385938-9.00007-9. Available at: https://www.sciencedirect.com/science/article/pii/B9780123859389000079

New nomenclature of para-amphibolite depending on its mineralogical aspects and chemical composition – An attempt

Sneha Chakroborty[1], Debarati Bhowmick[2], Srila Bhowmik[3]
Students of 5th Semester Geology Honours Course
[1]*chakrabortysneha14@gmail.com*, [2]*bhowmicktuhina@gmail.com*, [3]*srilabhowmik@gmail.com*

1. Introduction

Amphibolites are the most common metamorphic rocks formed by regional metamorphism under high pressure and high temperature. It usually occurs along with the mica schist and gneiss. The mineral composition of the amphibolites is simple and mostly contains hornblende and plagioclase, with variable amounts of anthophyllite, garnet, mica, quartz, and epidote etc. The rocks may originate from pelitic sediments, with amphibole (hornblende), plagioclase, and typically include green pyroxene. Amphibolite has a formula $X_2Y_5Si_8O_{22}(OH)_2$. It is an important group of generally dark-coloured, inosilicate minerals, forming prism or needle-like crystals, composed of double chain SiO_4 tetrahedra, linked at the vertices and generally containing ions of iron and /or magnesium in their structures. Long prismatic, acicular, or fibrous amphibole crystallizes in orthorhombic and / or monoclinic system.

It has a deep green colour. Amphibole is characterized by two sets of cleavage which is oriented at an angle of 56° and 124°, six-sided basal cross sections, characteristic colour and its pleochroism.

The development of schistosity is considerably less pronounced in amphibolites. They are mainly influenced by more or less parallel orientation of prismatic crystals of black hornblende. The rocks are often striped due to semi-parallel sort of mutual narrow bands, predominantly of rich black hornblende and light plagioclase. These rocks are characterized by nematoblastic or granoblastic texture (Figures 1and 2).

2. Types of Amphibolite:

1.Amphibolite
2.Ortho- amphibolite
3.Para-amphibolite
4.Chlorite amphibolite
5.Epidote amphibolite
6.Feather amphibolite
7.Post-eclogite amphibolite
8.Pyroxene amphibolite
9.Davianite

Amphibolite is divisible into three parts based on their structure: massive, schistose, gneissose/ banded.

Figure 1
Amphibolite (Streckeisen 2021)

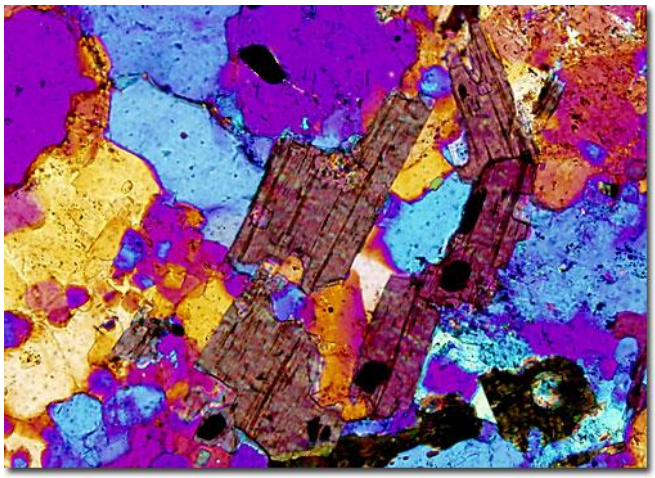

Figure 2
Amphibolite under microscope (FSU 2021)

2.1 Ortho-amphibolite

Metamorphic rocks composed primarily of amphibole with subordinate albite, epidote, zoisite, chlorite, quartz, titanite, and accessory leucoxene, ilmenite and magnetite which have a protolith of an igneous rock are known as ortho-amphibolite. The amphibolites may also occur from various neutrals and basic igneous rocks. The ortho-amphibolite (Figure 3) includes mainly amphibole (hornblende) and albite, and even small amounts of epidote, zoisite, chlorite, and quartz. It often contains incomplete metamorphic remains of protolith igneous rocks.

2.2 Para-amphibolite

Para-amphibolite generally have the same equilibrium mineral assemblage as ortho-amphibolite, with more biotite, and may include more quartz, plagioclase, and depending on the protolith, more calcite/aragonite and wollastonite. These amphibolites may occur out of marl, pelitic sediments, and clay limestone. The para-amphibolites (Figure 4) are balanced in composition. It contains biotite, more of quartz, albite, wollastonite, and calcite, in addition to hornblende and plagioclase, unlike ortho-amphibolites. It contains less of protolith (incomplete metamorphosed relics of sedimentary rocks) than ortho-amphibolite.

Figure 3: Ortho-amphibolite

Figure 4: Para-amphibolite

2.3 Geochemistry of Amphibolite

Often the easiest way to determine the true nature of an amphibolite is to inspect its field relationships; especially whether it is interfingered with other metasedimentary rocks, especially greywacke and other poorly sorted sedimentary rocks. If the amphibolite appears to transgress apparent protolith bedding surfaces it is an ortho-amphibolite, as this suggests it was a dyke. Thereafter, whole rock geochemistry will suitably identify ortho- from para-amphibolite.

Although ortho-amphibolites can often be distinguished chemically from para-amphibolites by their higher contents of Cr, Ni, and Ti, and lower Niggli k ratios, no criterion based on abundance levels is generally applicable because many basic igneous rocks have low Cr, Ni, and Ti contents, and alkali metasomatism in metamorphic terrains often disturbs the k ratio. Of much more value is the distinction between igneous and sedimentary trends of variation. This requires enough analyses to establish a reliable trend. Some critical plots are needed.

The Karroo dolerites from South Africa and the Connemara striped amphibolites from western Ireland are compared with amphibolites from Langøy (N. Norway), Bakersville-Roan area (N. Carolina, U.S.A.), and NW. Queensland (Australia). When the compositions are plotted the plots confirm the origin of the ortho-amphibolites from these regions but some of the supposed para-amphibolites may be ortho-amphibolites and more analyses are needed to define reliable trends of variation.

Para-amphibolite contains less of protolith (incomplete metamorphosed relics of sedimentary rocks) than ortho-amphibolite.

Figure 5: Calc-silicate rock (Wikipedia 2020)

3. Calc-Silicate

Calcsilicate rock is a metamorphic rock (Figure 5) mainly composed of calc-silicate minerals, such as diopside, grossular-andradite, clinozoisite-epidote and wollastonite less than 5% volume of carbonate minerals (usually dolomite or calcite). A calc–silicate rock is generally produced by metasomatic alteration of pre-existing rocks in which calcium silicate minerals such as diopside and wollastonite are produced. It is also formed by metamorphism of impure limestone or dolostone; related to skarns.

Figure 6: Larnite (RRUFF 2021)

Figure 7: Californite (Mindat 2021)

3.1 Geochemistry of Calc-Silicate

Calcium silicate is the chemical compound Ca2SiO4, also known as calcium orthosilicate and is sometimes formulated as 2CaO·SiO2. It is also referred to by the shortened trade name Cal-Sil or Calsil. It occurs naturally as the mineral *larnite* (Figure 6).

3.2 Classification of Calc-silicate rock

There are three types of rock based of proportion of calcium.

- Metamorphic rock
- Metacarbonate rock
- Calc-silicate rock

Sub-divisions of Calc-silicate rock: Two types of calc-silicate rocks are named: (a) Californite and (b) Tactite

(a) Californite: It is a variety of *Vesuvianite* (Figure 7), typically found in areas where contact metamorphism occurs.

(b) Tactite: It is a contact metamorphosed carbonate rock (Figure 8) which contains crystalline silicate minerals like garnet, diopside, vesuvian

Figure 8: Tactite (Alamy 2021)

3.3 Mineralogy of calc-silicate rock

Detailed microscopic study shows that calc-silicate rocks normally appear as 0.5 – 2.25 mm thick, mineralogical simple, reaction zones along the contact between Carbonate and Quartz-Feldspar rich metapelite layers.

Calc-silicates are rocks rich in Ca-Mg-silicate minerals but poor in carbonate.

- They form via the metamorphism of very impure calcite or dolomite limestones, or from limy mudstones (marls).
- Since calc–silicates contain significant amounts of other chemical components, such as Al, K and Fe, minerals such as zoisite (epidote group), garnet, Ca-plagioclase, K-feldspar, hornblende and diopside could formed. A generalized zonal sequence can be summarized as follows:
  - I. Ankerite Zone
    - → The lowest grade rocks
    - → It is characterised by the assemblage ankerite $Ca(Mg,Fe)(CO_3)_2$) + quartz + albite + muscovite ± chlorite
  - II- Biotite Zone
    - → This zone is characterised by the coexistence of biotite and chlorite without amphibole, via a reaction such as:

      $$Ms + Qtz + ankerite + H_2O \rightarrow Cal + Chl + Bt + CO_2$$
    - → The upper part of this zone is also characterised by the replacement of albite by a more Ca-rich plagioclase and a reduction in the amount of muscovite present:

      $$Chl + Cal + Ms + Qtz + Ab \rightarrow Bt + Pl + H_2O + CO_2$$
  - III- Amphibole Zone
    - → The appearance of Ca-amphibole is accompanied by a further increase in the Ca content of the plagioclase:

      $$Chl + Cal + Qtz + Pl \rightarrow Ca\text{-}amph + Ca\text{-}Pl + H_2O + CO_2$$
  - IV- Zoisite Zone

→ Zoisite ($Ca_2(Al,Fe)_3[SiO_4](OH)$) often first appears rimming plagioclase at contacts with calcite grains, suggesting growth is due to the reaction:

$$\text{Ca-plagioclase} + \text{calcite} + H_2O \rightarrow \text{zoisite} + CO_2$$

- V- Diopside Zone

→ At the highest grades diopside appears due to the breakdown of amphibole:

$$\text{Ca-amphibole} + \text{calcite} + \text{quartz} \rightarrow \text{diopside} + H_2O + CO_2$$

3.4 Textures of calc-silicate rock

A. Reaction textures:

Several high temperature metamorphic intergrowths and retrograde reaction textures are observed in calc-silicate rocks (Figure 9)

B. High temperature intergrowth textures

High temperature intergrowth textures of scapolite + grandite, garnet + clinopyroxene and plagioclase + grandite, garnet + clinopyroxene are observed in the intermediate zone. (Figure 10)

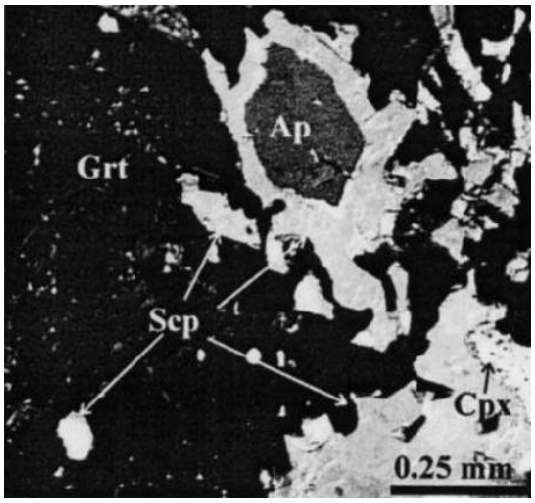

Figure 9: Reaction textures (Faryad 2002)

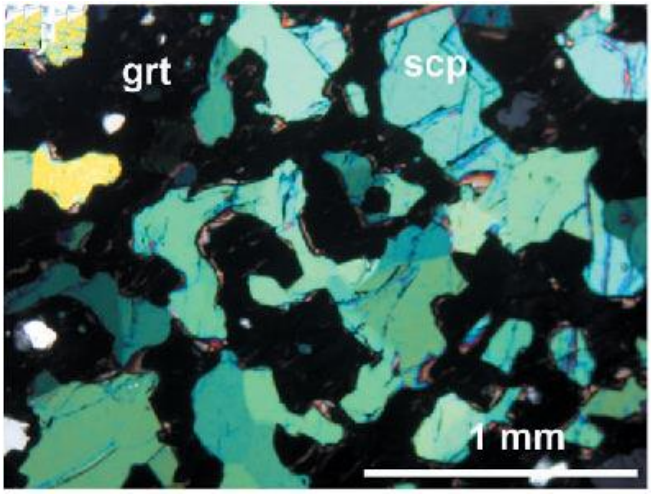

Figure 10: High temperature intergrowth textures (Satish-Kumar et al. 2006)

Garnet often shows resorbed grain boundaries and enclosed in larger scapolite grains. These intergrowth textures can be considered as symplectites, where mineral reactions have progressed considerably.

C. Retrograde Reaction Textures

Several stages of retrograde reaction textures (Figure 11) are identified. Garnet corona surrounding clinopyroxene or calcite is the prominent one observed. Thin rinds and corona of garnet are also observed surrounding scapolite, partially altered to plagioclase. Scapolite in some zones is replaced by plagioclase, calcite and minor amounts of quartz. Wollastonite, found as a relict, is surrounded by retrograde calcite and quartz. Thin rinds of garnet were also observed within the anorthite calcite quartz intergrowth, suggesting garnet formation after the breakdown of scapolite.

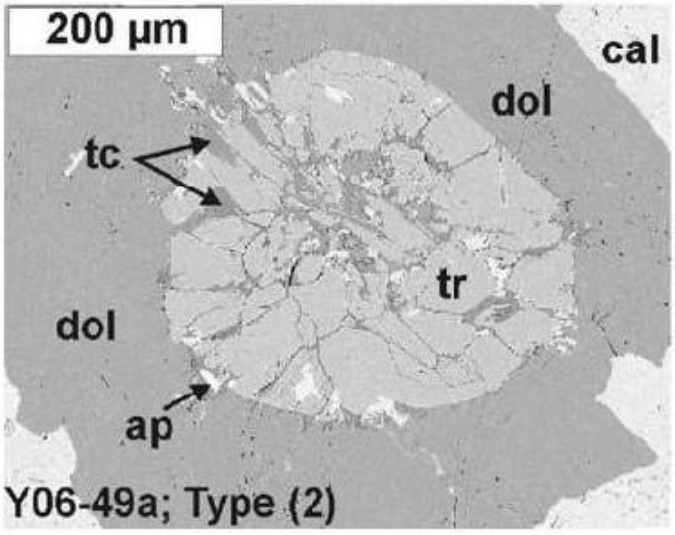

Figure 11: Retrograde Reaction Texture (Gallien et al. 2008)

4. Conclusion

Taking all these into considerations Dr. Chandan Kumar B, Central University of Kerala, 2014, suggested that amphibolites which he figured out in field study clearly show sedimentary structures like bedding planes and are associated conformably with other sediments like greywackes, banded iron formations, dolomitic limestones and impure quartzites. They also consist of detrital quartz grains. These amphibolites mainly consist of tabular and prismatic hornblende and sub-rounded to well-rounded quartz set in a meager fine-grained matrix of quartz, chlorite and sericite but they have negligible feldspars and when plotted in chemical classification diagram they fall into ortho-(igneous) amphibolite category. On the contrary another Geologist Federico Lucci, Università degli Studi di Bari Aldo, Moro, 2014 suggested that texture and fabric of the rock can surely help in this regard, but that they might reflect exhumation processes, or other younger events (deformation, alteration, hydrothermal transformation etc).

Maria Areias of University of Porto, 2014, proposed that the term “para-amphibolite” is outdated now and generally is avoided since it is very hard to think that a carbonatic rocks (or a pelitic rock) shows such impurities, to produce amphibole and plagioclase as a mafic protolith. She added that these rocks can have a direct igneous origin (ortho), a volcanogenic origin or originate from a quartzite with carbonate cemented protolith. According to USGS amphibolite refers to a metamorphic rock of igneous origin containing mainly amphibole and plagioclase. M. Cemal Göncüoğlu of Middle East Technical University, 2014 also suggested that the "para"-amphibolites he studied were very rich in calc-silicate minerals (Ca-rich pyroxene, Ca-rich amphibole, epidote etc) and included calcite. So, he again emphasized that currently the term para-amphibolite tends to be replaced by the term "calc-silicate rock".

ACKNOWLEDGEMENT

We are deeply indebted to our mentor Dr. Chandrabali Mukhopadhyay for her valuable support and suggestion. We are also thankful to all our professors of Geology Department for their constant moral support.

REFERENCES

[1] Alamy, 2021. Skarn (tactite) stone isolated on white. modified from Alamy (Internet open-source photo). Available at: https://www.alamy.com/stock-image-skarn-tactite-stone-isolated-on-white-169258944.html. Accessed on: 20-12-2021.

[2] Faryad, S.W. 2002. Metamorphic Conditions and Fluid Compositions of Scapolite-Bearing Rocks from the Lapis Lazuli Deposit at Sare Sang, Afghanistan. Journal of Petrology, V.43(4), pp.725–747.

[3] FSU, 2021. Hornblende Gneiss, *Polarized Light Microscopy Digital Image Gallery*, Optical Microscopy Primer: Introduction, Michael W. Davidson and The Florida State University. Available at: https://micro.magnet.fsu.edu/primer/index.html. Accessed on: 20-12-2021.

[4] Gallien F., Mogessie A., Bjerg E., Delpino S., deMachuca B.C., 2009. Contrasting fluid evolution of granulite-facies marbles: implications for a high-T intermediate-P terrain in the Famatinian Range, San-Juan, Argentina. Miner Petrology, V.95, pp.135–157.

[5] Mindat, 2021. Californite. Available at: https://www.mindat.org/min-11025.html. Accessed on: 20-12-2021.

[6] RRUFF, 2021. Larnite R070530. RRUFF Project website. Available at: https://rruff.info/Larnite. Accessed on: 20-12-2021.

[7] Satish-Kumar, M., Motoyoshi, Y., Suda, Y., Hiroi, Y. and Kagashima, S. 2006. Calc-silicate rocks and marbles from Lützow-Holm Complex, East Antarctica, with special reference to the mineralogy and geochemical characteristics of calc-silicate mega-boudins from Rundvågshetta. *Polar Geoscience*, V. 19, pp.37-61

[8] Streckeisen, A., 2021. Amphibolite, Available at: https://www.alexstrekeisen.it/english/meta/amphibolite.php. Accessed on: 20-12-2021.

[9] Wikipedia, 2020. Calc-silicate rock. Wikipedia: The Free Encyclopedia. Available at: https://en.wikipedia.org/wiki/Calc%E2%80%93silicate_rock. Accessed on: 20-12-2021.

JDC GeoBytes

2022

Department of Geology
Jogamaya Devi College